

**CHARACTERIZATION AND CATALYTIC
APPLICATIONS OF HYDROTHERMALLY
SYNTHESIZED POLYOXOTUNGSTATE
CLUSTERS CONTAINING ORGANIC-INORGANIC
HYBRID MATERIALS**

**A Thesis Submitted to
the Graduate School of Engineering and Sciences of
İzmir Institute of Technology
in Partial Fulfillment of the Requirements for the Degree of
DOCTOR OF PHILOSOPHY
in Chemistry**

**by
Özlem ECE**

**July 2019
İZMİR**

We approve the thesis of Özlem ECE

Examining Committee Members:


Prof. Dr. Mehtap EANES

Department of Chemistry, Izmir Institute of Technology


Prof. Dr. Funda DEMİRHAN

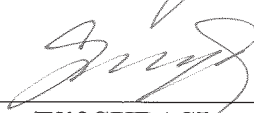
Department of Chemistry, Manisa Celal Bayar University


Assoc. Prof. Dr. Mustafa EMRULLAHOĞLU

Department of Chemistry, Izmir Institute of Technology


Prof. Dr. İşıl TOPALOĞLU SÖZÜER

Department of Chemistry, Izmir Institute of Technology


Prof. Dr. Elif SUBAŞI

Department of Chemistry, Dokuz Eylül University

12 July 2019


Prof. Dr. Mehtap EANES

Supervisor, Department of Chemistry
İzmir Institute of Technology


Prof. Dr. Ali ÇAĞIR

Co-Supervisor, Department of Chemistry
İzmir Institute of Technology


Prof. Dr. Ahmet Emin EROĞLU
Head of the Department of Chemistry


Prof. Dr. Aysun SOFUOĞLU
Dean of the Graduate School of
Engineering and Sciences

ACKNOWLEDGMENTS

I would like to extend my special appreciation to my research advisor, Prof. Dr. Mehtap EMİRDAĞ EANES and my co-advisor Prof. Dr. Ali ÇAĞIR for their support, endless patience and guidance through my PhD. thesis.

Special thanks to my friend Özge TÜNCEL for her all help, support and friendship through my PhD.

Next, I wish to express my thanks to all my friends at IZTECH especially Seçil Sevim ÜNLÜTÜRK, Seray Ece KESKİN and Büşra YILDIZ.

Additionally, my deepest gratitude goes to my family, my mother Pervin ECE, my father Nafiz ECE for their endless love, understanding, encouragement, patience and support throughout my entire life.

Finally, I would like to thank Dr. Hüseyin ÖZGENER and Biotechnology and Bioengineering Application and Research Center (İYTE-BİYOMER) for Fourier Transform Infrared Spectroscopy (FT-IR) analysis, Center of Materials Research (İYTE-MAM) researches for Powder X-ray Diffraction, Scanning Electron Microscope (SEM-EDX) and thermogravimetric analyses, Clemson University for Single Crystal X-ray Diffraction analyses.

ABSTRACT

CHARACTERIZATION AND CATALYTIC APPLICATIONS OF HYDROTHERMALLY SYNTHESIZED POLYOXOTUNGSTATE CLUSTERS CONTAINING ORGANIC-INORGANIC HYBRID MATERIALS

Many scientists have been interested in hydrothermal synthesis and characterization of polyoxometalate clusters containing organic-inorganic hybrid materials recently because of having different applications in lots of fields, especially, using as catalysis in chemical reactions.

In this study, three novel polyoxotungstate clusters were synthesized using hydrothermal method and catalytic activities of these three novel polyoxometalates and in addition two crystals previously synthesized in our group were studied.

The first compound, $[(4,4'\text{-bpyH}_2)_3][\text{PCuW}_{11}\text{O}_{39}]$ yellow crystals, crystallize in the space group $\text{P}2(1)/n$ of the monoclinic system with four formula units in a cell. The crystal is a Keggin polyoxometalate and includes free 4,4'-bipyridine groups between the clusters.

The second compound, $(4,4'\text{-bpyH}_2)[\text{H}_2\text{PW}_{12}\text{O}_{40}]_2 \cdot \text{H}_2\text{O}$ colorless crystals, crystallize in the space group Ia-3 of the cubic system with twelve formula units in a cell. The crystal is a Keggin polyoxometalate and consists of two polyoxotungstate clusters, a free 4,4'-bipyridine group and a water molecule.

The third and the last novel compound, $(4,4'\text{-bpyH}_2)_4[\text{H}_2\text{P}_2\text{W}_{18}\text{O}_{62}]_2$ dark yellow crystals, crystallize in the space group P-1 of the triclinic system with four formula units in a cell. The crystal is a Wells-Dawson polyoxometalate and contains two polyoxotungstate clusters and free 4,4'-bipyridine groups between clusters.

The catalytic study has been carried out using starch hydrolysis reactions by using hydrothermal synthesis and five different crystals were tried and conversion results were obtained. Starch samples converted to D-glucose with glucose yields above 90 wt.%. Catalyst reusability was performed for each crystal. No appreciable loss was observed in activity after five reaction cycles for each crystal.

ÖZET

HİDROTERMAL METOT İLE SENTEZLENEN POLİOKSOTUNGSTEN KÜMELERİ İÇEREN ORGANİK-İNORGANİK MELEZ MALZEMEMLERİN KARAKTERİZASYONU VE KATALİTİK UYGULAMALARI

Son zamanlarda, birçok alanda farklı uygulamalarının olması özellikle kimyasal reaksiyonlarda katalizör olarak kullanılmalarından dolayı birçok bilim adamı polioksometal kümeleri içeren organik-inorganik melez malzemelerin hidrotermal sentezi ve karakterizasyonu ile ilgilenmektedir.

Bu çalışmada, üç adet yeni polioksotungstat kümesi hidrotermal sentez ile sentezlenmiş ve bu yeni bileşikler ile birlikte iki adet daha önce grubumuzda sentezlenmiş olan kristallerin katalitik aktiviteleri çalışılmıştır.

İlk bileşik, $[(4,4'-bpyH_2)_3][PCuW_{11}O_{39}]$ sarı kristalleri, monoklinik sistemin P2(1)/n uzay grubunda olup, dört formül birimi içeren birim hücrede kristallenmiştir. Kristal, Keggin polioksometal yapısına sahiptir ve kristalin yapısındaki 4,4'-bipiridin grupları, $[PCuW_{11}O_{39}]^{6-}$ kümelerinin arasında serbest halde bulunmaktadır.

İkinci bileşik, $(4,4'-bpyH_2)[H_2PW_{12}O_{40}]_2 \cdot H_2O$ şeffaf kristalleri, kübik sistemin Ia-3 uzay grubunda olup, 12 formül birimi içeren birim hücrede kristallenmiştir. Kristal Keggin polioksometal yapısına sahiptir ve iki adet polioksotunstat kümesi ile kümeler arasında serbest halde bulunan 4,4'-bipiridin grubu ile su molekülünden oluşmaktadır.

Üçüncü ve son bileşik, $(4,4'-bpyH_2)_4[H_2P_2W_{18}O_{62}]_2$ koyu sarı kristalleri, triklinik sistemin P-1 uzay grubunda olup, dört formül birimi içeren birim hücrede kristallenmiştir. Kristal Wells-Dawson polioksometal yapısına sahiptir ve iki adet polioksotungstat kümesi ile kümeler arasında serbest halde bulunan 4,4'-bipiridin gruplarını içermektedir.

Katalitik çalışmada, hidrotermal sentez ve nişasta hidroliz reaksiyonları ile beş farklı kristal kullanılmış ve dönüşüm sonuçları elde edilmiştir. Nişasta örnekleri kütlece %90 glikoz verimi ile D-glikoza dönüşmüştür. Her bir kristal için yeniden kullanılabilirlik denemeleri yapılmıştır. Beş reaksiyon döngüsü sonucunda her bir kristalin katalitik aktivitesinde kayda değer bir azalısa rastlanmamıştır.

TABLE OF CONTENTS

LIST OF FIGURES	ix
LIST OF TABLES	xii
CHAPTER 1. INTRODUCTION	1
1.1. Organic-Inorganic Hybrid Materials.....	2
1.2. Hydrothermal Synthesis	3
CHAPTER 2. EXPERIMENTAL METHOD	5
2.1. Autoclaves.....	5
2.2. Hydrothermal Procedure	6
2.3. Characterization	6
2.3.1. Diffraction Techniques	7
2.3.1.1. X-ray Diffraction	7
2.3.1.1.1. Powder X-ray Diffraction	7
2.3.1.1.2. Single Crystal X-ray Diffraction	8
2.3.2. Microscopic Techniques	9
2.3.2.1. Optical Microscopy	10
2.3.2.2. Electron Microscopy	10
2.3.2.2.1. Scanning Electron Microscopy (SEM)	11
2.3.3. Spectroscopic Techniques	12
2.3.3.1. Infrared Spectroscopy.....	12
2.3.4. Thermogravimetric Analysis.....	13
CHAPTER 3. ORGANIC-INORGANIC HYBRID MATERIALS	14
3.1. Structures of Polyoxometalates	15
3.2. Catalysis of Polyoxometalates	17
3.3. Synthesis and Characterization of Polyoxometalates	19
3.3.1. Synthesis and Characterization of $(4,4'-\text{bpyH}_2)_3[\text{PCuW}_{11}\text{O}_{39}]$	19
3.3.1.1. X-ray Crystallographic Analysis of $(4,4'-\text{bpyH}_2)_3[\text{PCuW}_{11}\text{O}_{39}]$	21
3.3.1.2. Results and Discussion for $(4,4'-\text{bpyH}_2)_3[\text{PCuW}_{11}\text{O}_{39}]$	24

3.3.2. Synthesis and Characterization of (4,4'-bpyH ₂)[H ₂ PW ₁₂ O ₄₀] ₂ .H ₂ O	27
3.3.2.1. X-ray Crystallographic Analysis of (4,4'-bpyH ₂)[H ₂ PW ₁₂ O ₄₀] ₂ .H ₂ O	29
3.3.2.2. Results and Discussion for (4,4'-bpyH ₂)[H ₂ PW ₁₂ O ₄₀] ₂ .H ₂ O	32
3.3.3. Synthesis and Characterization of (4,4'-bpyH ₂) ₄ [H ₂ P ₂ W ₁₈ O ₆₂] ₂	35
3.3.3.1. X-ray Crystallographic Analysis of (4,4'-bpyH ₂) ₄ [H ₂ P ₂ W ₁₈ O ₆₂] ₂	37
3.3.3.2. Results and Discussion for (4,4'-bpyH ₂) ₄ [H ₂ P ₂ W ₁₈ O ₆₂] ₂	41
CHAPTER 4. CATALYTIC APPLICATIONS	44
4.1. Catalytic Procedure	44
4.2. Results and Discussion.....	45
4.2.1. Lugol's Iodine Test	45
4.2.2. FT-IR ATR Results	46
4.2.3. Optimization of Reaction Time and Temperature.....	48
4.2.4. Optimization of Catalyst Amount	51
4.2.5. Reusability of Catalysts.....	52
CHAPTER 5. CONCLUSION	58
REFERENCES	60
APPENDICES	
APPENDIX A. BOND LENGTHS (Å) FOR (4,4'-bpyH ₂) ₃ [PCuW ₁₁ O ₃₉]	63
APPENDIX B. BOND ANGLES (°) FOR (4,4'-bpyH ₂) ₃ [PCuW ₁₁ O ₃₉]	65
APPENDIX C. BOND LENGTHS (Å) FOR (4,4'-bpyH ₂)[H ₂ PW ₁₂ O ₄₀] ₂ .H ₂ O	69
APPENDIX D. BOND ANGLES (°) FOR (4,4'-bpyH ₂)[H ₂ PW ₁₂ O ₄₀] ₂ .H ₂ O.....	70
APPENDIX E. BOND LENGTHS (Å) FOR (4,4'-bpyH ₂) ₄ [H ₂ P ₂ W ₁₈ O ₆₂] ₂	72
APPENDIX F. BOND ANGLES (°) FOR (4,4'-bpyH ₂) ₄ [H ₂ P ₂ W ₁₈ O ₆₂] ₂	76
APPENDIX G. BOND VALENCE SUMS OF (4,4'-bpyH ₂) ₃ [PCuW ₁₁ O ₃₉]	85
APPENDIX H. BOND VALENCE SUMS OF (4,4'-bpyH ₂)[H ₂ PW ₁₂ O ₄₀] ₂ .H ₂ O	87

LIST OF FIGURES

<u>Figure</u>	<u>Page</u>
Figure 1.1. Selected interactions in hybrid materials and their strength.....	2
Figure 1.2. Graph of the P-T conditions of water at various degrees of fill	4
Figure 2.1. Parts and schematic representation of a stainless-steel autoclave	6
Figure 2.2. The X-ray Spectrometer	8
Figure 2.3. J.P. Selecta Zoom Stereo Microscope	10
Figure 2.4. Scanning Electron Microscope (SEM)	11
Figure 3.1. Different functions of organonitrogen ligand	14
Figure 3.2. Polyhedral representations of (a) decavanadate ($V_{10}O_{28}$) ⁶⁻ and (b) Keggin ($PMo_{12}O_{40}$) ³⁻ (c) Wells-Dawson ($P_2W_{18}O_{62}$) ⁶⁻ anions.....	16
Figure 3.3. (a) Combination of three octahedra to form a trimetallic group M_3O_{13} . (b) Structure of the Keggin type POM	16
Figure 3.4. (a) Combination of two octahedra to form a dimetallic group M_2O_{10} . (b) Structure of the Dawson type POM	17
Figure 3.5. Amylose and amylopectin bonds of starch.....	18
Figure 3.6. SEM/EDX spectrum of $(4,4'-bpyH_2)_3[PCuW_{11}O_{39}]$	20
Figure 3.7. XRD spectrum of $(4,4'-bpyH_2)_3[PCuW_{11}O_{39}]$	20
Figure 3.8. TGA graph of $(4,4'-bpyH_2)_3[PCuW_{11}O_{39}]$	21
Figure 3.9. The view of $[PCuW_{11}O_{39}]^5-$ Keggin polyanion cluster	24
Figure 3.10. The chain structure of $[PCuW_{11}O_{39}]^5-$ Keggin polyanions	25
Figure 3.11. The unitcell view of $(4,4'-bpyH_2)_3[PCuW_{11}O_{39}]$	26
Figure 3.12. SEM/EDX spectrum of $(4,4'-bpyH_2)[H_2PW_{12}O_{40}]_2.H_2O$	28
Figure 3.13. XRD spectrum of $(4,4'-bpyH_2)[H_2PW_{12}O_{40}]_2.H_2O$	28
Figure 3.14. TGA graph of $(4,4'-bpyH_2)[H_2PW_{12}O_{40}]_2.H_2O$	29
Figure 3.15. The view of Keggin polyanion cluster	32
Figure 3.16. The polyhedral structure of Keggin polyanions	33
Figure 3.17. The unitcell view of $(4,4'-bpyH_2)[H_2PW_{12}O_{40}]_2.H_2O$	34
Figure 3.18. SEM/EDX spectrum of $(4,4'-bpyH_2)_4[H_2P_2W_{18}O_{62}]_2$	36
Figure 3.19. XRD spectrum of $(4,4'-bpyH_2)_4[H_2P_2W_{18}O_{62}]_2$	36
Figure 3.20. TGA graph of $(4,4'-bpyH_2)_4[H_2P_2W_{18}O_{62}]_2$	37
Figure 3.21. The view of Well-Dawson polyanion cluster	41

<u>Figure</u>	<u>Page</u>
Figure 3.22. The polyhedral structure of Well-Dawson polyanions.....	42
Figure 3.23. The unitcell view of $(4,4'\text{-bpyH}_2)_4[\text{H}_2\text{P}_2\text{W}_{18}\text{O}_{62}]_2$	43
Figure 4.1. Hydrolysis reaction of starch	45
Figure 4.2. Lugol's test of the reactions with five different crystals and without any catalyst.	46
Figure 4.3. FT-IR ATR spectra of the reactions with five different catalysts and with no catalyst.....	47
Figure 4.4. Lugol's test of the reaction with $(4,4'\text{-bpyH}_2)_2(4,4'\text{-bpyH})[\text{PCoW}_{11}\text{O}_{39}]\cdot\text{H}_2\text{O}$ crystal for temperature.....	48
Figure 4.5. Lugol's test of the reaction with $(4,4'\text{-bpyH}_2)_2(4,4'\text{-bpyH})[\text{PCoW}_{11}\text{O}_{39}]\cdot\text{H}_2\text{O}$ crystal for time.	49
Figure 4.6. FT-IR ATR spectra of the starch hydrolysis reactions with the catalyst $(4,4'\text{-bpyH}_2)_2(4,4'\text{-bpyH})[\text{PCoW}_{11}\text{O}_{39}]\cdot\text{H}_2\text{O}$ at 150 °C from 1 to 5 h.....	50
Figure 4.7. Lugol's test of the reaction with $(4,4'\text{-bpyH}_2)_2(4,4'\text{-bpyH})[\text{PCoW}_{11}\text{O}_{39}]\cdot\text{H}_2\text{O}$ crystal for catalyst amount... ...	51
Figure 4.8. Lugol's test of the reaction with $(4,4'\text{-bpyH}_2)_2(4,4'\text{-bpyH})[\text{PCoW}_{11}\text{O}_{39}]\cdot\text{H}_2\text{O}$ crystal for five cycles.....	52
Figure 4.9. Lugol's test of the reaction with $(4,4'\text{-bpyH}_2)_2[\text{H}_2\text{PW}_{12}\text{O}_{40}]_2\cdot\text{H}_2\text{O}$ crystal for five cycles.....	53
Figure 4.10. Lugol's test of the reaction with $(4,4'\text{-bpyH}_2)_3[\text{PCuW}_{11}\text{O}_{39}]$ crystal for for five cycles.....	53
Figure 4.11. Lugol's test of the reaction with $(4,4'\text{-bpyH}_2)_4[\text{H}_2\text{P}_2\text{W}_{18}\text{O}_{62}]_2$ crystal for five cycles.....	54
Figure 4.12. Lugol's test of the reaction with $(4,4'\text{-bpyH}_2)_2(4,4'\text{-bpyH})[\text{PCuW}_{11}\text{O}_{39}]\cdot\text{H}_2\text{O}$ crystal for five cycles.....	54
Figure 4.13. Plot of glucose yield vs reaction cycles of the reaction with the catalyst $(4,4'\text{-bpyH}_2)_2(4,4'\text{-bpyH})[\text{PCoW}_{11}\text{O}_{39}]\cdot\text{H}_2\text{O}$	55
Figure 4.14. Plot of glucose yield vs reaction cycles of the reaction with the catalyst $(4,4'\text{-bpyH}_2)_2[\text{H}_2\text{PW}_{12}\text{O}_{40}]_2\cdot\text{H}_2\text{O}$	55
Figure 4.15. Plot of glucose yield vs reaction cycles of the reaction with the catalyst $(4,4'\text{-bpyH}_2)_3[\text{PCuW}_{11}\text{O}_{39}]$	56

<u>Figure</u>	<u>Page</u>
Figure 4.16. Plot of glucose yield vs reaction cycles of the reaction with the catalyst $(4,4'\text{-bpyH}_2)_4[\text{H}_2\text{P}_2\text{W}_{18}\text{O}_{62}]_2$	56
Figure 4.17. Plot of glucose yield vs reaction cycles of the reaction with the catalyst $(4,4'\text{-bpyH}_2)_2(4,4'\text{-bpyH})[\text{PCuW}_{11}\text{O}_{39}]\cdot\text{H}_2\text{O}$	57

LIST OF TABLES

<u>Table</u>	<u>Page</u>
Table 3.1. Crystallographic data for (4,4'-bpyH ₂) ₃ [PCuW ₁₁ O ₃₉]	22
Table 3.2. Selected bond lengths (Å) for (4,4'-bpyH ₂) ₃ [PCuW ₁₁ O ₃₉].....	23
Table 3.3. Selected bond angles (°) for (4,4'-bpyH ₂) ₃ [PCuW ₁₁ O ₃₉]	23
Table 3.4. Crystallographic data for (4,4'-bpyH ₂)[H ₂ PW ₁₂ O ₄₀] ₂ .H ₂ O	30
Table 3.5. Selected bond lengths (Å) for (4,4'-bpyH ₂)[H ₂ PW ₁₂ O ₄₀] ₂ .H ₂ O	31
Table 3.6. Selected bond angles (°) for (4,4'-bpyH ₂)[H ₂ PW ₁₂ O ₄₀] ₂ .H ₂ O	31
Table 3.7. Crystallographic data for (4,4'-bpyH ₂) ₄ [H ₂ P ₂ W ₁₈ O ₆₂] ₂	38
Table 3.8. Selected bond lengths (Å) for (4,4'-bpyH ₂) ₄ [H ₂ P ₂ W ₁₈ O ₆₂] ₂	39
Table 3.9. Selected bond angles (°) for (4,4'-bpyH ₂) ₄ [H ₂ P ₂ W ₁₈ O ₆₂] ₂	40

CHAPTER 1

INTRODUCTION

Solid state chemistry is interested in synthesis, structure, properties and applications of solid materials. It has also a strong correspondence with solid-state physics, mineralogy, crystallography, ceramics, metallurgy, thermodynamics, materials science and electronics with a focus on the synthesis of novel materials and their characterization. Solid phase materials which solid state chemistry deals with, mostly involve inorganic compounds. Organic solids are also involved in solid phase materials because of presenting curious physical properties like high electrical property and the reactions of organic solids are connected to topochemical control.

Mainly, inorganic solids are non-molecular and their structure is determined by the manner in which atoms or ions are packed together in three dimensions. Their various structures are the center of appreciation of solid state chemistry and involve description and classification of crystal structures by space groups and factors that affect and control the crystal structures.

The defect structure is an important structural aspect for solid materials. It effects on mechanical strength, electrical conductivity and chemical reactivity. Moreover, it allows the various composition of solids in the framework of the same overall crystal structure. Therefore, it is possible to control or modify many properties by changing the compositions.

Vapour phase transport, precipitation, electrochemical methods, ceramic methods, solvothermal and hydrothermal methods are the synthesis methods of solids.¹ Among these methods, hydrothermal synthesis is a common method to synthesize organic-inorganic hybrid materials since the other solid state synthesis methods are usually carried out by high temperature (1000°C) solid-solid interactions and this hydrothermal method is suitable in order to produce stable organic-inorganic hybrid materials.

In recent years, polyoxometalates (POMs), have been widely used as catalysts for both homogeneous and heterogeneous reactions due to their high acid strength and high thermal stability. The aim of this PhD thesis is to synthesize novel

polyoxotungstate clusters containing organic-inorganic hybrid materials by hydrothermal method and study their catalytic activities.

1.1. Organic-Inorganic Hybrid Materials

Organic-inorganic materials can be applied in several branches of chemistry and they attracted the attention of the scientists especially the beginning of 21st century due to their different characteristic properties although mixing of them was carried out in ancient times. These materials are not only represent an alternative for designing of new materials but also have applications in many areas like optics, electronics, energy and medicine.

There are two types of interactions in organic-inorganic hybrid materials which are shown in Figure 1.1. The first type of interaction is the weak interaction between the two components, Van der Waals, H-bonding or weak electrostatic interactions. The second type of interaction is the strong chemical interaction between the components.² In these materials, organic part can control the nucleation and growth of the inorganic oxide part and affect its structure. Also, more complex structures can be produced by using secondary metal complexes.³

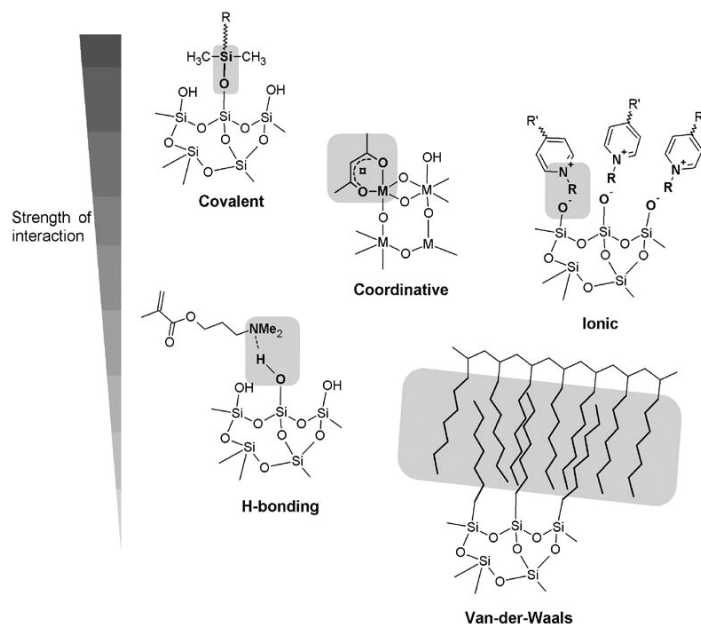


Figure 1.1. Selected interactions in hybrid materials and their strength.
 (Source: Kickelbick²)

1.2. Hydrothermal Synthesis

Hydrothermal synthesis is named as a heterogeneous reaction in an aqueous media above 100°C and 1 bar in a closed system in order to dissolve and recrystallize materials that are relatively insoluble under normal conditions.⁴

The hydrothermal technique has attracted the attention of scientists from different branches of science. Today, it is an interdisciplinary subject and the technique is mostly used by geologists, biologists, physicists, chemists, ceramists, hydrometallurgists, material scientists, engineers, and so on.

In the Earth, water is one of the most important solvents and it acts very differently from its standard conditions as a reaction medium under hydrothermal conditions.

Water is beneficial for the environment and cheaper than other solvents. Moreover, it can act as a catalyst for the formation of various types of materials by changing temperature and pressure. Other advantages of water are nontoxicity, nonflammability, noncarcinogenicity, nonmutagenicity, and thermodynamic stability. On the other hand, water is very volatile, so it can be removed easily from the product.

Also, water has a polarity that can be controlled by temperature and pressure. This makes water as an advantageous solvent. For experimental hydrothermal synthesis, to understand the PT conditions of water, it is first necessary to know how it changes under various states of pressure, volume and temperature.

An extensive study of pressure-temperature conditions of water was reported by Laudise. At the beginning, when an autoclave is filled to 32%, the liquid level does not change until the critical temperature as shown in Figure 1.2. The density of both the liquid and gas is 0.32 g/cm³ when it comes to the critical point. If an autoclave is filled more than 32% with water, it is filled at temperatures before critical temperature.

If an autoclave is filled less than 32%, the liquid level drops and gas fills the autoclave at temperatures under critical temperature when temperature increases. As a result that, liquid is lost. If the filling is in higher percentage, the temperature at which the autoclave becomes filled with liquid, decreases.⁵

In addition to these, supercritical water is an excellent reaction media with its low viscosity and high mobility to synthesize novel metastable phases and grow best quality single crystals for analysis. Superheated water can solvate various reagents and

is a fine reaction media for both better transport and intermixing of reagents. The properties of hydrothermal solutions that have conditions between 100-150°C and 150-375°C, carry the characteristics of supercritical state.

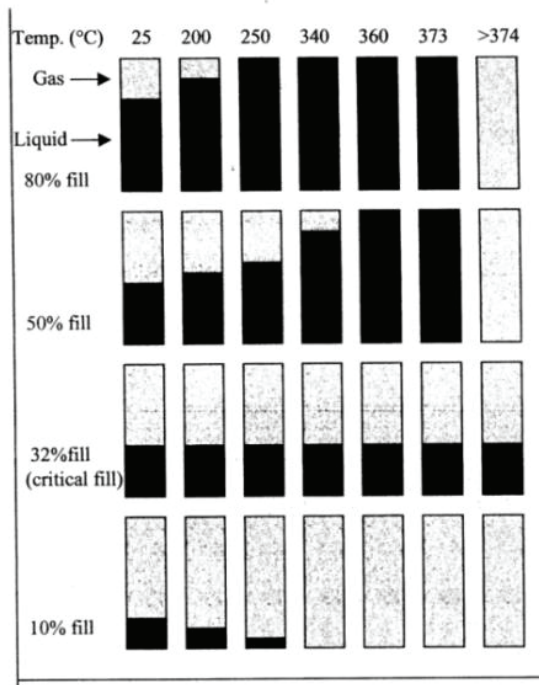


Figure 1.2. Graph of the P-T conditions of water at various degrees of fill.
(Source: Laudise⁵)

Furthermore, hydrothermal reaction does not need much more time compared to traditional methods. Although a solid state reaction can be done in a few weeks, hydrothermal reaction can be performed in a few days.⁶

CHAPTER 2

EXPERIMENTAL METHOD

2.1. Autoclaves

A pressure vessel that is capable of including highly corrosive solvent at high temperatures and pressures is used for crystal synthesis and growth with hydrothermal synthesis method. This special hydrothermal apparatus is named as ‘autoclave’.⁷

In the 19th century, the first autoclave was made in Europe and than started to used in the 20th century in all over the world. An ideal autoclave should involve the following properties;

- Inertness to oxidizing agents, acids and bases
- Easy to operate and maintain
- A suitable size and shape to obtain a desired temperature gradient
- Leak-proof with unlimited capabilities to the required pressure and temperature
- High mechanical strength to resist high pressure and temperature experiments for long duration

Stainless steel, iron, nickel, cobalt based super alloys, titanium and its alloys are corrosion resistant, high-strength alloys that are suitable for producing autoclaves. The reagents and solvents are corrosive and they can attack the vessel in high temperatures and pressures during the hydrothermal experiments so it requires a suitable lining for the inner wall of the autoclave.

In order to synthesize high purity crystals in highly corrosive conditions, teflon beakers or liners are used. They should sit inside the autoclave without leaving any space. Teflon is the most popularly used lining material but it cannot be used at more than 300°C since it dissociates affecting the pH of unbuffered, near-neutral solutions above this temperature.⁸ The other parts of the stainless-steel autoclave are lower pressure stainless-steel disc, upper pressure stainless-steel disc, corrosion disc and rupture. Also, at the top it has a stainless-steel lid in order to close the stainless-steel autoclave. Figure 2.1 shows parts and shematic representation of a stainless steel autoclave.

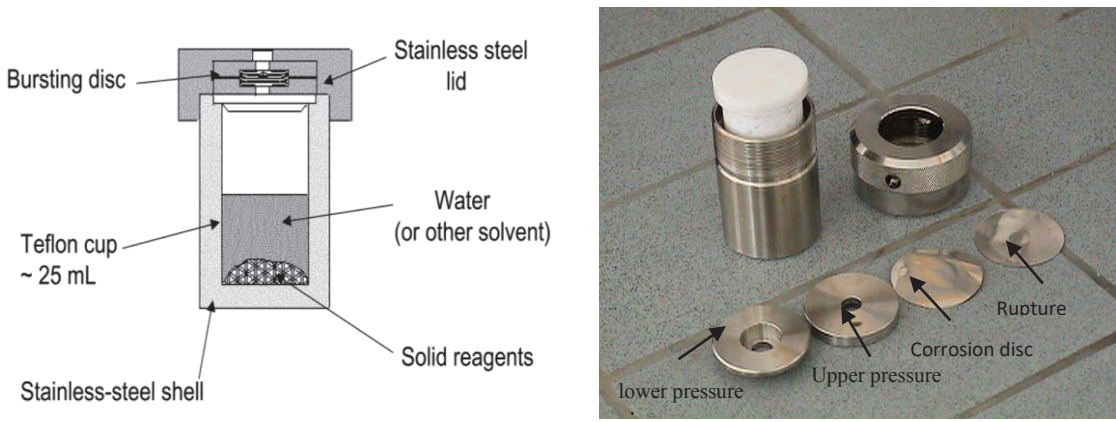


Figure 2.1. Parts and schematic representation of a stainless-steel autoclave.
(Source: Şahin⁹)

2.2. Hydrothermal Procedure

Hydrothermal reactions generally take place between 100-250°C in stainless steel autoclaves. Teflon is an inert material, so it does not interact with the starting materials so teflon vessels (23 ml) are used in autoclaves. Firstly, teflon vessels are filled with starting materials (transition metal oxide, organic component, secondary metal salt, phosphoric acid) and reaction solution (water). Secondly, teflon vessels are inserted in autoclaves and put in an oven. Above 100°C, water is vaporized and solves the initial compounds that could not be solved easily in normal conditions. Reactions are kept 3 days at the intended temperature. After the end of this period, autoclaves are cooled slowly to room temperature. Crystals having the best quality are formed in the cooling period. Lastly, products are filtered by vacuum filtration and washed at least 3 times with pure water to remove the traces of solvent from the products. The crystals are observed under the optical microscope and analyzed with Powder X-ray Diffractometer, spectroscopic techniques, Scanning Electron Microscope-EDX, Single Crystal X-ray Diffractometer and their structures are determined by ShelXTL crystal structure program.

2.3. Characterization

Diffraction techniques, microscopic techniques and spectroscopic techniques are the three main techniques that are generally used in order to characterize the organic-

inorganic hybrid crystalline materials. Additionally, thermogravimetric analysis gives informations about the organic components of the organic-inorganic hybrid crystalline materials.

2.3.1. Diffraction Techniques

Diffraction methods are used for the identification and quantification of constituents of crystalline structures. The basic principle of diffraction methods is based on the Bragg equation, which defines the relation between the wavelength of the radiation, the angle of the incident radiation and the crystal lattice geometry of the object irradiated.

2.3.1.1. X-ray Diffraction

Certainly, X-ray diffraction methods are the most effective methods in solid state chemistry and have been applied in order to characterize the crystals and determine their structures. These methods require an X-ray source (monochromatic or of variable λ), the sample (single crystal, powder or solid piece) and a detector (radiation counter or photographic film) that takes the diffracted X-rays.

2.3.1.1.1. Powder X-ray Diffraction

The spectroscopic technique known as the X-ray powder diffractometry, or simply X-ray diffractometry, is the most widely used diffraction method. X-ray diffractometry (XRD), is originally used for examining the crystal structure of powder samples; thus, traditionally it is called X-ray powder diffractometry (Figure 2.2).

Powder diffraction is a common method to tell which crystalline compounds or phases present but it does not give any direct information about their chemical composition. Each crystal has a typical powder pattern like a fingerprint for identification purposes. The two variables in powder pattern are peak position and intensity. An invaluable reference source is the Powder Diffraction File (Joint Committee on Powder Diffraction Standards, USA), previously known as ASTM file, is

used for identifying the unknown crystals. It includes the powder patterns of about 35000 materials and new entries are added at the current rate of ~ 2000 p.a.¹⁰ The synthesized crystals were analyzed by Philips X'Pert Pro Powder X-ray Diffractometer.

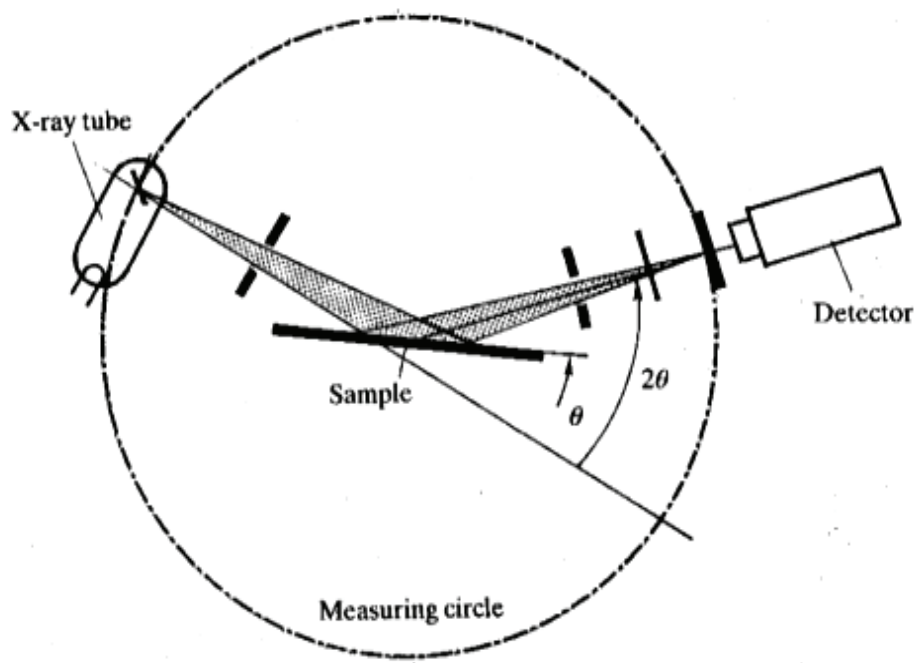


Figure 2.2. The X-ray Spectrometer.
(Source: Smart et al.¹⁰)

2.3.1.1.2. Single Crystal X-ray Diffraction

It is possible to solve and refine a full crystalline structure of a new material by measuring the position and intensity of the hkl reflections by using single crystal X-ray diffraction method. The unit cell dimensions, space group and the precise atomic positions of crystals are also determined. Generally, these can be done with speed and accuracy and this method is one of the most powerful structural methods in chemistry.¹⁰

Single crystal X-ray diffraction is a non destructive analysis and the possibilities of success are very high that have increased over the last 15 years with the progress in the experimental devices, the improvement of crystal-structure solution and refinement methodologies.

In single crystal X-ray diffraction analysis, the samples should be unfracturated and optically clear single crystals. Crystals size should be between 0.1 and 0.2 millimeters in three directions of space. They are selected by using an optical microscope (x40) which includes a polarizing attachment and observing if light extinguishes regularly every 90° when turning the stage of the microscope.

A selected crystal is fixed on the tip of a thin glass fibre using epoxy or cement, or in a loop including specific oil, which fits inside the goniometer head of the diffractometer. After that, the crystal is aligned along the beam direction. Stability properties of the crystals are necessary. Crystals can be sensitive to light, air and moisture, or susceptible to loss of crystallisation solvent. In that case, a special treatment is required. They can be fitted into sealed glass capillaries or the data collection can be performed at low temperature.

After the crystal is mounted on the diffractometer, the suitable parameters for each measurement such as the distance to the detector and the space of the Ewald sphere are selected and then the intensity data are collected. Data are usually obtained between 3° and 30° 2θ when using molybdenum radiation. A complete data collection requires between 3 to 12 hours, depending on the specimen and the diffractometer. Some measured intensities allow the calculation of the unit cell parameters. Later, all the intensities are indexed and a list of hkl reflections is obtained.¹¹

Single crystal X-ray diffractions of the synthesized crystals were performed using a Rigaku AFC8S diffractometer equipped with Mo K α ($\lambda=0.71073\text{ \AA}$) radiation and a Mercury CCD area detector. Data collection and processing, involving corrections for absorption, Lorentz and polarization effects were performed by using the CrystalClear software package. Candidate space groups were determined depending on systematic absences of the data.

2.3.2. Microscopic Techniques

Ordinarily, it is better to look at solid samples under magnification to examine them that are observed to be similar may be seen very different under the microscope because of their various shapes and optical properties.

Microscopy can be divided into two groups: optical microscopy and electron microscopy.

2.3.2.1. Optical Microscopy

Optical microscopy, often referred to as light microscopy, is used to investigate particles down to a few micrometers under high magnification. Optical microscopy is the oldest and cheapest microscopic method furthermore, its sample preparation is easy. However, a conventional optical microscope uses visible radiation (wavelength 400–700 nm) and cannot resolve images of samples smaller than half the wavelength of the light. So, it is better to prefer electron microscopy for submicrometer-sized particles.¹ Figure 2.3 shows a J.P. Selecta Zoom Stereo Microscope which was used.



Figure 2.3. J.P. Selecta Zoom Stereo Microscope.

2.3.2.2. Electron Microscopy

Electron microscopy is a type of microscopy that uses a beam of electrons to create an image of the specimen and is generally preferred for the characterization of solids in order to identify the structure, morphology, crystal size and the distribution of elements. An electron microscope works with a similar principle with an optical microscope but it has much higher magnifications and a greater resolving power than an optical microscope for observing smaller objects in finer detail.¹⁰

2.3.2.2.1. Scanning Electron Microscopy (SEM)

Observation and characterization of the heterogeneous organic and inorganic materials on a nanometer (nm) to micrometer (μm) scale is possible in scanning electron microscopy (SEM). It is a popular technique for scientists as a reason of taking three-dimensional-like images of the surfaces of a very wide range of materials. The main components of SEM are the lens system, electron gun, electron collector, visual and photorecording cathode ray tubes (CRTs) and associated electronics.¹²

According to the principle of the SEM, a very fine probe of electrons changing energies from a few hundred eV to tens of keV is focused at the surface of the sample and scanned across it in a raster or pattern of parallel lines. Signal comes from electrons or radiations can be collected in every position of the incident electron probe. The ratio between the dimensions of the final image display and the sample is called as magnification that is produced by the scanning microscope. A wide range of magnification can be used. The samples sometimes need to be coated with gold or graphite for preventing charge building up on the surface.¹³ Figure 2.4 shows a scanning electron microscope. In this study, FEI QUANTA 250 FEG Scanning Electron Microscope was used to analyze the synthesized crystals.



Figure 2.4. Scanning Electron Microscope (SEM).

2.3.3. Spectroscopic Techniques

Spectroscopy is the study of the absorption, emission or scattering of electromagnetic radiation by atoms or molecules. Some of the types of spectroscopic techniques are vibrational spectroscopy, visible and ultraviolet spectroscopy, nuclear magnetic resonance spectroscopy, electron spectroscopies, electron spin resonance spectroscopy, Mössbauer spectroscopy, X-ray spectroscopies and mass spectrometry. All of these spectroscopic techniques work as absorbing or emitting energy by substances under certain conditions.

Data obtained from spectroscopy is generally presented as a spectrum. The spectrum includes X and Y axes. X axis shows the frequency, f , or wavelength, λ , of the appropriate radiation and Y axis shows the intensity of absorption or emission.

In this study, infrared (IR) spectroscopy, a type of vibrational spectroscopy was used to determine the products of the catalytic reactions of the synthesized organic-inorganic hybrid crystals.

2.3.3.1. Infrared Spectroscopy

Infrared spectroscopy is the study of the interaction between infrared light and molecules. In this technique, vibrational modes which involve groups or pairs of atoms are excited to higher energy states by absorption of radiation of appropriate frequency. Although IR spectra is mostly used for the determination of organic compounds, in inorganic solids, covalently bonded linkages can give intense IR peaks. IR spectrum is the plot of intensity of absorption or percent transmittance of the material. IR spectrum of solids gives lots of peaks. Each peak shows a particular vibrational transition. A composition of all peaks demonstrates the molecular samples and sometimes the nonmolecular samples.¹

Attenuated total reflection (ATR) is the most widely used technique in infrared spectroscopy. This technique requires little or no sample preparation and results can be taken with a little care. In this technique, the sample is placed in a contact with the sensing element and the spectrum is obtained from this contact.¹⁴

The IR spectra of the synthesized crystals were taken by Perkin-Elmer Spectrum 100 FT-IR Spectrometer between 4000-400 cm^{-1} .

2.3.4. Thermogravimetric Analysis

Thermogravimetric analysis is one of the types of thermal analysis in which the mass of a substance is investigated as a function of temperature or time as the sample specimen is subjected to a controlled temperature program in a controlled atmosphere. The measurement is generally performed in air or in an inert atmosphere, such as Helium or Argon, and the weight is recorded as a function of increasing temperature. Occasionally, the measurement is performed in a lean oxygen atmosphere (1 to 5% O₂ in N₂ or He) to slow down oxidation.¹ Perkin Elmer Diamond TG/DTA instrument was used to analyze the crystals.

CHAPTER 3

ORGANIC-INORGANIC HYBRID MATERIALS

Hybrid materials which includes both organic and inorganic parts are simple and suitable for designing on the molecular level. Inorganic part of these materials involves transition metal oxides and p-block elements and organic part of them includes organic diamine ligands. Secondary metal complexes are also used more complex structures. They make bridges between the metal oxide and organic component which cannot make bonds directly with metal oxide structure.

There are different involvements of organonitrogen ligands in metal oxides. These are charge compensating cation, ligand bound directly to the metal oxide, ligand bound to secondary metal site, ligand on the secondary metal that bound to metal oxide structure and bringing ligand between secondary metal complexes which are shown from a to e respectively in Figure 3.1.

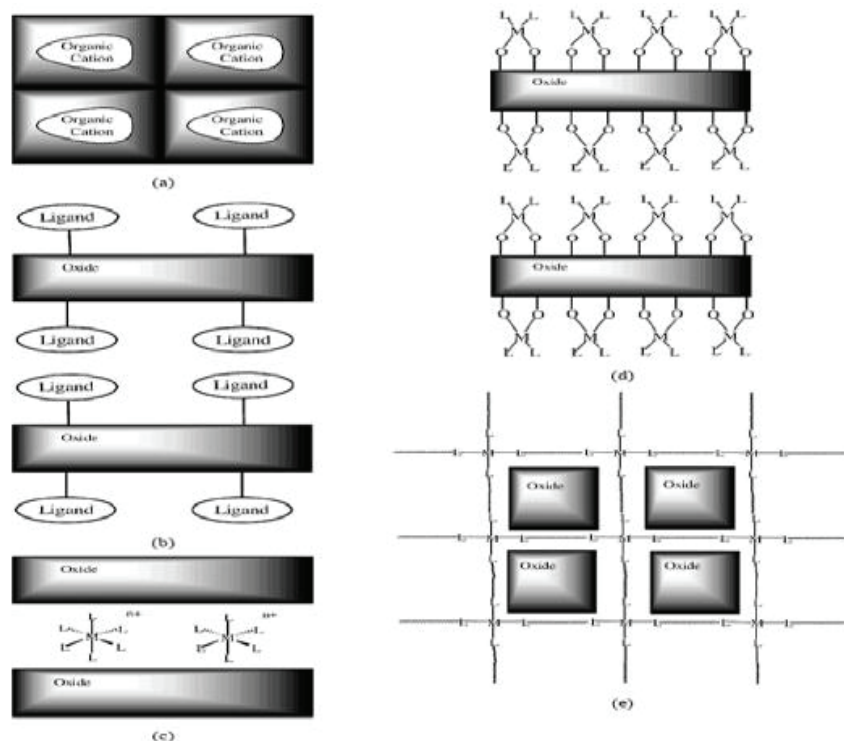


Figure 3.1. Different functions of organonitrogen ligand.
(Source: Hagrman et al.³)

Crystalline open-framework inorganic materials have been attracted attention because of their various structures and their studies in catalysis, adsorption and ion exchange.¹⁵

Open-framework metal phosphates are usually synthesized in different sizes by using organic amines under hydrothermal conditions. They have several structures like one-dimensional linear chains which include corner-shared four-membered rings, one-dimensional ladders that have edge-shared four-membered rings, two-dimensional layers, three dimensional structures with channels and zero-dimensional metal phosphate monomers which involve four-membered rings.¹⁶

The simplest units of open-framework metal phosphates are ordinarily four-membered rings and because of their greater stability, three-dimensional open-frameworks are formed much more frequently than the two or one-dimensional ones.

Organic amine groups in open-framework metal phosphates that mentioned before, act as a structure directing or space-filling agent. These groups can also stabilize the structure through hydrogen-bonding or other interactions and help in charge compensation of the compound.¹⁷

Polyoxometalates (POMs) compose of anionic metal-oxygen clusters formed as a result of the connection of $[MO]_x$ polyhedra of the early transition metals which have their biggest oxidation states. The polyoxometalate structures, can be named as hetero- or isopolyacids and hetero- or isopolyanions or polyoxoanions.

Molybdenum(VI) and tungsten(VI) structures are the most preferred polyoxo structures because of their empty d-orbitals for metal-oxygen π -bonding and suitable combination of ionic radius and charge.¹⁸

According to lots of reviews polyoxometalates have many applications in material science, medicine, catalysis and so forth.

3.1. Structures of Polyoxometalates

Polyoxometalates (POMs) consist of isopolyanions (IPAs) and heteropolyanions (HPAs) based on the number of different atoms except oxygens. Isopolyanions have $M_nO_{(4nm)}^{(2nm)-}$ formula, heteropolyanions have $X_sM_nO_m^{y-}$ formula. Figure 3.2 shows the polyhedral representations of an isopolyanion (decavanadate) and heteropolyanions (Keggin and Wells-Dawson anions). M can be molybdenum (Mo), tungsten (W),

vanadium (V), niobium (Nb) and tantalum (Ta); X in heteropolyanions can be Si(V), P(IV), As(III), Ge(IV).¹⁹

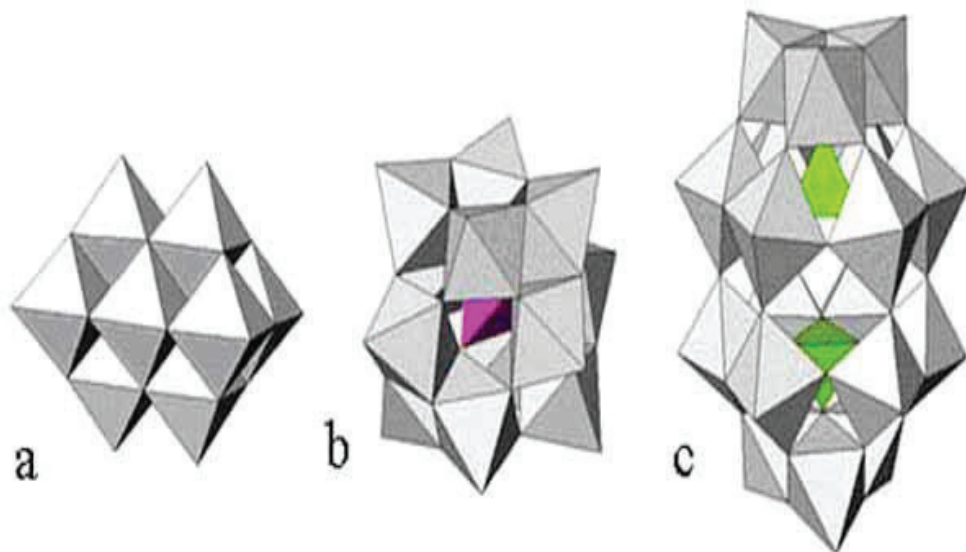


Figure 3.2. Polyhedral representations of (a) decavanadate ($V_{10}O_{28}$)⁶⁻ and (b) Keggin ($PMo_{12}O_{40}$)³⁻ (c) Wells-Dawson anions ($P_2W_{18}O_{62}$)⁶⁻. (Source: Casan-Pastor et al.²⁰)

In the structures of heteropolyanions, XO_4 is the center of the molecule and surrounded by MO_6 octahedrons where M_3O_{13} is connected by sharing edges and to the XO_4 center by sharing corners. Keggin structure $[XM_{12}O_{40}]^{x-8}$ and the Wells-Dawson $[X_2M_{18}O_{62}]^{2x-16}$ structure shown in Figure 3.3 and Figure 3.4 are the most common types of the studied structures.²¹

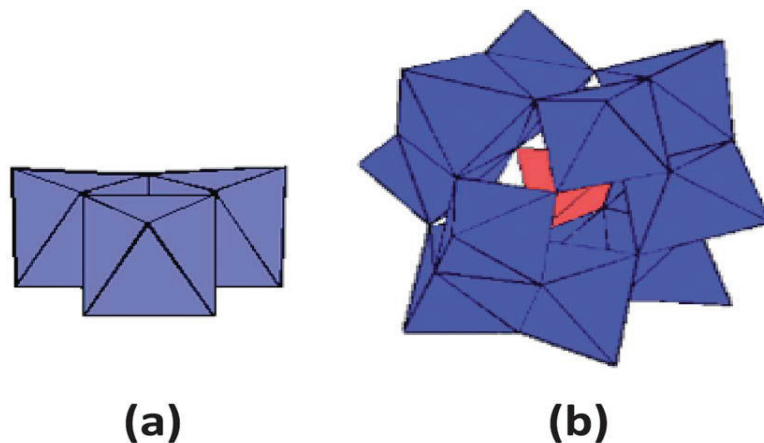


Figure 3.3. (a) Combination of three octahedra to form a trimetallic group M_3O_1
(b) Structure of the Keggin type POM. (Source: Ammam¹⁹)

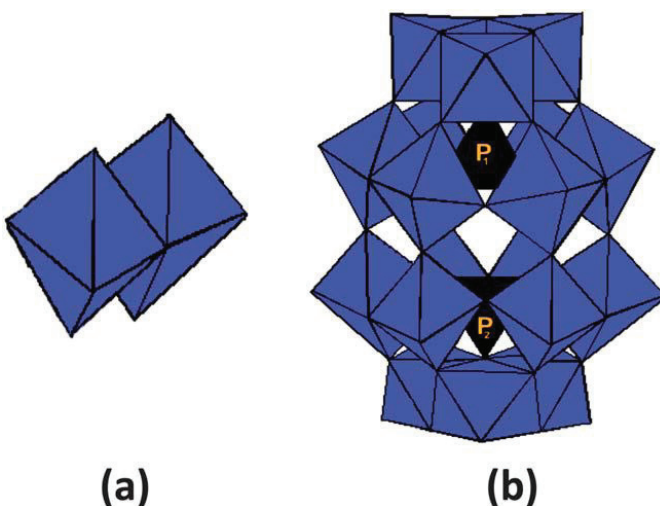


Figure 3.4. (a) Combination of two octahedra to form a dimetallic group M_2O_{10} .
 (b) Structure of the Dawson type POM. (Source: Ammam¹⁹)

3.2. Catalysis of Polyoxometalates

In the previous years, the harmful effects of chemical substances on environment has been a subject of the world. So that, preservation and protection of the environment for future generations has been encouraged and green chemistry is one of the important topic for this effort. In other words, green chemistry includes the chemical products and processes that minimise the use of destructive materials. One of the solutions of green chemistry is the application of solid acid catalysts. These substances can be used in many industries rather than corrosive liquid acids.

Various types of materials have been used as solid acid catalysts. For example; clays, zeolites, sulfated metal oxides and polyoxometalates (POMs). Each of these materials has unique properties which can have an effect upon the catalytic activity. Among these solid acids, polyoxometalates show a class of structurally well-defined clusters with a huge variety in size, metal-oxygen framework topology, composition and function.

Because of their high acid strength and thermal stability, POMs have been commonly used as catalysts for both homogeneous and heterogeneous reactions such as esterification, etherification, epoxidation, oxidation, hydrolysis, Friedel-Crafts alkylation, hydration of olefin and polymerization of tetrahydrofuran.²² Also, the

catalytic usage of polyoxometalates has been a favorite topic because the acidic and redox properties of polyoxometalates can be controlled at atomic or molecular levels.²³

Occasionally, catalyst systems have disadvantages, for example, there can be some difficulties with catalyst recovery from the reaction mixture and reuse. In order to prevent these problems, heterogeneous catalysts containing various transition metals such as Ti, Mn, W, V, Co has been largely studied.²⁴

In the world, energy independence and security come before many subjects for lots of countries. It must be known that, the common sources of energy are restricted and they are not renewable. For the humankind, it is important to find new energy sources that are renewable and eco-friendly.²⁵

Starch is one of the basic ingredient of various biomass and one of the important renewable sources in the nature. It is found in many agricultural foods like potatoes, corn, rice, wheat and pasta. It consists of amylose (20-25 %, 1,4- α -linked glucosyl units in linear form, water insoluble), and amylopectin (75-80 %, 1,6- α -linked branched, water soluble) which are illustrated in Figure 3.5.

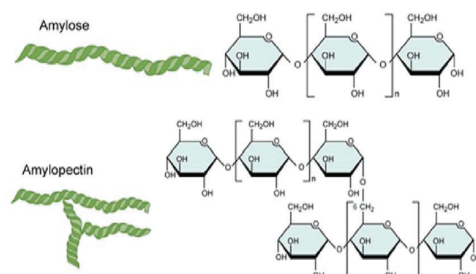


Figure 3.5. Amylose and amylopectin bonds of starch.
(Source: Sanyang et al.²⁶)

The methods which include enzymatic and acidic hydrolysis have been used widely for producing glucose from starch. The industry generally prefer the enzymatic method rather than the acidic one because it is environmentally friendly and having high yields under mild conditions although it is an expensive method.²⁷ In the literature, there are different studies which are alternative to enzymatic method. Euis Hermati et al. reported the production of glucose from starch by using microwave irradiation and activated carbon for 5 min at 200-220 °C but they could not eliminate the byproducts completely.²⁸ Orozco et al. reported the hydrolysis of starch using hot compressed water includes high pressure CO₂ for producing glucose in order to used in biohydrogen

production. However, hydroxy methyl furfural (HMF) was observed as a byproduct and it was eliminated by using activated carbon.²⁹ Yamaguchi et al., used carbon based solid catalyst involving acidic -COOH, phenolic OH and SO₃H functional groups.³⁰

In this thesis, as an alternative way for the starch hydrolysis techniques obtained in the literature, catalytic activity of the synthesized polyoxometalates was studied as an acidic hydrolysis by using hydrothermal method.

3.3. Synthesis and Characterization of Polyoxometalates

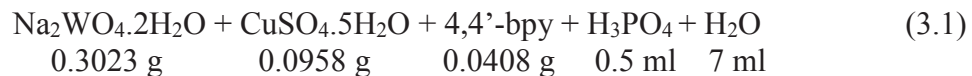
In this study, the synthesis and characterization of three novel crystals were done. The crystals were synthesized by hydrothermal reaction and characterized by SEM-EDX, powder X-ray diffraction analysis, single crystal X-ray diffraction analysis and thermogravimetric analysis methods.

3.3.1. Synthesis and Characterization of (4,4'-bpyH₂)₃[PCuW₁₁O₃₉]

(4,4'-bpyH₂)₃[PCuW₁₁O₃₉] yellow crystals were synthesized by hydrothermal reaction of Na₂WO₄.2H₂O (0.3023 g), CuSO₄.5H₂O (0.0958 g), 4,4'-bipyridine (0.0408 g), 5M H₃PO₄ (0.5 ml) and H₂O (7.0 ml) at 170°C for 3 days in a 23 ml Teflon-lined autoclave. Na₂WO₄.2H₂O (Sigma-Aldrich, 99%), CuSO₄.5H₂O (Merck, 99%), 4,4'-bipyridine (Merck, 98%), 5M H₃PO₄ (Sigma-Aldrich, 85%) were used without needing any purification.

After all reactants were added into the teflon vessel, the mixture was stirred for 5 minutes under laboratory conditions. Then, teflon vessel was placed into the steel autoclave and heated at 170°C for 3 days in oven. When the reaction finished, the autoclave was slowly cooled to the room temperature. The product was filtered by using vacuum filtration and washed a few times with pure water. The yellow crystals were observed on filter paper by optical microscope. Crystals were characterized by SEM-EDX, powder X-ray diffraction, single crystal X-ray diffraction and thermogravimetric analysis methods.

As it is seen from the SEM/EDX results of the yellow crystals indicated in Figure 3.6, the compound includes Cu, W, O, P, C, N elements in the weight percentages 1.23%, 42.24%, 27.05%, 1.08%, 23.79% and 4.61% respectively.



↓
170 °C 3 days

yellow crystals

The synthesized compound was analyzed by powder X-ray diffraction method. The powder peaks of the compound included in Figure 3.7 did not match well with any compound in the XRD database.

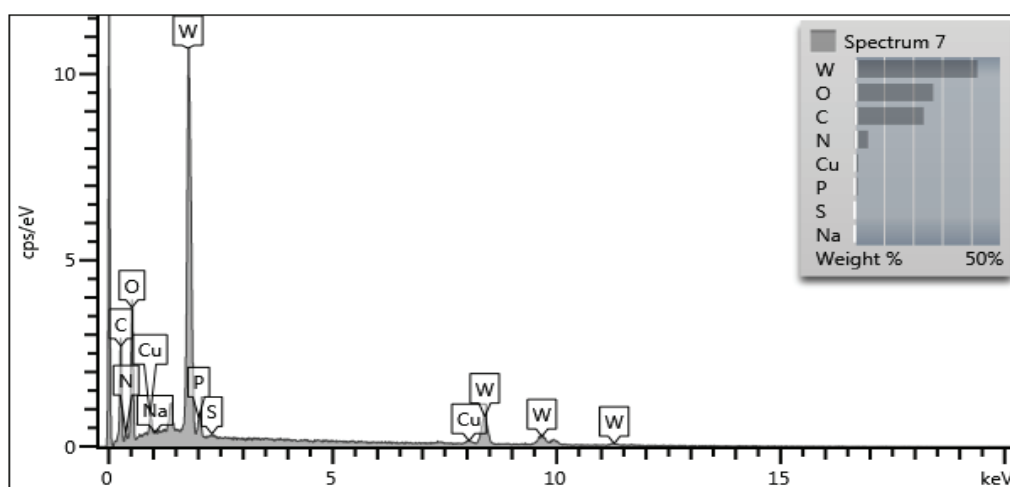


Figure 3.6. SEM/EDX spectrum of $(4,4'\text{-bpyH}_2)_3[\text{PCuW}_{11}\text{O}_{39}]$.

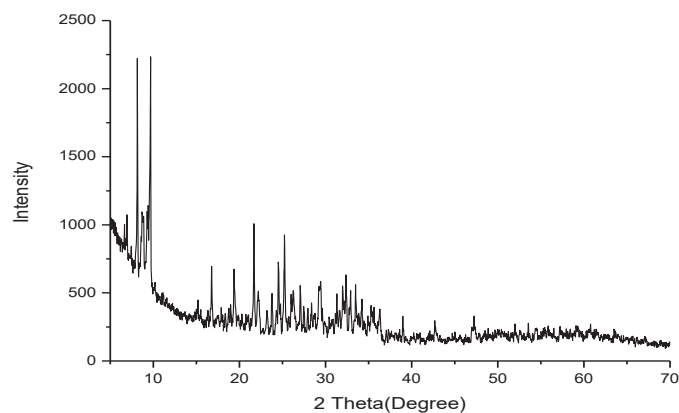


Figure 3.7. XRD spectrum of $(4,4'\text{-bpyH}_2)_3[\text{PCuW}_{11}\text{O}_{39}]$.

The change in the weight of $(4,4'\text{-bpyH}_2)_3[\text{PCuW}_{11}\text{O}_{39}]$ was measured as a function of temperature and the presence of the organic groups was determined. The thermogravimetric analysis of the compound whose graph is shown in Figure 3.8 was performed between 30 and 1000°C in nitrogen atmosphere. The first weight loss of 1.0% occurs between 100 and 700°C, and is assigned to the removal of impurities and the surface water. The second continuous weight loss of approximately 15.0% (calcd. 14.7%), occurs in the temperature range 700–1000°C and corresponds to the release of three 4,4'-bipyridine molecules.

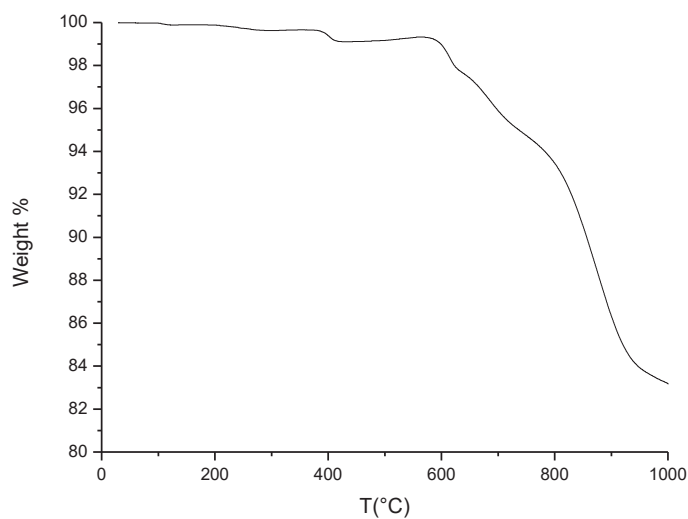


Figure 3.8. TGA graph of $(4,4'\text{-bpyH}_2)_3[\text{PCuW}_{11}\text{O}_{39}]$.

3.3.1.1. X-ray Crystallographic Analysis of $(4,4'\text{-bpyH}_2)_3[\text{PCuW}_{11}\text{O}_{39}]$

Single crystal X-ray diffraction of the resulting crystals was applied by using a Rigaku AFC8S diffractometer equipped with Mo K α ($\lambda=0.71073\text{ \AA}$) radiation and a Mercury CCD area detector. Data collection and processing involving corrections for absorption and Lorentz and polarization effects were applied by using the CrystalClear software package (Version 1.3. Rigaku Corporation, Japan and MSC, The Woodlands, Texas, USA). Candidate space groups were established due to the systematic absences of the data. The structures were solved by direct methods and refined by full-matrix least squares on F2 using the SHELXTL software package. All atoms were refined anisotropically in the structures.

Crystallographic data are given in Table 3.1. Selected bond lengths (Å) and bond angles (degree) for $(4,4'\text{-bpyH}_2)_3[\text{PCuW}_{11}\text{O}_{39}]$ are given in Table 3.2 and Table 3.3 respectively. The complete tables are shown in Appendix A and Appendix B.

Table 3.1. Crystallographic data for $(4,4'\text{-bpyH}_2)_3[\text{PCuW}_{11}\text{O}_{39}]$.

	(1)
Empirical Formula	$\text{C}_{30}\text{H}_{30}\text{CuN}_6\text{O}_{39}\text{PW}_{11}$
Formula weight	2731.21
Space group	P2(1)/n
a, Å	13.519(3)
b, Å	26.824(5)
c, Å	15.199(3)
α , °	90.00
β , °	99.47(3)
γ , °	90.00
V, Å ³	5436.4(19)
Z	4
D _{calc} , Mg/m ³	3.337
Parameters	793
μ , mm ⁻¹	21.562
θ range, °	2.65-25.98
Reflections	
Collected	48701
Independent	10579
Observed [$I \geq 2\sigma(I)$]	9590
R (int)	0.0655
Final R (obs. data) ^a	
R ₁	0.0854
wR ₂	0.1144
Final R (all data)	
R ₁	0.0929
wR ₂	0.1156
Goodness of fit on F ²	2.479
Largest diff. peak, e/Å ³	5.178
Largest diff. hole, e/Å ³	-3.312

Table 3.2. Selected bond lengths (\AA) for $(4,4'\text{-bpyH}_2)_3[\text{PCuW}_{11}\text{O}_{39}]$.

W(1) – O(34)	1.711(16)	W(8) – O(45)	1.868(17)
W(1) – O(1)	1.910(17)	W(9) – O(5)	1.975(17)
W(2) – O(32)	1.711(15)	W(9) – O(37)	1.688(14)
W(2) – O(4)	1.896(16)	W(9) – O(46)	1.905(16)
W(3) – O(7)	1.713(15)	W(10) – O(30)	1.711(16)
W(3) – O(8)	1.885(16)	W(10) – O(21)	1.878(18)
W(4) – O(31)	1.712(16)	W(11) – O(27)	1.881(19)
W(4) – O(11)	1.865(16)	W(11) – O(47)	1.920(16)
W(5) – O(19)	1.708(16)	W(12) – O(22)	1.883(17)
W(5) – O(14)	1.858(16)	W(12) – O(45)	1.893(16)
W(6) – O(33)	1.710(16)	P(1) – O(40)	1.539(15)
W(6) – O(47)	1.833(17)	P(1) – O(39)	1.563(13)
W(7) – O(35)	1.720(17)	P(1) – O(28)	1.583(15)
W(7) – O(24)	1.903(18)	P(1) – O(15)	1.608(16)
W(8) – O(36)	1.691(14)	Cu(12) – O(27)	1.932(18)

 Table 3.3. Selected bond angles ($^\circ$) for $(4,4'\text{-bpyH}_2)_3[\text{PCuW}_{11}\text{O}_{39}]$.

O(34) – W(1) – O(1)	103.5(8)	W(9) – O(40) – W(11)	88.3(4)
O(34) – W(1) – O(29)	102.6(8)	W(7) – O(40) – W(11)	88.6(5)
O(32) – W(2) – O(13)	101.0(8)	O(40) – P(1) – O(28)	109.6(9)
O(32) – W(2) – O(4)	99.9(8)	O(39) – P(1) – O(28)	110.4(8)
O(7) – W(3) – O(8)	101.7(8)	W(10) – O(26) – W(8)	125.7(8)
O(7) – W(3) – O(6)	101.5(8)	W(4) – O(11) – W(12)	123.4(8)
O(31) – W(4) – O(11)	100.7(8)	W(2) – O(28) – W(12)	90.3(5)
O(31) – W(4) – O(12)	104.7(7)	W(4) – O(28) – W(12)	88.7(5)
O(19) – W(5) – O(14)	105.2(8)	W(3) – O(6) – W(1)	126.2(9)
O(19) – W(5) – O(16)	104.2(8)	W(12) – O(22) – W(7)	145.5(11)
O(33) – W(6) – O(47)	102.4(8)	W(4) – O(12) – W(10)	153.3(8)
O(33) – W(6) – O(43)	100.6(8)	W(10) – O(21) – W(6)	128.0(9)
O(35) – W(7) – O(24)	99.8(8)	W(8) – O(39) – W(10)	89.9(4)
O(35) – W(7) – O(23)	103.0(7)	W(6) – O(39) – W(10)	89.3(5)
O(36) – W(8) – O(45)	102.9(7)	W(1) – O(2) – W(4)	151.7(10)
O(36) – W(8) – O(23)	102.9(8)	W(1) – O(5) – W(9)	151.7(10)
O(25) – W(9) – O(46)	91.7(7)	P(1) – O(28) – W(2)	126.2(8)
O(37) – W(9) – O(8)	101.6(7)	P(1) – O(28) – W(4)	127.6(9)
O(30) – W(10) – O(21)	102.4(9)	P(1) – O(40) – W(9)	128.5(9)
O(30) – W(10) – O(1)	103.2(9)	P(1) – O(40) – W(7)	125.8(7)
O(27) – W(11) – O(47)	104.6(8)	P(1) – O(39) – W(8)	125.3(8)
O(27) – W(11) – O(24)	99.1(8)	P(1) – O(39) – W(6)	125.2(7)
O(22) – W(12) – O(45)	90.7(8)	P(1) – O(15) – W(5)	125.2(8)
O(22) – W(12) – O(27)	99.8(7)	P(1) – O(15) – W(3)	124.1(9)
O(45) – W(12) – O(27)	99.9(8)	P(1) – O(40) – W(11)	123.0(9)

3.3.1.2. Results and Discussion for $(4,4'\text{-bpyH}_2)_3[\text{PCuW}_{11}\text{O}_{39}]$

The crystal $(4,4'\text{-bpyH}_2)_3[\text{PCuW}_{11}\text{O}_{39}]$ was synthesized by hydrothermal method from the reaction of $\text{Na}_2\text{WO}_4\cdot 2\text{H}_2\text{O}$, $\text{CuSO}_4\cdot 5\text{H}_2\text{O}$, 4,4'-bipyridine and H_3PO_4 .

As a result of single crystal X-ray diffraction, it is determined that the structure contains $[\text{PCuW}_{11}\text{O}_{39}]^{5-}$ Keggin polyanion clusters, 4,4'-bipyridine ligands and water molecules. Keggin polyanion cluster includes 12 edge-and-corner sharing WO_6 octahedra and there is a PO_4 tetrahedra at the center that is shown in Figure 3.9. $[\text{PCuW}_{11}\text{O}_{39}]^{5-}$ polyanion cluster shares its one oxygen with another $[\text{PCuW}_{11}\text{O}_{39}]^{5-}$ polyanion cluster and forms the chain structure that is illustrated in Figure 3.10. The chain structures and water molecules have C-H...O hydrogen bond interactions between each other.

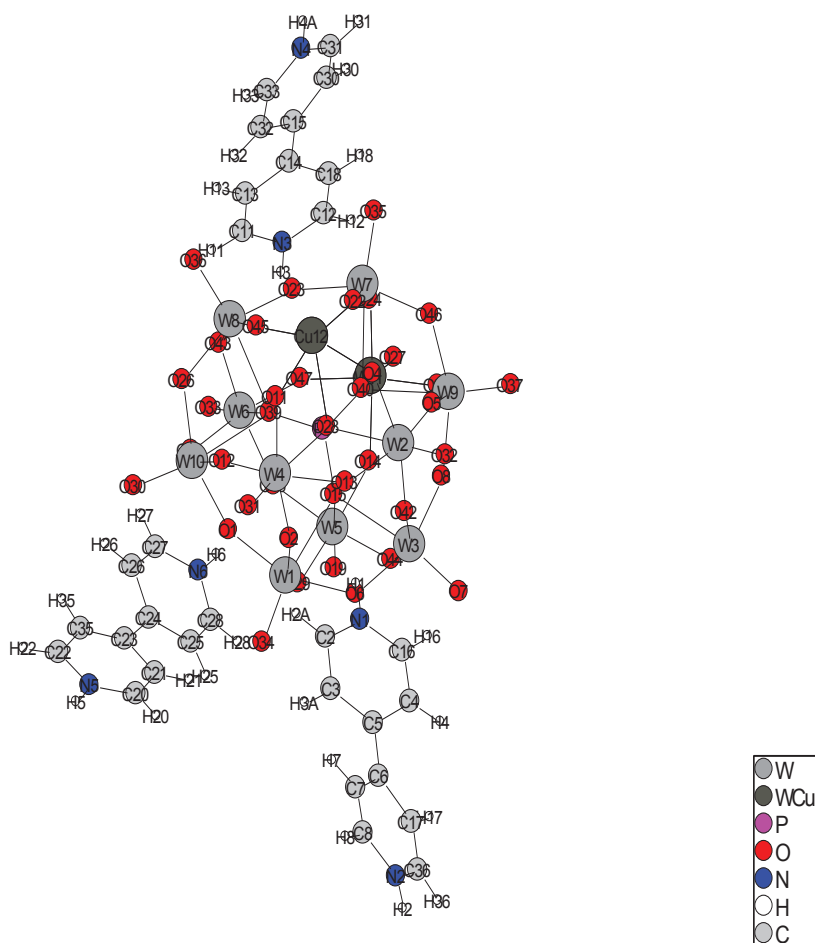


Figure 3.9. The view of $[\text{PCuW}_{11}\text{O}_{39}]^{5-}$ Keggin polyanion cluster.

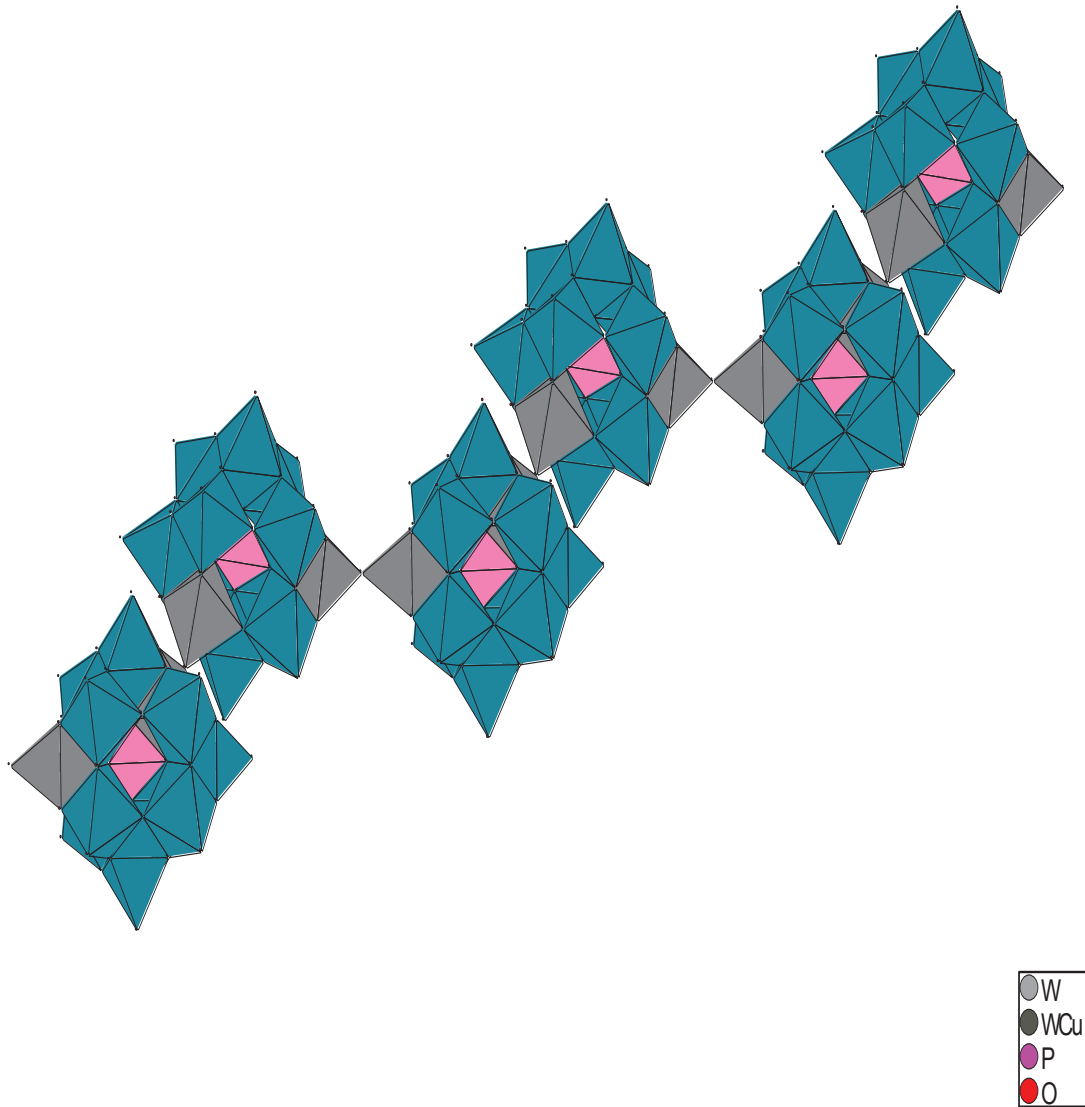


Figure 3.10. The chain structure of $[PCuW_{11}O_{39}]^{5-}$ Keggin polyanions.

In the unitcell that is indicated in Figure 3.11 , there are four polyanion clusters and 4,4'-bipyridine ligands between these clusters. WO_6 octahedral structures include three different W-O bonds. These are; W-Ot (terminal) bonds whose distances range from 1.688(23) to 1.721(16) Å which indicates a W=O multiple bond, W-Ob (bridging) bonds whose distances range from 1.904(16) to 1.997(33) Å and W-Oc (central) bonds range from 2.365(29) to 2.457(15) Å respectively. Besides, the distances of P-O bond distances are between 1.539(15) and 1.608(16) Å.

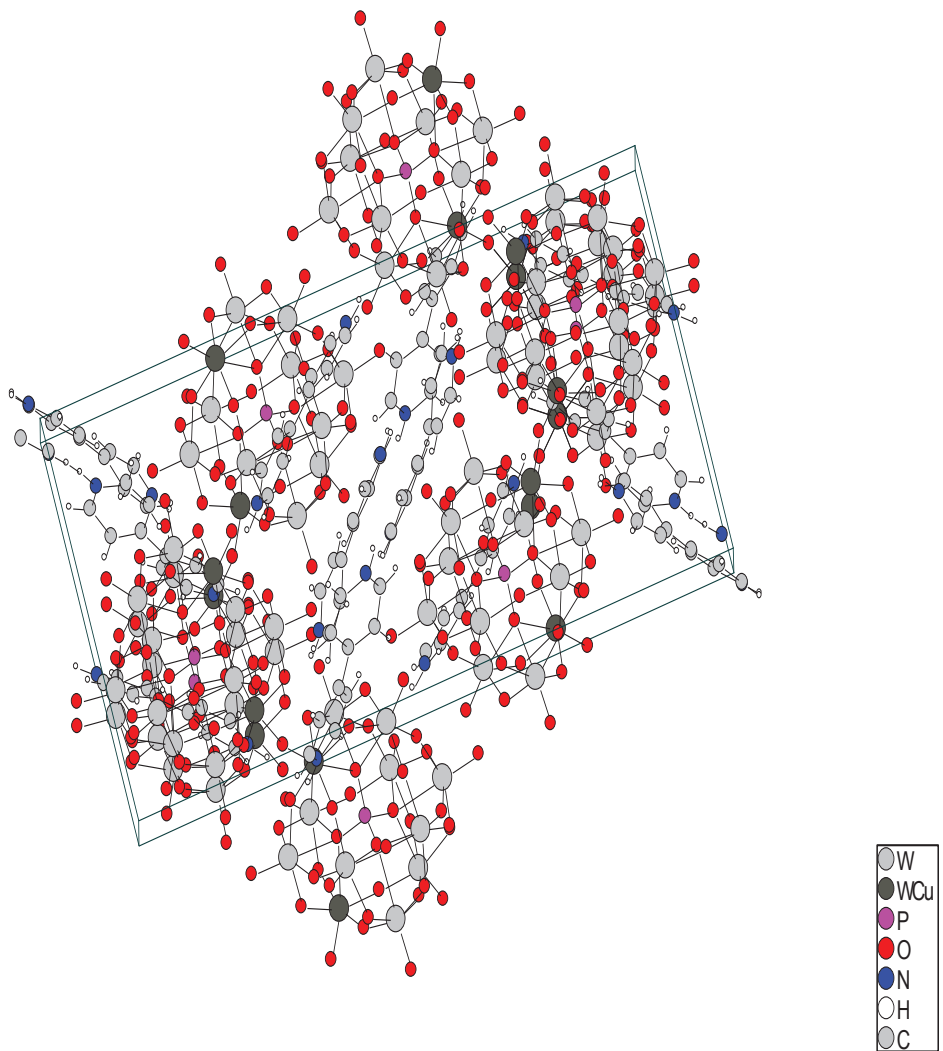


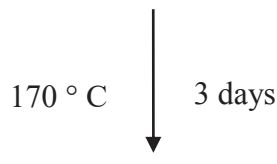
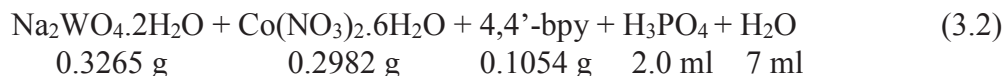
Figure 3.11. The unitcell view of $(4,4'\text{-bpyH}_2)_3[\text{PCuW}_{11}\text{O}_{39}]$.

The bond valence sums of $(4,4'\text{-bpyH}_2)_3[\text{PCuW}_{11}\text{O}_{39}]$ were calculated by Bond Valence Sum, BVS method developed by ID Brown. The results of these calculations show that, the oxidation states of W, P, O and Cu atoms of the structure are 6+, 5+, 2- and 1+ respectively. Only the valence sums of W(11) and W(12) are 5.275 and 5.367 alternately and these atoms share the same position with Cu(11) and Cu(12). These cobalt atoms are in the same crystallographic position with 50% occupancy factor. The compound needs 5+ valence cations and they are provided by 4,4'-bipyridine ligands. These ligands change into $4,4'\text{-bpyH}_2^{2+}$ cation easily in acidic medium. It is thought that, the organic part of the synthesized material includes bipyridinium cation and bipyridinium radical cation. Bond valence sums table of $(4,4'\text{-bpyH}_2)_3[\text{PCuW}_{11}\text{O}_{39}]$ is shown in Appendix G.

3.3.2. Synthesis and Characterization of (4,4'-bpyH₂) [H₂PW₁₂O₄₀]₂.H₂O

(4,4'-bpyH₂)₂[H₂PW₁₂O₄₀]₂.H₂O colorless crystals were synthesized by hydrothermal reaction of Na₂WO₄.2H₂O (0.3265 g), Co(NO₃)₂.6H₂O (0.2982 g), 4,4'-bipyridine (0.1054 g), 5M H₃PO₄ (2.0 ml) and H₂O (7.0 ml) at 170°C for 3 days in a 23 ml Teflon-lined autoclave. Na₂WO₄.2H₂O (Sigma-Aldrich, 99%), Co(NO₃)₂.6H₂O (Merck, 99%), 4,4'-bipyridine (Merck, 98%), 5M H₃PO₄ (Sigma-Aldrich, 85%) were used without needing any purification.

After all reactants were added into the teflon vessel, the mixture was stirred for 10 minutes under laboratory conditions. Then, teflon vessel was placed into the steel autoclave and heated at 170°C for 3 days in oven. When the reaction finished, the autoclave was slowly cooled to the room temperature. The product was filtered by using vacuum filtration and washed a few times with pure water. The colorless crystals were observed on filter paper by optical microscope. Crystals were characterized by SEM-EDX, powder X-ray diffraction, single crystal X-ray diffraction and thermogravimetric analysis methods.



As it is seen from the SEM/EDX results of the yellow crystals indicated in Figure 3.12, the compound includes W, O, P, C, N elements in the weight percentages 51.34%, 27.95%, 0.88%, 17.79% and 1.73% respectively.

The synthesized compound was analyzed by powder X-ray diffraction method. The powder peaks of the compound included in Figure 3.13 did not match well with any compound in the XRD database.

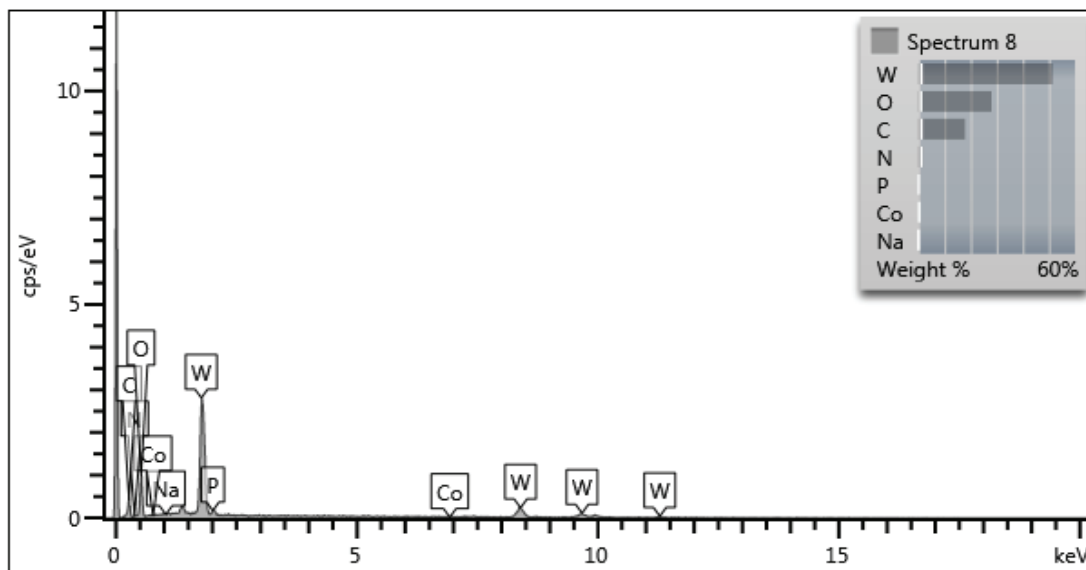


Figure 3.12. SEM/EDX spectrum of $(4,4'\text{-bpyH}_2)[\text{H}_2\text{PW}_{12}\text{O}_{40}]_2\text{H}_2\text{O}$.

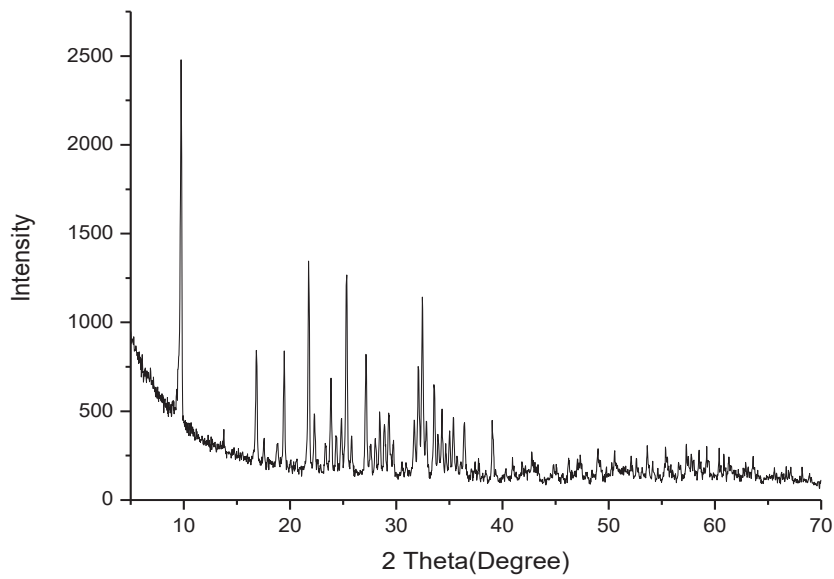


Figure 3.13. XRD spectrum of $(4,4'\text{-bpyH}_2)[\text{H}_2\text{PW}_{12}\text{O}_{40}]_2\text{H}_2\text{O}$.

The change in the weight of $(4,4'\text{-bpyH}_2)[\text{H}_2\text{PW}_{12}\text{O}_{40}]_2\text{H}_2\text{O}$ was measured as a function of temperature and the presence of the organic groups was determined. The thermogravimetric analysis of the crystal whose graph is shown in Figure 3.14 was performed between 30 and 1000°C in nitrogen atmosphere. The first weight loss of

1.0% occurs between 100 and 600 °C, and is assigned to the removal of impurities and surface water. The second continuous weight loss of approximately 3.0% (calcd. 2.66%), occurs in the temperature range 600–700 °C and corresponds to the release of 4,4'-bipyridine molecule. Lastly, the weight loss between 700–800 °C indicates the removal of impurities.

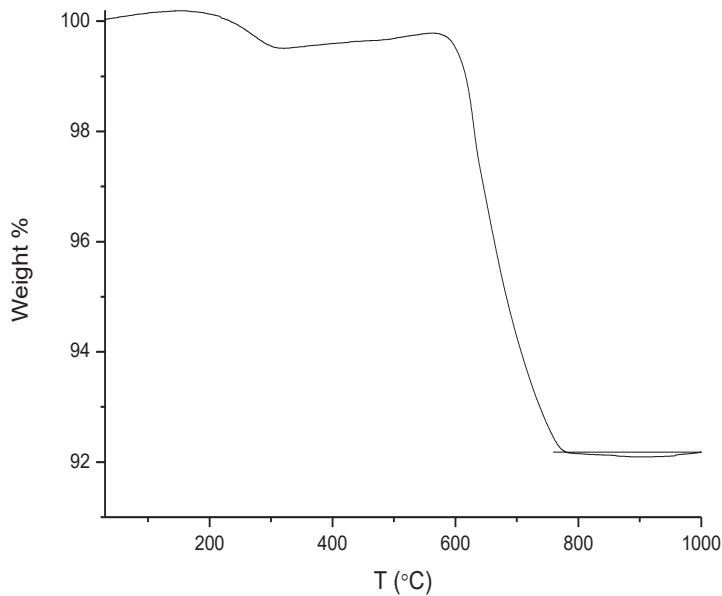


Figure 3.14. TGA graph of (4,4'-bpyH₂)[H₂PW₁₂O₄₀]₂.H₂O.

3.3.2.1. X-ray Crystallographic Analysis of (4,4'-bpyH₂)[H₂PW₁₂O₄₀]₂.H₂O

Single crystal X-ray diffraction of the resulting crystals was applied by using a Rigaku AFC8S diffractometer equipped with Mo K α ($\lambda=0.71073$ Å) radiation and a Mercury CCD area detector. Data collection and processing involving corrections for absorption and Lorentz and polarization effects were applied by using the CrystalClear software package (Version 1.3. Rigaku Corporation, Japan and MSC, The Woodlands, Texas, USA). Candidate space groups were established due to the systematic absences of the data. The structures were solved by direct methods and refined by full-matrix least squares on F₂ using the SHELXTL software package. All atoms were refined anisotropically in the structures.

Crystallographic data are given in Table 3.4. Selected bond lengths (Å) and bond angles (degree) for (4,4'-bpyH₂)[H₂PW₁₂O₄₀]₂.H₂O are given in Table 3.5 and Table 3.6 respectively. The complete tables are shown in Appendix C and Appendix D.

Table 3.4. Crystallographic data for (4,4'-bpyH₂)[H₂PW₁₂O₄₀]₂.H₂O.

(1)	
Empirical Formula	P ₂ W ₂₄ O ₈₀ C ₁₀ H ₈ N ₂
Formula weight	3011.35
Space group	Ia-3
a, Å	25.936(3)
b, Å	25.936(3)
c, Å	25.936(3)
α, °	90.00
β, °	90.00
γ, °	90.00
V, Å ³	17446(3)
Z	12
D _{calc} , Mg/m ³	3.440
Parameters	234
μ, mm ⁻¹	23.734
θ range, °	1.92-25.23
Reflections	
Collected	73659
Independent	2637
Observed [I≥2σ(I)]	2513
R (int)	0.1000
Final R (obs. data) ^a	
R ₁	0.0560
wR ₂	0.1366
Final R (all data)	
R ₁	0.0592
wR ₂	0.1388
Goodness of fit on F ²	1.196
Largest diff. peak, e/Å ³	1.901
Largest diff. hole, e/Å ³	-2.178

Table 3.5. Selected bond lengths (\AA) for $(4,4'\text{-bpyH}_2)[\text{H}_2\text{PW}_{12}\text{O}_{40}]_2\text{.H}_2\text{O}$.

W(1) – O(2)	1.647(13)	W(3) – O(7)	1.859(19)
W(1) – O(10)	1.844(18)	W(3) – O(1)	1.929(16)
W(1) – O(1)	1.853(18)	W(3) – O(7)	1.956(18)
W(1) – O(3)	1.924(18)	W(3) – O(13)	2.450(2)
W(1) – O(10)	1.940(2)	W(3) – O(13)	2.490(2)
W(1) – O(14)	2.420(2)	W(4) – O(8)	1.647(14)
W(2) – O(12)	1.669(18)	W(4) – O(9)	1.850(2)
W(2) – O(5)	1.836(17)	W(4) – O(11)	1.894(19)
W(2) – O(4)	1.869 (19)	W(4) – O(9)	1.907(19)
W(2) – O(4)	1.921(18)	W(4) – O(5)	1.950(2)
W(2) – O(11)	1.900(17)	W(4) – O(16)	2.433(2)
W(2) – O(15)	2.430(2)	P(1) – O(13)	1.500(2)
W(2) – O(15)	2.480(2)	P(1) – O(14)	1.620(4)
W(3) – O(6)	1.676(15)	P(2) – O(15)	1.490(2)
W(3) – O(3)	1.856(16)	P(2) – O(16)	1.590(3)

Table 3.6. Selected bond angles ($^\circ$) for $(4,4'\text{-bpyH}_2)[\text{H}_2\text{PW}_{12}\text{O}_{40}]_2\text{.H}_2\text{O}$.

O(2) – W(1) – O(10)	103.4(11)	W(2) – O(5) – W(4)	140.5(11)
O(2) – W(1) – O(1)	101.7(9)	W(4) – O(11) – W(2)	140.6(11)
O(3) – W(1) – O(10)	82.6(9)	W(1) – O(10) – W(1)	140.0(15)
O(2) – W(1) – O(14)	158.8(10)	W(4) – O(16) – W(4)	93.4(9)
O(12) – W(2) – O(11)	100.7(11)	O(13) – P(1) – O(14)	72.5(8)
O(5) – W(2) – O(11)	155.1(10)	O(13) – P(1) – O(14)	107.5(8)
O(12) – W(2) – O(5)	104.1(11)	O(14) – P(1) – O(14)	180.0(4)
O(12) – W(2) – O(4)	102.1(11)	O(15) – P(2) – O(15)	66.4(6)
O(11) – W(2) – O(4)	85.2(9)	O(15) – P(2) – O(15)	113.6(6)
O(12) – W(2) – O(15)	160.0(11)	O(15) – P(2) – O(15)	180.0(2)
O(1) – W(3) – O(13)	64.1(8)	O(15) – P(2) – O(16)	75.1(8)
O(7) – W(3) – O(13)	93.2(8)	O(15) – P(2) – O(16)	104.9(8)
O(6) – W(3) – O(3)	102.2(10)	O(16) – P(2) – O(16)	180.0(2)
O(6) – W(3) – O(7)	101.4(10)	P(1) – O(13) – W(3)	126.8(12)
O(7) – W(3) – O(13)	64.7(8)	O(15) – P(2) – O(15)	180.0(2)
O(1) – W(3) – O(13)	64.1(8)	O(15) – P(2) – O(16)	75.1(8)
O(8) – W(4) – O(11)	100.7(9)	O(15) – P(2) – O(16)	104.9(8)
O(9) – W(4) – O(11)	88.5(10)	O(16) – P(2) – O(16)	180.0(2)
O(8) – W(4) – O(9)	105.0(11)	P(1) – O(13) – W(3)	126.8(12)
O(8) – W(4) – O(11)	100.7(9)	P(1) – O(13) – W(3)	124.6(12)
O(11) – W(4) – O(5)	86.9(8)	W(4) – O(16) – W(4)	93.4(9)
O(9) – W(4) – O(9)	89.1(11)	W(1) – O(10) – W(1)	140.0(15)
W(3) – O(3) – W(1)	140.6(11)	O(13) – P(1) – O(13)	111.4(8)
W(3) – O(7) – W(3)	138.1(13)	O(13) – P(1) – O(13)	68.6(8)
W(4) – O(9) – W(4)	141.3(14)	O(13) – P(1) – O(13)	180.0(19)

3.3.2.2. Results and Discussion for (4,4'-bpyH₂)[H₂PW₁₂O₄₀]₂.H₂O

The crystal (4,4'-bpyH₂)[H₂PW₁₂O₄₀]₂.H₂O was synthesized by hydrothermal method from the reaction of Na₂WO₄.2H₂O, Co(NO₃)₂.6H₂O, 4,4'-bipyridine and H₃PO₄.

As a result of single crystal X-ray diffraction, it is determined that the structure contains two [H₂PW₁₂O₄₀]⁻ Keggin polyanion clusters, 4,4'-bipyridine ligand and water molecules. Keggin polyanion cluster includes 12 edge-and-corner sharing WO₆ octahedra and there is a PO₄ tetrahedra at the center that is shown in Figure 3.15 and polyhedral structure is illustrated in Figure 3.16. The clusters and water molecules have C-H...O hydrogen bond interactions between each other.

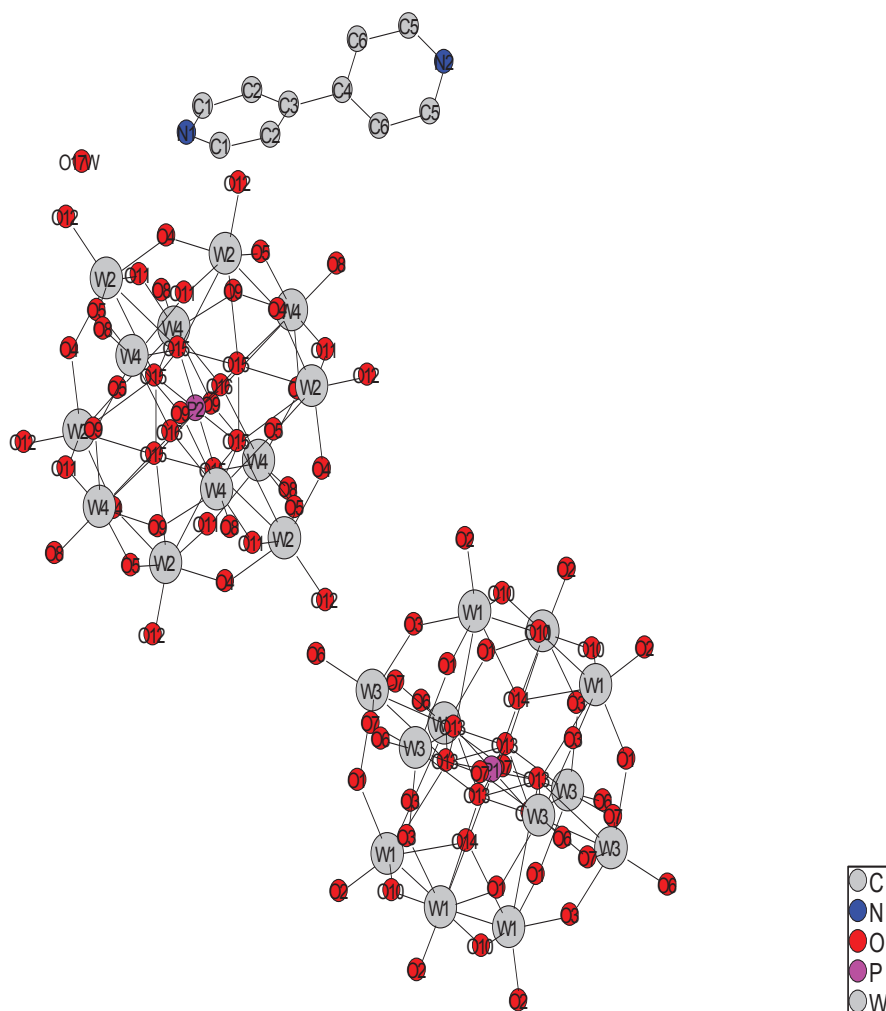


Figure 3.15. The view of Keggin polyanion cluster.

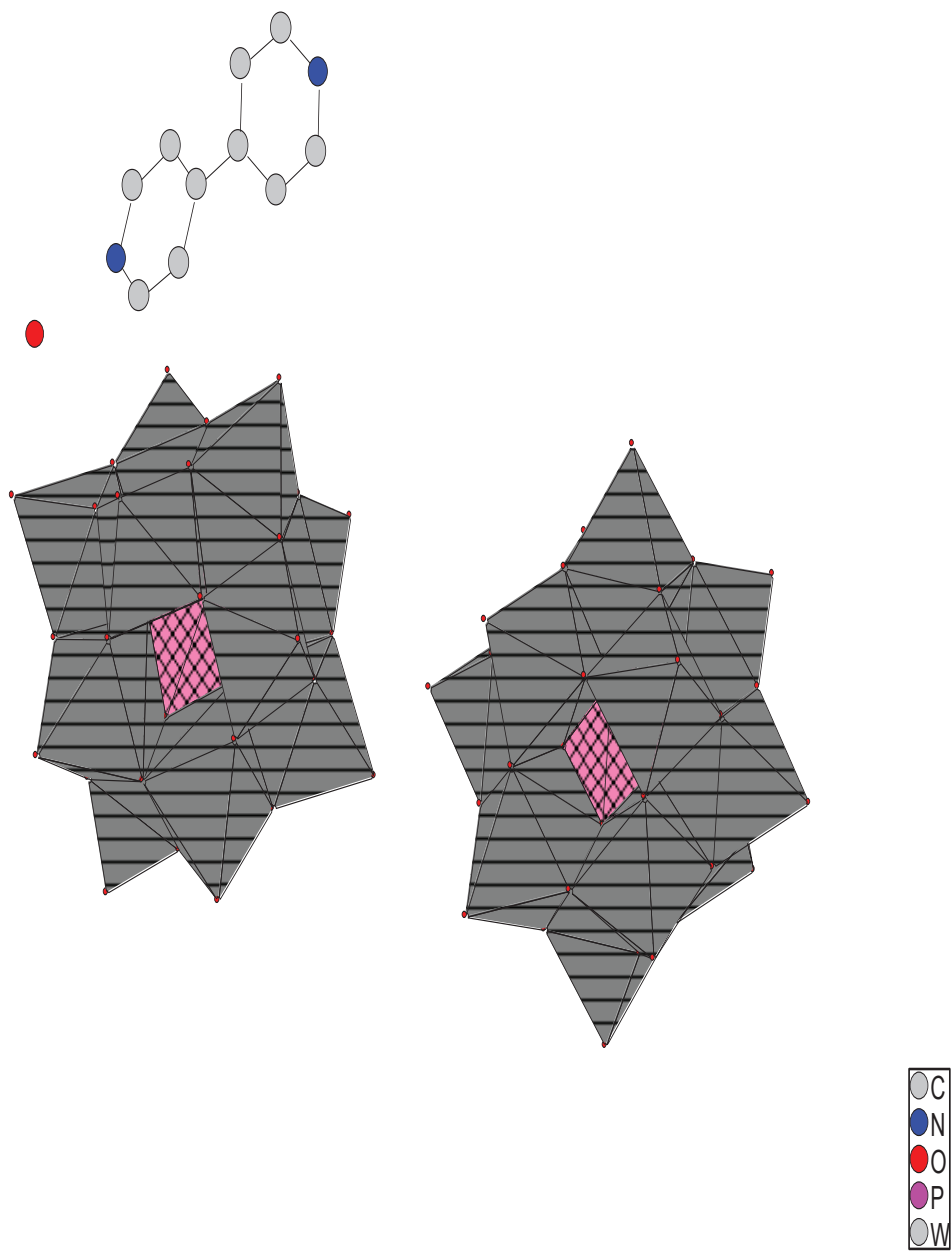


Figure 3.16. The polyhedral structure of Keggin polyanions.

In the unitcell that is indicated in Figure 3.17, there are twelve polyanion clusters and 4,4'-bipyridine ligands and water molecules between these clusters. WO_6 octahedral structures include three different W-O bonds. These are; W-O_t (terminal) bonds whose distances range from 1.647(13) to 1.676(15) Å which represents a W=O multiple bond, W-O_b (bridging) bonds whose distances range from 1.836(17) to 1.956(18) Å and W-O_c (central) bonds range from 2.420(2) to 2.490(2) Å respectively. Besides, the distances of P-O bond distances are between 1.50(2) and 1.62(4) Å.

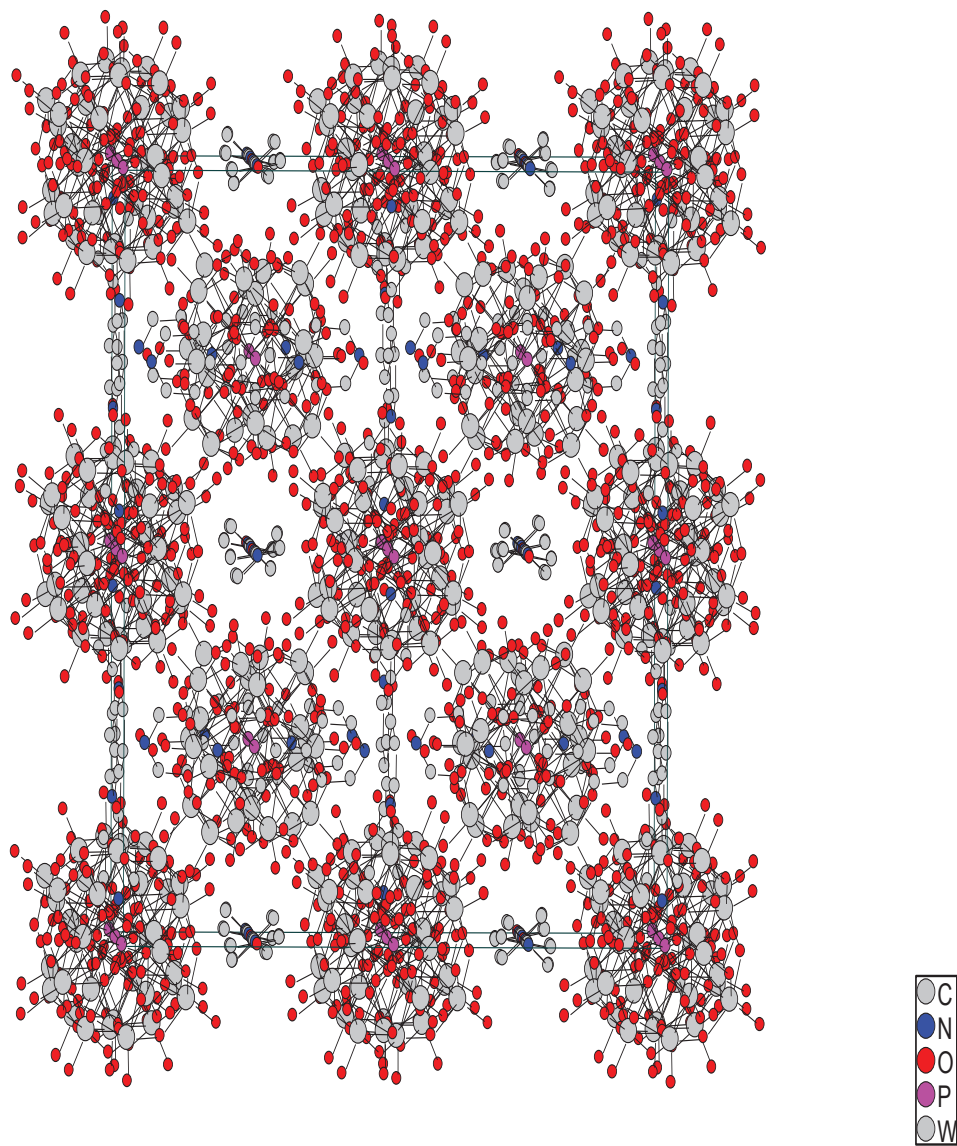


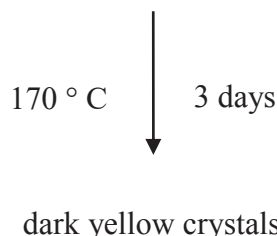
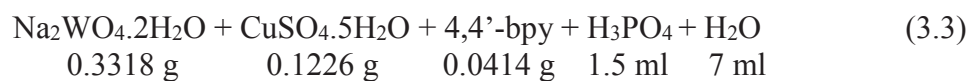
Figure 3.17. The unitcell view of $(4,4'\text{-bpyH}_2)[\text{H}_2\text{PW}_{12}\text{O}_{40}]_2\cdot\text{H}_2\text{O}$.

The bond valence sums of $(4,4'\text{-bpyH}_2)[\text{H}_2\text{PW}_{12}\text{O}_{40}]_2\cdot\text{H}_2\text{O}$ were calculated by Bond Valence Sum, BVS method developed by ID Brown. The results of these calculations show that, the oxidation states of W, P, O atoms of the structure are 6+, 5+, and 2- respectively. The compound needs 2+ valence cations and they are provided by 4,4'-bipyridine ligand. These ligand changes into $4,4'\text{-bpyH}_2^{2+}$ cation easily in acidic medium. It is thought that, the organic part of the synthesized material includes bipyridinium cation. Bond valence sums table of $(4,4'\text{-bpyH}_2)[\text{H}_2\text{PW}_{12}\text{O}_{40}]_2\cdot\text{H}_2\text{O}$ is shown in Appendix H.

3.3.3. Synthesis and Characterization of $(4,4'\text{-bpyH}_2)_4[\text{H}_2\text{P}_2\text{W}_{18}\text{O}_{62}]_2$

$(4,4'\text{-bpyH}_2)_4[\text{H}_2\text{P}_2\text{W}_{18}\text{O}_{62}]_2$ dark yellow rod-like crystals were synthesized by hydrothermal reaction of $\text{Na}_2\text{WO}_4\cdot 2\text{H}_2\text{O}$ (0.3318 g), $\text{CuSO}_4\cdot 5\text{H}_2\text{O}$ (0.1226 g), 4,4'-bipyridine (0.0414 g), 5M H_3PO_4 (1.5 ml) and H_2O (7.0 ml) at 170°C for 3 days in a 23 ml Teflon-lined autoclave. $\text{Na}_2\text{WO}_4\cdot 2\text{H}_2\text{O}$ (Sigma-Aldrich, 99%), $\text{CuSO}_4\cdot 5\text{H}_2\text{O}$ (Merck, 99%), 4,4'-bipyridine (Merck, 98%), 5M H_3PO_4 (Sigma-Aldrich, 85%) were used without needing any purification.

After all reactants were added into the teflon vessel, the mixture was stirred for 5 minutes under laboratory conditions. Then, teflon vessel was placed into the steel autoclave and heated at 170°C for 3 days in oven. When the reaction finished, the autoclave was slowly cooled to the room temperature. The product was filtered by using vacuum filtration and washed a few times with pure water. The dark yellow crystals were observed on filter paper by optical microscope. Crystals were characterized by SEM-EDX, powder X-ray diffraction, single crystal X-ray diffraction and thermogravimetric analysis methods.



As it is seen from the SEM/EDX results of the dark yellow crystals indicated in Figure 3.18, the compound includes W, O, P, C, N elements in the weight percentages 52.10%, 17.73%, 0.93%, 27.29% and 1.91% respectively.

The synthesized compound was analyzed by powder X-ray diffraction method. The powder peaks of the compound included in Figure 3.19 did not match well with any compound in the XRD database.

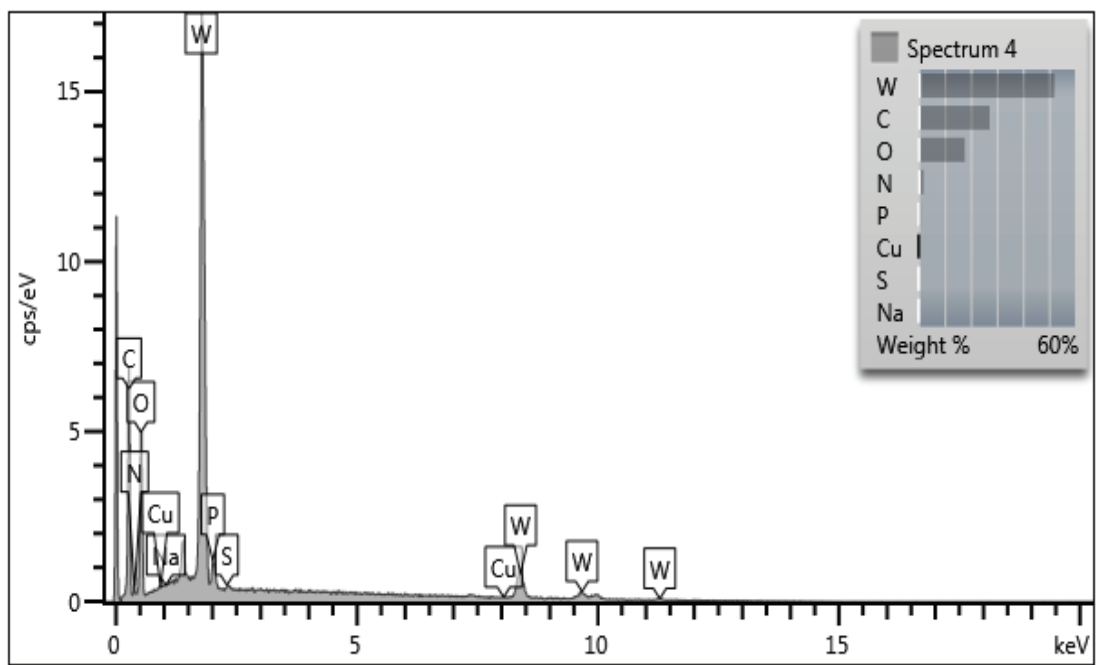


Figure 3.18. SEM/EDX spectrum of $(4,4'\text{-bpyH}_2)_4[\text{H}_2\text{P}_2\text{W}_{18}\text{O}_{62}]_2$.

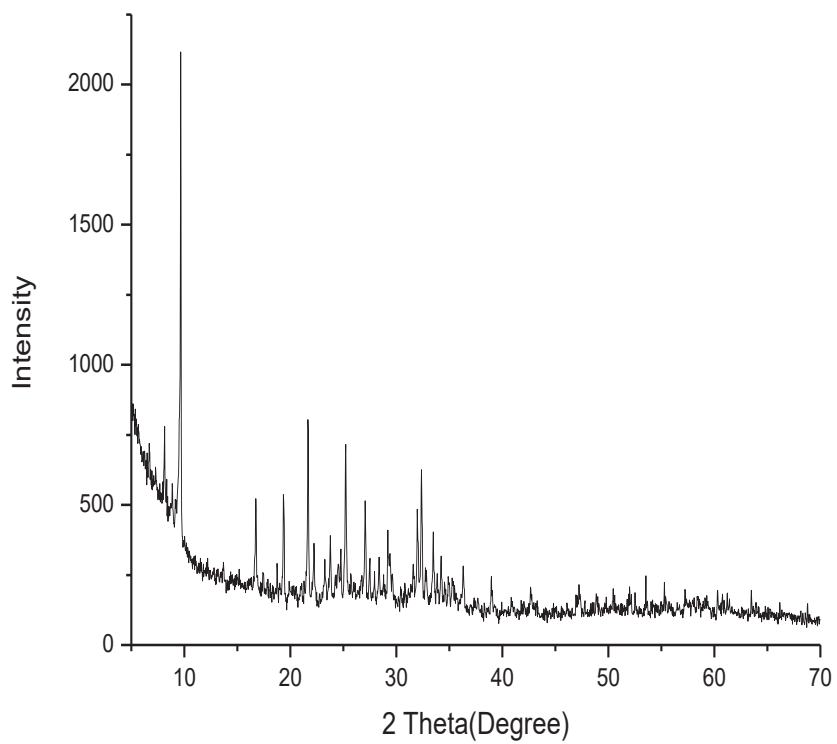


Figure 3.19. XRD spectrum of $(4,4'\text{-bpyH}_2)_4[\text{H}_2\text{P}_2\text{W}_{18}\text{O}_{62}]_2$.

The change in the weight of $(4,4'\text{-bpyH}_2)_4[\text{H}_2\text{P}_2\text{W}_{18}\text{O}_{62}]_2$ was measured as a function of temperature and the presence of the organic groups was determined. The thermogravimetric analysis of the crystal whose graph is shown in Figure 3.20 was performed between 30 and 1000°C in nitrogen atmosphere. The first weight loss of 1.0% occurs between 100 and 700°C, and is assigned to the removal of impurities. The second continuous weight loss of approximately 7.0% (calcd. 6.75%), occurs in the temperature range 700–900°C and corresponds to the release of three 4,4'bipyridine molecules. Lastly, the weight loss between 900–1000°C indicates the removal of impurities.

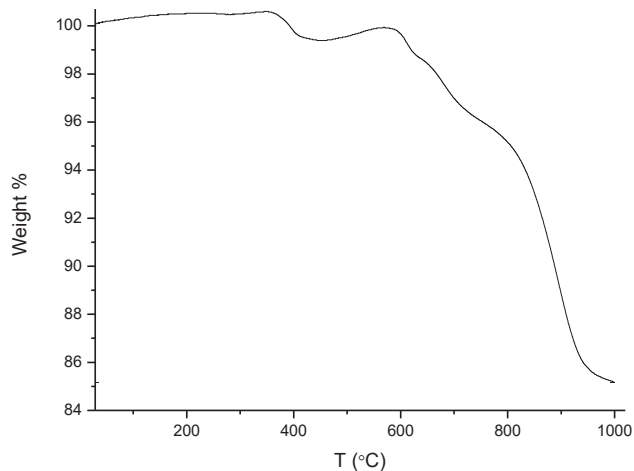


Figure 3.20. TGA graph of $(4,4'\text{-bpyH}_2)_4[\text{H}_2\text{P}_2\text{W}_{18}\text{O}_{62}]_2$.

3.3.3.1. X-ray Crystallographic Analysis of $(4,4'\text{-bpyH}_2)_4[\text{H}_2\text{P}_2\text{W}_{18}\text{O}_{62}]_2$

Single crystal X-ray diffraction of the resulting crystals was applied by using a Rigaku AFC8S diffractometer equipped with Mo K α ($\lambda=0.71073$ Å) radiation and a Mercury CCD area detector. Data collection and processing involving corrections for absorption and Lorentz and polarization effects were applied by using the CrystalClear software package (Version 1.3. Rigaku Corporation, Japan and MSC, The Woodlands, Texas, USA).

Candidate space groups were established due to the systematic absences of the data. The structures were solved by direct methods and refined by full-matrix least

squares on F² using the SHELXTL software package. All atoms were refined anisotropically in the structures.

Crystallographic data are given in Table 3.7. Selected bond lengths (Å) and bond angles (degree) for (4,4'-bpyH₂)₄[H₂P₂W₁₈O₆₂]₂ are given in Table 3.8 and Table 3.9 respectively. The complete tables are shown in Appendix E and Appendix F.

Table 3.7. Crystallographic data for (4,4'-bpyH₂)₄[H₂P₂W₁₈O₆₂]₂.

(1)	
Empirical Formula	P ₄ W ₃₆ O ₁₂₄ C ₄₀ H ₄₄ N ₈
Formula weight	4375.09
Space group	P-1
a, Å	13.519(3)
b, Å	22.400(5)
c, Å	27.374(6)
α, °	79.83(3)
β, °	77.44(3)
γ, °	80.21(3)
V, Å ³	7889(3)
Z	4
D _{calc} , Mg/m ³	3.683
Parameters	901
μ, mm ⁻¹	25.064
θ range, °	1.9681-26.69
Reflections	
Collected	74178
Independent	32579
Observed [I≥2σ(I)]	23195
R (int)	0.0831
Final R (obs. data) ^a	
R ₁	0.1127
wR ₂	0.3037
Final R (all data)	
R ₁	0.1408
wR ₂	0.3489
Goodness of fit on F ²	1.207
Largest diff. peak, e/Å ³	12.061
Largest diff. hole, e/Å ³	-11.134

Table 3.8. Selected bond lengths (\AA) for $(4,4'\text{-bpyH}_2)_4[\text{H}_2\text{P}_2\text{W}_{18}\text{O}_{62}]_2$.

W(1) – O(36)	1.67(3)	W(23) – O(32)	1.69(2)
W(1) – O(23)	1.89(2)	W(23) – O(10)	1.86(2)
W(2) – O(33)	1.73(2)	W(24) – O(31)	1.71(2)
W(2) – O(18)	1.84(2)	W(24) – O(11)	1.91(2)
W(3) – O(48)	1.72(3)	W(25) – O(108)	1.72(3)
W(3) – O(4)	1.93(2)	W(25) – O(9)	1.89(2)
W(4) – O(61)	1.71(2)	W(26) – O(103)	1.68(3)
W(4) – O(52)	1.89(2)	W(26) – O(109)	1.88(3)
W(5) – O(86)	1.75(3)	W(27) – O(114)	1.75(3)
W(5) – O(19)	1.91(2)	W(27) – O(37)	1.87(2)
W(6) – O(49)	1.72(2)	W(28) – O(29)	1.72(2)
W(6) – O(22)	1.86(2)	W(28) – O(79)	1.86(2)
W(7) – O(7)	1.73(3)	W(29) – O(104)	1.63(2)
W(7) – O(21)	1.85(2)	W(29) – O(55)	1.87(2)
W(8) – O(106)	1.73(3)	W(30) – O(92)	1.74(2)
W(8) – O(14)	1.87(2)	W(30) – O(93)	1.90(2)
W(9) – O(58)	1.95(2)	W(31) – O(116)	1.84(3)
W(9) – O(53)	1.96(2)	W(31) – O(62)	1.86(2)
W(10) – O(30)	1.70(3)	W(32) – O(121)	1.71(3)
W(10) – O(63)	1.89(3)	W(32) – O(109)	1.90(3)
W(11) – O(44)	1.65(3)	W(33) – O(122)	1.70(3)
W(11) – O(43)	1.88(2)	W(33) – O(82)	1.85(3)
W(12) – O(111)	1.72(3)	W(34) – O(124)	1.80(4)
W(12) – O(38)	1.87(3)	W(34) – O(81)	1.90(3)
W(13) – O(17)	1.72(3)	W(35) – O(40)	1.92(2)
W(13) – O(24)	1.91(2)	W(35) – O(82)	1.95(3)
W(14) – O(41)	1.72(2)	W(36) – O(96)	1.76(3)
W(14) – O(15)	1.87(2)	W(36) – O(83)	1.87(2)
W(15) – O(60)	1.74(2)	W(36) – O(91)	2.32(3)
W(15) – O(42)	1.83(2)	P(1) – O(67)	1.51(2)
W(16) – O(25)	1.72(2)	P(1) – O(66)	1.53(2)
W(16) – O(20)	1.844(18)	P(1) – O(76)	1.58(3)
W(17) – O(80)	1.75(2)	P(2) – O(68)	1.52(2)
W(17) – O(53)	1.90(2)	P(2) – O(98)	1.52(3)
W(18) – O(12)	1.87(2)	P(2) – O(70)	1.59(2)
W(18) – O(88)	1.89(2)	P(2) – O(74)	1.65(2)
W(19) – O(102)	1.69(3)	P(3) – O(72)	1.46(2)
W(19) – O(16)	1.86(2)	P(3) – O(71)	1.48(2)
W(20) – O(119)	1.73(3)	P(3) – O(69)	1.53(2)
W(20) – O(2)	1.86(2)	P(3) – O(77)	1.57(2)
W(21) – O(105)	1.74(3)	P(4) – O(85)	1.51(2)
W(21) – O(115)	1.85(2)	P(4) – O(78)	1.52(3)
W(22) – O(79)	1.95(2)	P(4) – O(73)	1.56(2)
W(22) – O(16)	1.95(2)	P(4) – O(91)	1.63(3)
W(22) – O(98)	2.45(2)	Cu(1) – O(29)	4.00(4)

Table 3.9. Selected bond angles ($^{\circ}$) for $(4,4'$ -bpyH₂)₄[H₂P₂W₁₈O₆₂]₂.

O(36) – W(1) – O(23)	100.1(11)	O(11) – W(24) – O(77)	84.1(8)
O(36) – W(1) – O(52)	104.3(11)	O(64) – W(24) – O(77)	84.8(9)
O(33) – W(2) – O(18)	98.5(10)	O(9) – W(25) – O(13)	86.7(9)
O(59) – W(2) – O(69)	72.7(8)	O(95) – W(25) – O(13)	86.7(10)
O(48) – W(3) – O(4)	98.6(11)	O(5) – W(26) – O(78)	81.8(8)
O(48) – W(3) – O(89)	96.4(11)	O(40) – W(26) – O(78)	81.6(9)
O(52) – W(4) – O(66)	82.0(9)	O(37) – W(27) – O(12)	163.4(10)
O(10) – W(4) – O(66)	72.7(9)	O(27) – W(27) – O(12)	88.7(10)
O(86) – W(5) – O(19)	100.7(10)	O(5) – W(28) – O(68)	81.6(8)
O(86) – W(5) – O(50)	97.4(11)	O(3) – W(28) – O(68)	73.6(7)
O(49) – W(6) – O(22)	97.0(11)	O(55) – W(29) – O(13)	164.1(9)
O(49) – W(6) – O(26)	99.4(10)	O(8) – W(29) – O(13)	87.7(10)
O(7) – W(7) – O(21)	99.3(11)	O(92) – W(30) – O(28)	100.5(10)
O(7) – W(7) – O(39)	102.0(11)	O(93) – W(30) – O(28)	85.9(10)
O(89) – W(8) – O(74)	85.2(9)	O(62) – W(31) – O(90)	90.2(10)
O(97) – W(8) – O(74)	71.5(9)	O(6) – W(31) – O(90)	87.4(9)
O(54) – W(9) – O(94)	103.3(11)	O(110) – W(32) – O(85)	72.4(10)
O(54) – W(9) – O(46)	99.6(12)	O(117) – W(32) – O(85)	81.3(10)
O(30) – W(10) – O(63)	101.7(12)	O(82) – W(33) – O(118)	87.8(12)
O(30) – W(10) – O(1)	95.9(12)	O(56) – W(33) – O(118)	158.1(11)
O(44) – W(11) – O(43)	96.7(11)	O(37) – W(34) – O(85)	83.4(9)
O(44) – W(11) – O(47)	100.1(11)	O(83) – W(34) – O(85)	83.4(9)
O(38) – W(12) – O(71)	81.8(9)	O(40) – W(35) – O(91)	85.7(10)
O(24) – W(12) – O(71)	73.1(9)	O(82) – W(35) – O(91)	71.2(11)
O(17) – W(13) – O(24)	98.7(12)	O(96) – W(36) – O(87)	101.8(12)
O(17) – W(13) – O(55)	100.1(12)	O(83) – W(36) – O(87)	86.2(10)
O(15) – W(14) – O(67)	82.2(8)	O(67) – P(1) – O(65)	111.2(12)
O(8) – W(14) – O(67)	84.8(8)	O(66) – P(1) – O(65)	113.0(12)
O(60) – W(15) – O(42)	102.7(11)	O(68) – P(2) – O(98)	113.4(13)
O(60) – W(15) – O(15)	99.6(10)	O(68) – P(2) – O(70)	110.7(11)
O(20) – W(16) – O(70)	86.2(7)	O(72) – P(3) – O(71)	111.8(12)
O(1) – W(16) – O(70)	84.2(9)	O(72) – P(3) – O(69)	109.6(13)
O(80) – W(17) – O(53)	99.5(10)	O(85) – P(4) – O(73)	111.5(13)
O(80) – W(17) – O(50)	101.9(11)	O(78) – P(4) – O(73)	112.0(13)
O(51) – W(18) – O(12)	100.0(11)	W(11) – O(43) – W(16)	124.0(12)
O(51) – W(18) – O(88)	104.9(11)	W(20) – O(45) – W(10)	124.8(11)
O(102) – W(19) – O(16)	103.8(12)	W(9) – O(46) – W(25)	122.1(13)
O(102) – W(19) – O(35)	101.7(12)	W(18) – O(47) – W(11)	153.7(12)
O(2) – W(20) – O(81)	88.6(11)	W(21) – O(4) – W(3)	162.2(13)
O(45) – W(20) – O(81)	157.7(11)	W(28) – O(5) – W(26)	162.4(12)
O(99) – W(21) – O(56)	91.4(11)	W(31) – O(6) – W(24)	123.2(12)
O(4) – W(21) – O(56)	165.0(10)	W(25) – O(9) – W(14)	151.6(12)
O(79) – W(22) – O(98)	85.6(9)	W(23) – O(10) – W(4)	125.3(13)
O(79) – W(22) – O(16)	83.9(10)	W(24) – O(11) – W(15)	147.9(13)
O(32) – W(23) – O(84)	98.2(11)	W(18) – O(12) – W(27)	150.2(13)
O(10) – W(23) – O(84)	89.5(10)	W(29) – O(13) – W(25)	148.9(13)

3.3.3.2. Results and Discussion for $(4,4'\text{-bpyH}_2)_4[\text{H}_2\text{P}_2\text{W}_{18}\text{O}_{62}]_2$

The crystal $(4,4'\text{-bpyH}_2)_4[\text{H}_2\text{P}_2\text{W}_{18}\text{O}_{62}]_2$ was synthesized by hydrothermal method from the reaction of $\text{Na}_2\text{WO}_4\cdot 2\text{H}_2\text{O}$, $\text{CuSO}_4\cdot 5\text{H}_2\text{O}$, 4,4'-bipyridine and H_3PO_4 .

As a result of single crystal X-ray diffraction, it is determined that the structure contains $[\text{H}_2\text{P}_2\text{W}_{18}\text{O}_{62}]^{4-}$ Well-Dawson polyanion clusters and 4,4'-bipyridine ligands. Well-Dawson polyanion cluster includes 18 edge-and-corner sharing WO_6 octahedra and there are two PO_4 tetrahedra at the center that is shown in Figure 3.21. $[\text{H}_2\text{P}_2\text{W}_{18}\text{O}_{62}]^{4-}$ and its polyhedral structure is illustrated in Figure 3.22. The clusters and water molecules have C-H...O hydrogen bond interactions between each other.

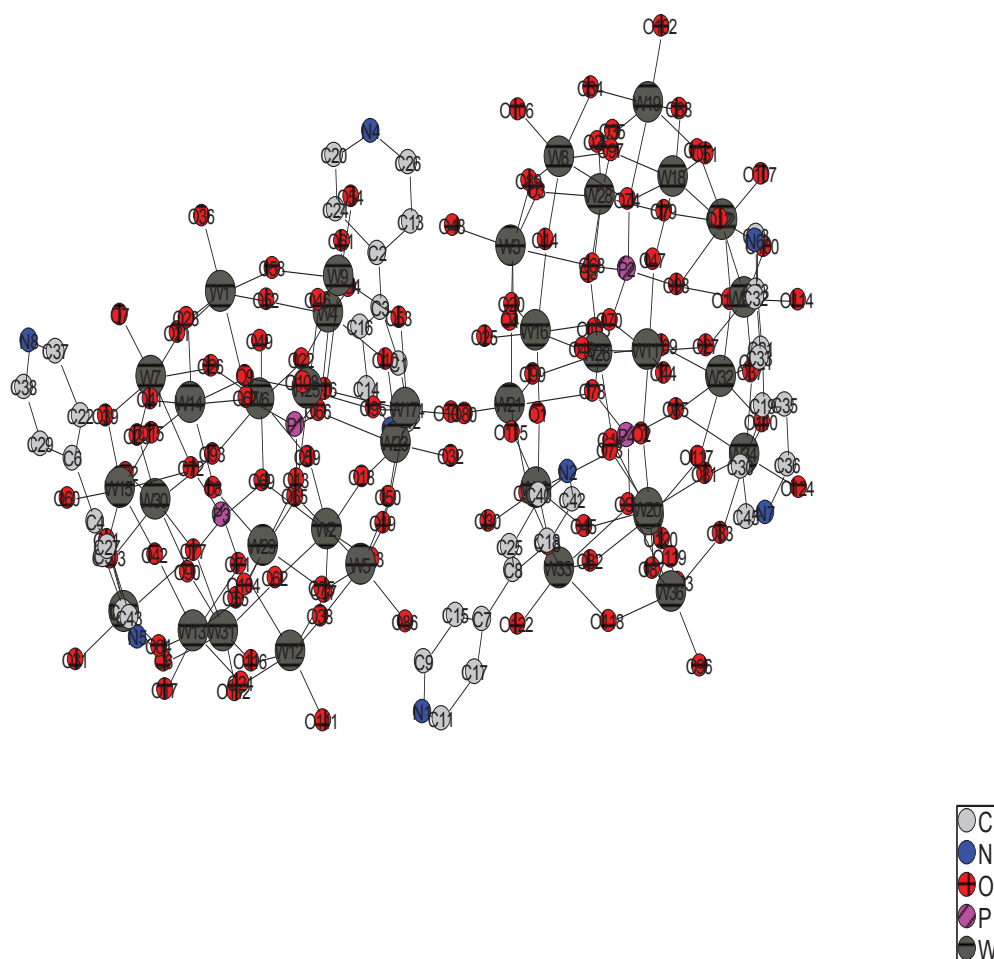


Figure 3.21. The view of Well-Dawson polyanion cluster.

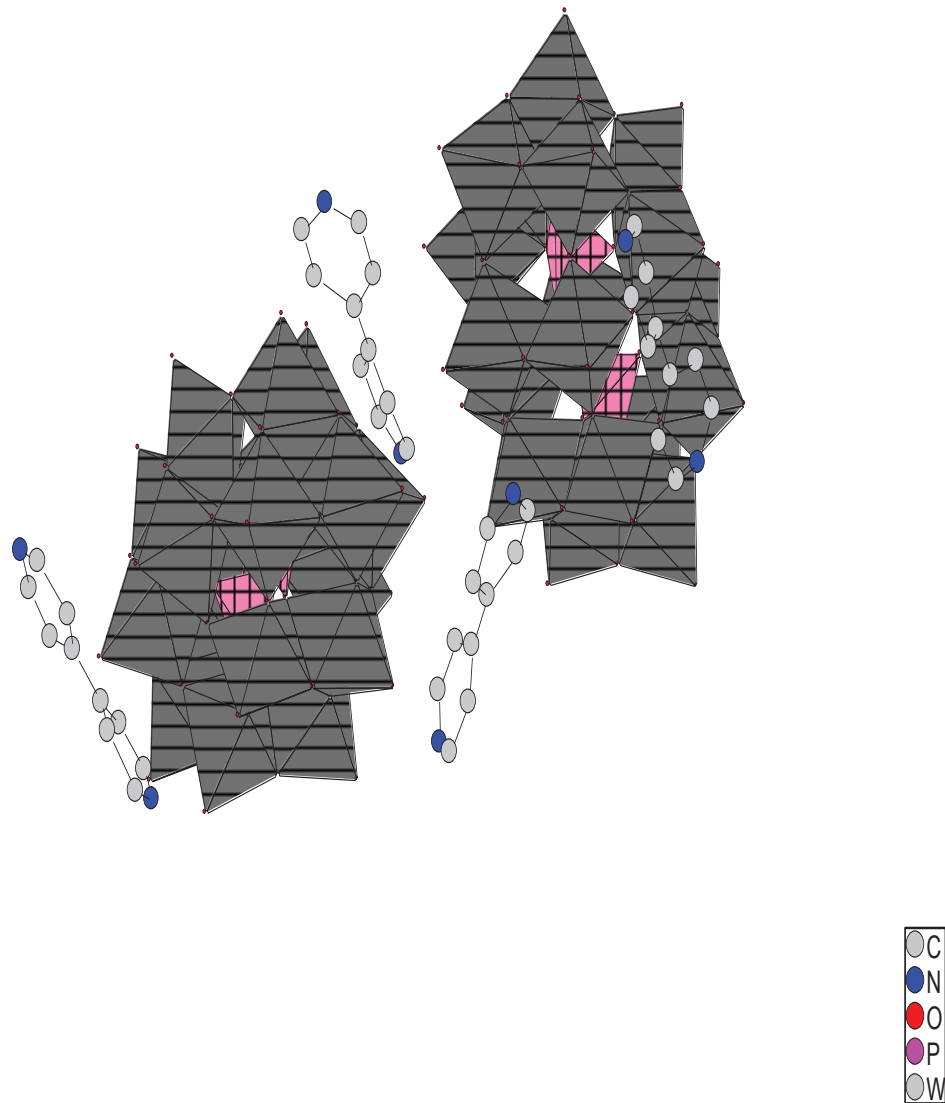


Figure 3.22. The polyhedral structure of Well-Dawson polyanions.

In the unitcell that is indicated in Figure 3.23, there are four polyanion clusters and 4,4'-bipyridine ligands between these clusters. WO_6 octahedral structures include three different W-O bonds. These are; W-Ot (terminal) bonds whose distances range from 1.647(30) to 1.757(42) Å which represents a $\text{W}=\text{O}$ multiple bond, W-Ob (bridging) bonds whose distances range from 1.854(33) to 1.963(41) Å and W-Oc (central) bonds range from 2.311(31) to 2.422(50) Å respectively. Besides, the distances of P-O bond distances are between 1.457(33) and 1.652(28) Å.

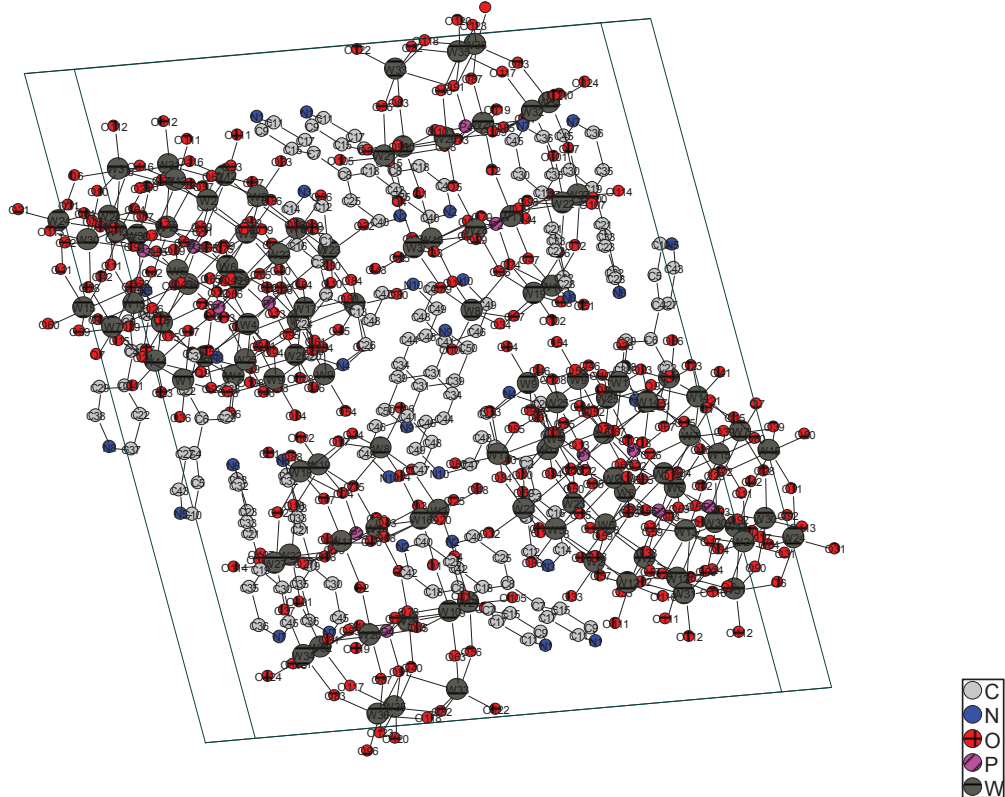


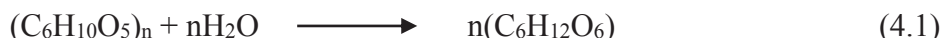
Figure 3.23. The unitcell view of $(4,4'\text{-bpyH}_2)_4[\text{H}_2\text{P}_2\text{W}_{18}\text{O}_{62}]_2$.

The bond valence sums of $(4,4'\text{-bpyH}_2)_4[\text{H}_2\text{P}_2\text{W}_{18}\text{O}_{62}]_2$ shown in Table 3.12 were calculated by Bond Valence Sum, BVS method developed by ID Brown. The results of these calculations show that, the oxidation states of W, P, O atoms of the structure are 6+, 5+, and 2- respectively. The compound needs 8+ valence cations and they are provided by 4,4'-bipyridine ligands. These ligands change into $4,4'\text{-bpyH}_2^{2+}$ cations easily in acidic medium. It is thought that, the organic part of the synthesized material includes bipyridinium cations. Bond valence sums table of the crystal $(4,4'\text{-bpyH}_2)_4[\text{H}_2\text{P}_2\text{W}_{18}\text{O}_{62}]_2$ is shown in Appendix I.

CHAPTER 4

CATALYTIC APPLICATIONS

In this study, catalytic activities of the synthesized three novel polyoxometalates; $[(4,4'\text{-bpyH}_2)_3][\text{PCuW}_{11}\text{O}_{39}]$, $(4,4'\text{-bpyH}_2)[\text{H}_2\text{PW}_{12}\text{O}_{40}]_2\cdot\text{H}_2\text{O}$, $(4,4'\text{-bpyH}_2)_4[\text{H}_2\text{P}_2\text{W}_{18}\text{O}_{62}]_2$ and two known crystals previously synthesized in our group which are formulated as $[(4,4'\text{-bpyH}_2)_2(4,4'\text{-bpyH})][\text{PCuW}_{11}\text{O}_{39}]\cdot\text{H}_2\text{O}^{31}$ and $[(4,4'\text{-bpyH}_2)_2(4,4'\text{-bpyH})][\text{PCoW}_{11}\text{O}_{39}]\cdot\text{H}_2\text{O}^{32}$ were studied. The crystals were used as catalysts for the hydrolysis of starch to glucose.



In the literature, starch was converted to glucose by using a micellar heteropolyacid catalyst, $[\text{C}_{16}\text{H}_{33}\text{N}(\text{CH}_3)_3]_3\text{H}_2\text{PW}_{12}\text{O}_{40}$ (abbreviated as $(\text{C}_{16}\text{TA})\text{H}_2\text{PW}$).³³ and a carbon based solid acid catalyst, $\text{H}_4\text{SiW}_{12}\text{O}_{40}/\text{activated carbon}$ (abbreviated as HSiW/C).³⁴ In both of the studies, hydrothermal method was chosen. Different from these studies, in our work, polyoxotungstate clusters containing organic-inorganic hybrid materials were used as catalysts for the hydrolysis of starch to glucose with hydrothermal method.

4.1. Catalytic Procedure

In the hydrolysis of starch, 0.10 g starch, 10.0 mg catalyst and 7.0 ml distilled water were mixed and heated at 150°C in a stainless steel autoclave lined with Teflon for 5h in oven. When the reaction finished, autoclave was cooled to room temperature and the mixture was filtered to separate the catalyst and centrifugated to separate unreacted starch from the solution. Starch was purchased from Carlo Erba Reagents. It was used without further purification. In order to understand the reaction is finished or not, Lugol's iodine reagent was used. The products were analyzed by FTIR-ATR spectroscopy. Also, to calculate yield(%), the following formula were used.

$$\text{Yield}(\%) = \left(\frac{\text{main product mass}}{\text{a mass in the loaded sample}} \right) \times 100\% \quad (4.2)$$

4.2. Results and Discussion

In this study, the hydrolyzed solutions from the reactions were tested by Lugol's iodine solution and determined by Fourier transform infrared-attenuated total reflection (FTIR-ATR) spectroscopy.

4.2.1. Lugol's Iodine Test

Lugol's iodine solution is a solution of potassium iodide with iodine in water. Reaction of starch with Lugol's iodine solution gives a blue-black colour. A negative test gives yellow-orange colour. This test was used in this study to obtain the hydrolysis of starch which is illustrated in Figure 4.1. The solution of 20.0 g potassium iodide (KI) and 10.0 g iodine (I₂) in 100.0 ml water was prepared for Lugol's iodine test. Then, this solution was dropped into each reaction sample in test tubes. It was determined that, each of the five reaction sample for five different catalysts gave yellow-orange colour. It shows there are no more starches in the solution at the end of each reaction.

Control experiment was also done at 150°C for 5 h without using any catalyst. As a result, the reaction gave blue colour with iodine solution which shows the presence of starch. In Figure 4.2, the numbers from 1 to 5 show the reactions with (4,4'-bpyH₂)₂(4,4'-bpyH)[PCoW₁₁O₃₉].H₂O and (4,4'-bpyH₂)[H₂PW₁₂O₄₀]₂.H₂O crystal catalysts, (4,4'-bpyH₂)₃[PCuW₁₁O₃₉], (4,4'-bpyH₂)₄[H₂P₂W₁₈O₆₂]₂ crystal catalysts and (4,4'-bpyH₂)₂(4,4'-bpyH)[PCuW₁₁O₃₉].H₂O crystal catalyst respectively.

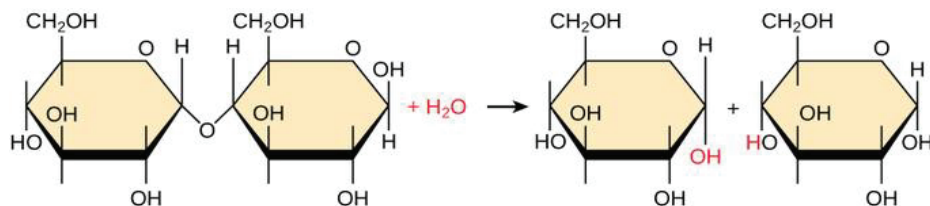


Figure 4.1. Hydrolysis reaction of starch.
(Source: Stax³⁵)



Figure 4.2. Lugol's test of the reactions with five different crystals and without any catalyst.

4.2.2. FT-IR ATR Results

The FT-IR ATR analysis was applied for each hydrolyzate of optimization reactions of five catalysts after determined the yellow-orange colours in the Lugol's iodine test. Figure 4.3 shows the FT-IR ATR spectra of these five reactions and the reaction with no catalyst. The peaks at $\sim 3350\text{ cm}^{-1}$, $\sim 2920\text{ cm}^{-1}$, $\sim 2850\text{ cm}^{-1}$, $\sim 1450\text{ cm}^{-1}$, $\sim 1200\text{ cm}^{-1}$, $\sim 1035\text{ cm}^{-1}$ show the stretch of OH, asymmetric vibration of CH, symmetric vibration of CH, bending vibration of CH, vibration of COC and characteristic vibration of CO bonds of glucose respectively.³⁶ When COC and CO spectrum peaks of the reactions under optimum conditions with catalyst and without catalyst, it was observed that the characteristic peaks of CO bonds of glucose are sharper than the peaks of COC bonds in the spectra of the reactions with catalyst, differently from the peaks of bonds in the spectrum of the reaction without catalyst. This shows the breakage of the COC bonds in the starch by the crystal catalysts.

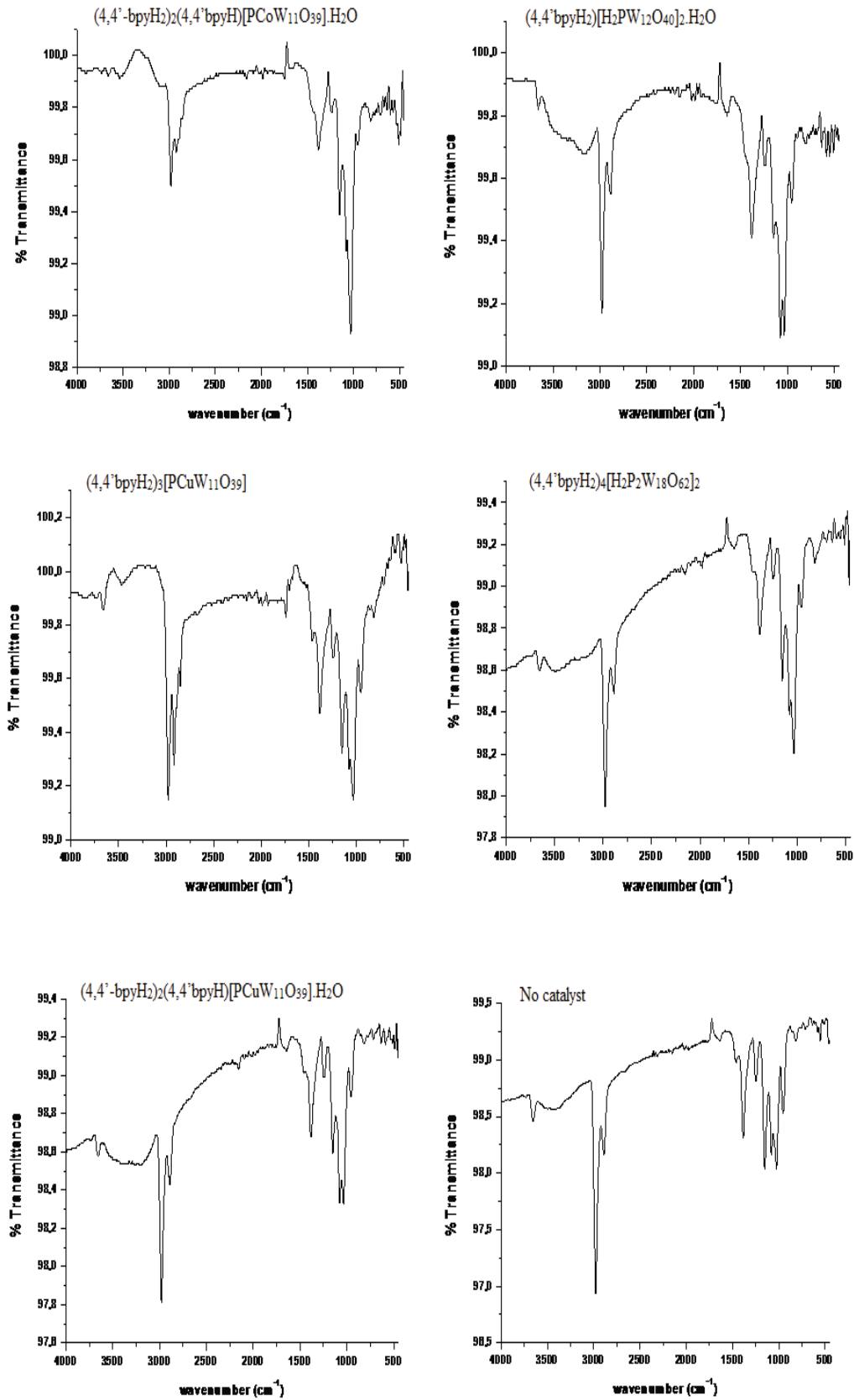
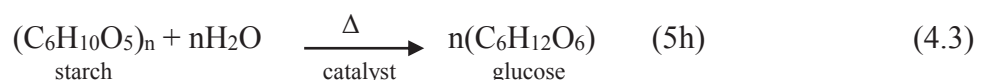


Figure 4.3. FT-IR ATR spectra of the reactions with five different catalysts and with no catalyst.

4.2.3. Optimization of Reaction Time and Temperature

Starch hydrolysis reactions were carried out at two different temperatures (120 °C and 150 °C) for 5h with $(4,4'-\text{bpyH}_2)_2(4,4'-\text{bpyH})[\text{PCoW}_{11}\text{O}_{39}]\cdot\text{H}_2\text{O}$ catalysts. The catalysts were separated from the solutions by filtration.

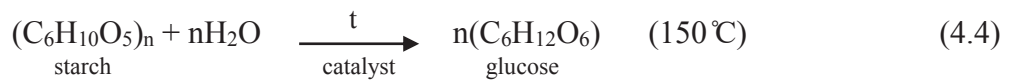


In Lugol's iodine tests, it was observed that at 120 °C, the reaction sample gave blue colour. It shows the presence of unreacted starch in the solution. However, at 150 °C reaction sample gave yellow-orange colour which show there is no more starch in the solution. The test results are shown in Figure 4.4.



Figure 4.4. Lugol's test of the reaction with $(4,4'-\text{bpyH}_2)_2(4,4'-\text{bpyH})[\text{PCoW}_{11}\text{O}_{39}]\cdot\text{H}_2\text{O}$ crystal for temperature.

After finding the optimum reaction temperature, effect of time on starch hydrolysis was determined. Starch hydrolysis reactions with the catalyst $(4,4'-\text{bpyH}_2)_2(4,4'-\text{bpyH})[\text{PCoW}_{11}\text{O}_{39}]\cdot\text{H}_2\text{O}$ were carried out at 150 °C for 1 to 5 h.



In Lugol's iodine tests, the reaction for 5 h gave yellow-orange colours but the other reactions for 1 to 4 h gave blue-violet colours. The test results are shown in Figure 4.5. Also, FT-IR ATR analysis of $(4,4'-bpyH_2)_2(4,4'-bpyH)[PCoW_{11}O_{39}].H_2O$ catalyst was done for each time from 1 to 5 h. It was observed that the characteristic peak of CO bond of glucose gets sharper from 1 to 5 h. These results in Figure 4.6 show that the optimum time is 5h for the hydrolysis reactions with these crystal catalysts.



Figure 4.5. Lugol's test of the reaction with $(4,4'-bpyH_2)_2(4,4'-bpyH)[PCoW_{11}O_{39}].H_2O$ crystal for time.

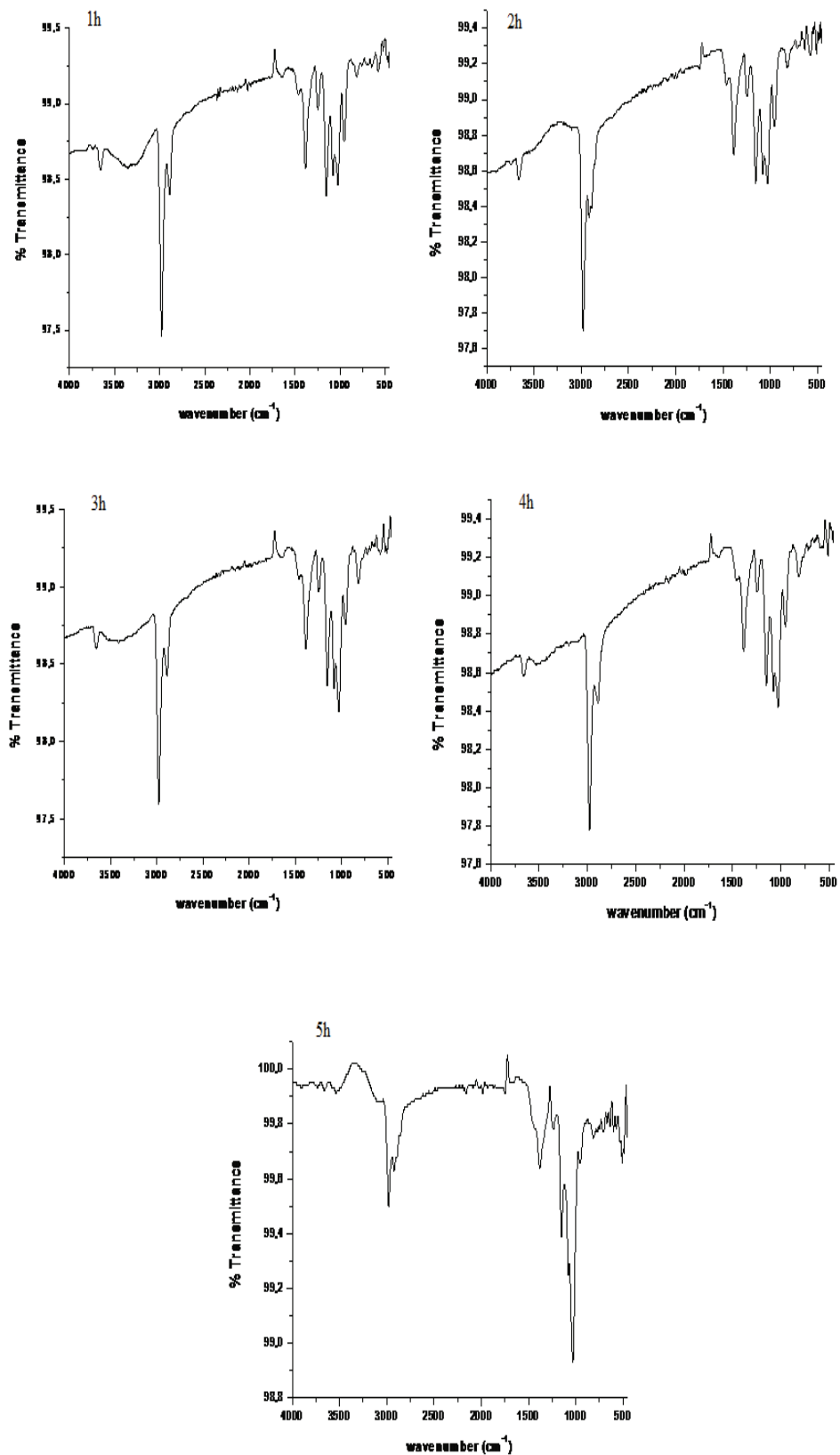
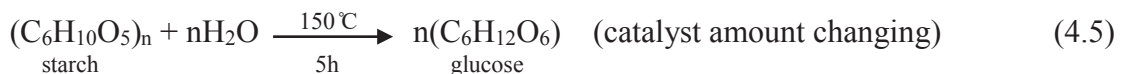


Figure 4.6. FT-IR ATR spectra of the starch hydrolysis reactions with the catalyst (4,4'-bpyH₂)₂(4,4'-bpyH)[PCoW₁₁O₃₉].H₂O at 150 °C from 1 to 5 h.

4.2.4. Optimization of Catalyst Amount

After finding the optimum reaction temperature and time for starch hydrolysis optimum catalyst amount was determined. Starch hydrolysis reactions with the catalyst $(4,4'-\text{bpyH}_2)_2(4,4'-\text{bpyH})[\text{PCoW}_{11}\text{O}_{39}]\cdot\text{H}_2\text{O}$ were carried out at 150°C and 5 h for 1 mg, 5 mg and 10 mg catalyst amounts respectively.



In Lugol's iodine tests, the reactions for 1 mg and 5 mg catalyst amounts gave reddish colours but the reaction for 10 mg gave yellow-orange colour. The reddish colours show the present of dextrin molecules in the solution. However, the colour of the reaction for 10 mg catalyst amount shows the presentation of glucose molecules rather than dextrin molecules. Dextrin molecules are the molecules which are the same formula with starch molecules $(\text{C}_6\text{H}_{10}\text{O}_5)_n$ but their chains are smaller than starch molecules. The chain numbers change from 10 to 30. The test results are shown in Figure 4.7.

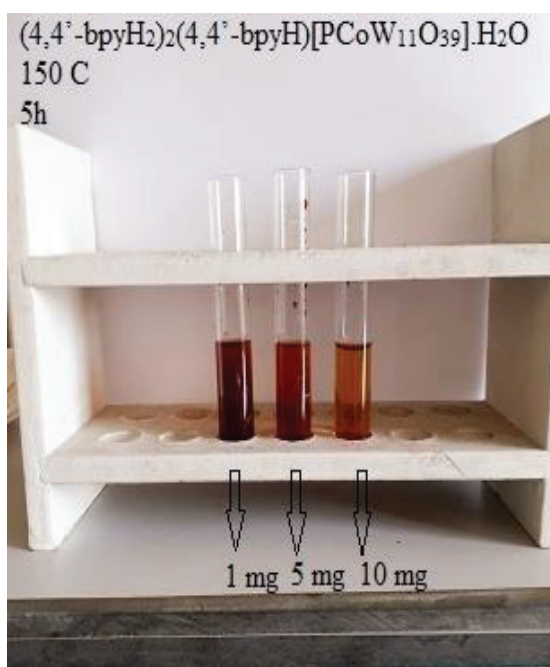


Figure 4.7. Lugol's test of the reaction with $(4,4'-\text{bpyH}_2)_2(4,4'-\text{bpyH})[\text{PCoW}_{11}\text{O}_{39}]\cdot\text{H}_2\text{O}$ crystal for catalyst amount.

4.2.5. Reusability of Catalysts

The reusability of catalysts was tested for five reaction runs under optimum conditions (150 °C, 5 h). In each reaction cycle, fresh starch and water were added to the catalyst remaining. In Lugol's iodine tests, reaction samples gave yellow-orange colours which show there are no more starches in the solutions. The glucose yields were obtained for each cycle. In each case, the glucose yield was above 90 wt.%. They were nearly the theoretical yield of D-glucose expected from starch 111 wt.%. The results which are illustrated in Figure 4.8, Figure 4.9, Figure 4.10, Figure 4.11 and Figure 4.12 show that the catalysts are reusable.



Figure 4.8. Lugol's test of the reaction with (4,4'-bpyH₂)₂(4,4'-bpyH)[PCoW₁₁O₃₉].H₂O crystal for five cycles.

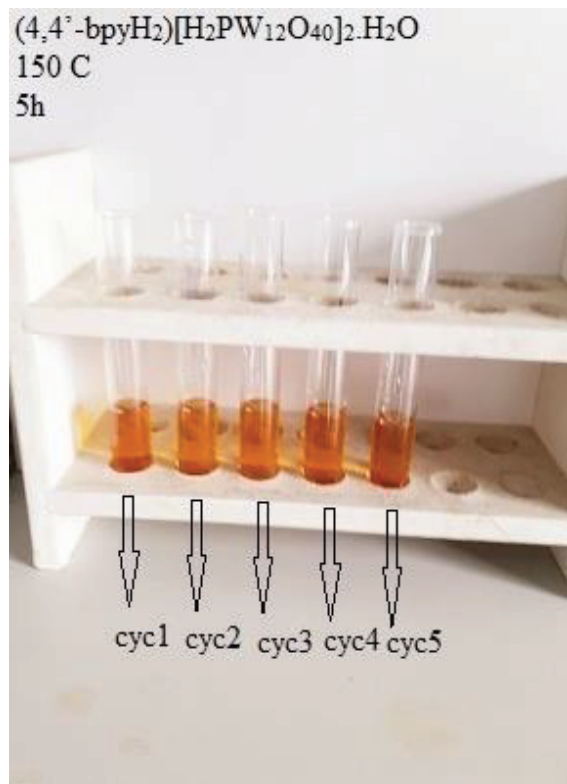


Figure 4.9. Lugol's test of the reaction with (4,4'-bpyH₂)₂[H₂PW₁₂O₄₀]₂.H₂O crystal for five cycles.



Figure 4.10. Lugol's test of the reaction with (4,4'-bpyH₂)₃[PCuW₁₁O₃₉] crystal for five cycles.



Figure 4.11. Lugol's test of the reaction with (4,4'-bpyH₂)₄[H₂P₂W₁₈O₆₂]₂ crystal for five cycles.



Figure 4.12. Lugol's test of the reaction with (4,4'bpyH₂)₂(4,4'bpyH)[PCuW₁₁O₃₉].H₂O crystal for five cycles.

The yields of the reactions of $(4,4'\text{-bpyH}_2)_2(4,4'\text{-bpyH})[\text{PCoW}_{11}\text{O}_{39}]\cdot\text{H}_2\text{O}$ obtained from cycle 1 to 5 are 95.04%, 95.08%, 95.11%, 95.05% and 95.90% respectively which are shown in Figure 4.13.

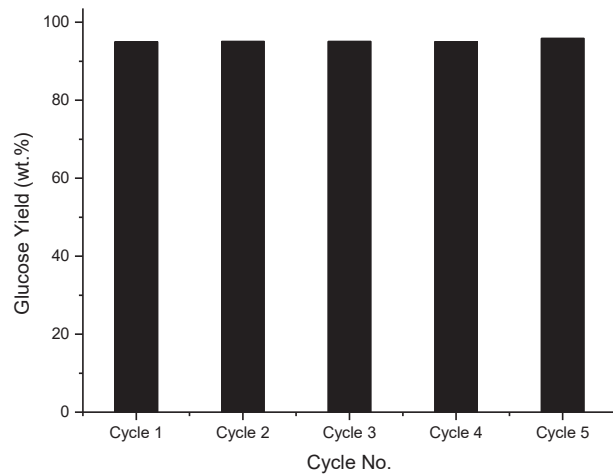


Figure 4.13. Plot of glucose yield vs reaction cycles of the reaction with the catalyst $(4,4'\text{-bpyH}_2)_2(4,4'\text{-bpyH})[\text{PCoW}_{11}\text{O}_{39}]\cdot\text{H}_2\text{O}$.

The yields of the reactions of $(4,4'\text{-bpyH}_2)[\text{H}_2\text{PW}_{12}\text{O}_{40}]_2\cdot\text{H}_2\text{O}$ obtained from cycle 1 to 5 are 93.57%, 94.70%, 94.25%, 93.83% and 96.25% respectively which are shown in Figure 4.14.

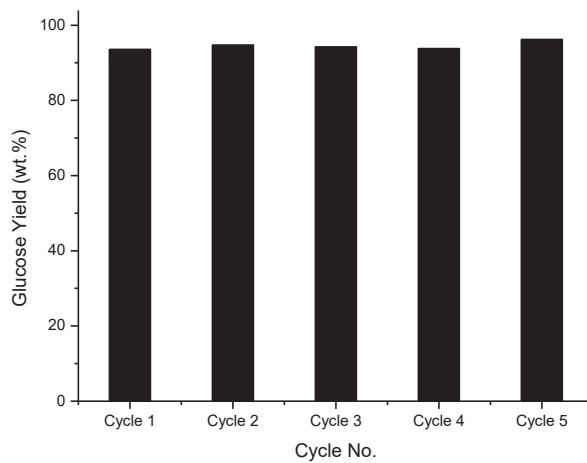


Figure 4.14. Plot of glucose yield vs reaction cycles of the reaction with the catalyst $(4,4'\text{-bpyH}_2)[\text{H}_2\text{PW}_{12}\text{O}_{40}]_2\cdot\text{H}_2\text{O}$.

The yields of the reactions of $(4,4'-\text{bpyH}_2)_3[\text{PCuW}_{11}\text{O}_{39}]$ obtained from cycle 1 to 5 are 94.08%, 93.42%, 93.56%, 93.40% and 91.90% respectively which are shown in Figure 4.15.

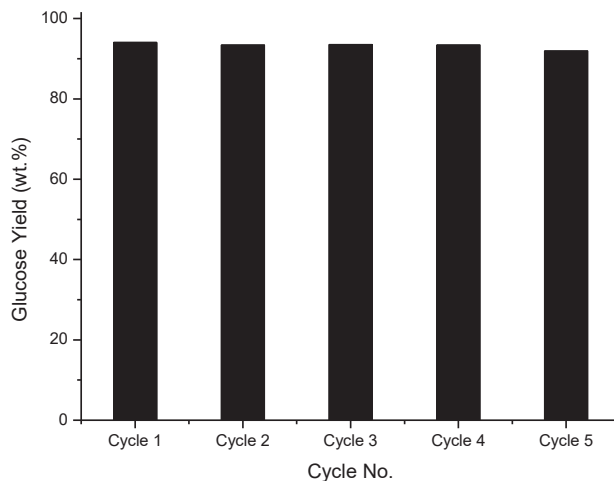


Figure 4.15. Plot of glucose yield vs reaction cycles of the reaction with the catalyst $(4,4'-\text{bpyH}_2)_3[\text{PCuW}_{11}\text{O}_{39}]$.

The yields of the reactions of $(4,4'-\text{bpyH}_2)_4[\text{H}_2\text{P}_2\text{W}_{18}\text{O}_{62}]_2$ obtained from cycle 1 to 5 are 92.55%, 93.38%, 92.84%, 92.54% and 93.95% respectively which are shown in Figure 4.16.

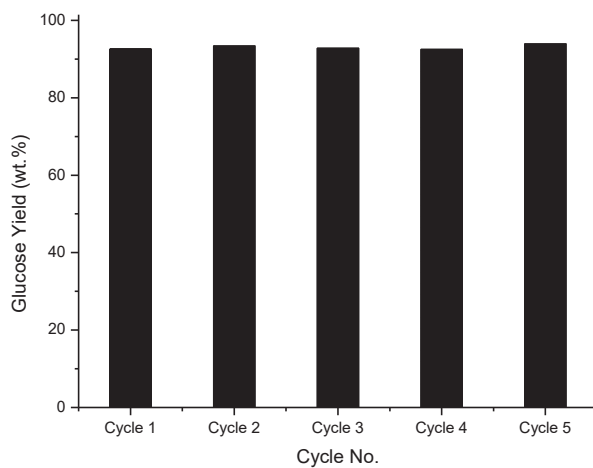


Figure 4.16. Plot of glucose yield vs reaction cycles of the reaction with the catalyst $(4,4'-\text{bpyH}_2)_4[\text{H}_2\text{P}_2\text{W}_{18}\text{O}_{62}]_2$.

The yields of the reactions of $(4,4'\text{-bpyH}_2)_2(4,4'\text{-bpyH})[\text{PCuW}_{11}\text{O}_{39}]\cdot\text{H}_2\text{O}$ obtained from cycle 1 to 5 are 94.07%, 93.83%, 93.58%, 92.84% and 93.55% respectively which are shown in Figure 4.17.

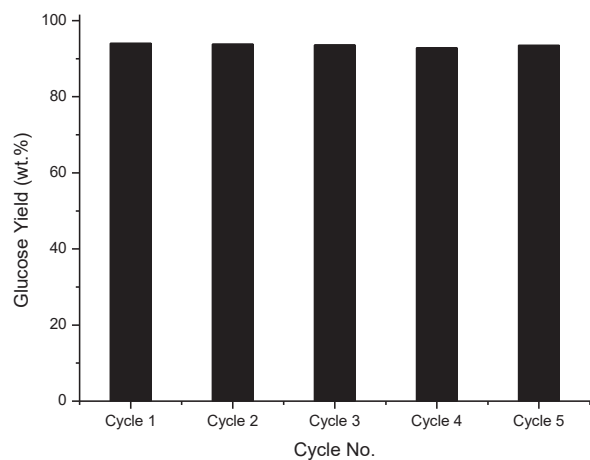


Figure 4.17. Plot of glucose yield vs reaction cycles of the reaction with the catalyst $(4,4'\text{-bpyH}_2)_2(4,4'\text{-bpyH})[\text{PCuW}_{11}\text{O}_{39}]\cdot\text{H}_2\text{O}$.

CHAPTER 5

CONCLUSION

In this PhD. thesis, characterization and catalytic applications of hydrothermally synthesized polyoxotungstate clusters containing organic-inorganic hybrid materials were studied. Tungsten transition metal was used to form the inorganic framework, 4,4'-bipyridine was used as the organic ligands of the hybrid materials. At the end of the hydrothermal reactions, several crystals were synthesized and characterized by using different methods. These methods are; powder X-ray diffraction, optical microscopy, scanning electron microscopy (SEM), single crystal X-ray diffraction and thermogravimetric analysis. The compounds synthesized in this study, include three novel crystals whose structures were solved by SHELXTL program. Therefore, the catalytic applications of these three novel crystals and two known crystals were studied.

The first synthesized novel compound is $[(4,4'\text{-bpyH}_2)_3][\text{PCuW}_{11}\text{O}_{39}]$ yellow crystals. They are synthesized by using the hydrothermal reaction of $\text{Na}_2\text{WO}_4\cdot 2\text{H}_2\text{O}$, $\text{CuSO}_4\cdot 5\text{H}_2\text{O}$, 4,4'-bipyridine and H_3PO_4 in a Teflon-lined autoclave at 170°C for 3 days. The compound crystallizes in the space group $\text{P}2(1)/n$ of the monoclinic system with four formula units in a cell with dimensions $a=13.519(3)$ Å, $b=26.824(5)$ Å, $c=15.199(3)$ Å and its volume is $17446(3)$ Å³. The crystal is a Keggin polyoxometalate and includes free 4,4'-bipyridine groups between the clusters.

The second synthesized novel compound is $(4,4'\text{-bpyH}_2)[\text{H}_2\text{PW}_{12}\text{O}_{40}]_2\cdot \text{H}_2\text{O}$ colorless crystals. They are synthesized by using the hydrothermal reaction of $\text{Na}_2\text{WO}_4\cdot 2\text{H}_2\text{O}$, $\text{Co}(\text{NO}_3)_2\cdot 6\text{H}_2\text{O}$, 4,4'-bipyridine and H_3PO_4 in a Teflon-lined autoclave at 170°C for 3 days. The compound crystallizes in the space group Ia-3 of the cubic system with twelve formula units in a cell with dimensions $a=25.936(3)$ Å, $b=25.936(3)$ Å, $c=25.936(3)$ Å and its volume is $5436.4(19)$ Å³. The crystal is a Keggin polyoxometalate and consists of two polyoxotungstate clusters, a free 4,4'-bipyridine group and a water molecule.

The third and the last compound is $(4,4'\text{-bpyH}_2)_4[\text{H}_2\text{P}_2\text{W}_{18}\text{O}_{62}]_2$ dark yellow crystals. They are synthesized by using the hydrothermal reaction of $\text{Na}_2\text{WO}_4\cdot 2\text{H}_2\text{O}$, $\text{CuSO}_4\cdot 5\text{H}_2\text{O}$, 4,4'-bipyridine and H_3PO_4 in a Teflon-lined autoclave at 170°C for 3

days. The compound crystallizes in the space group P-1 of the triclinic system with four formula units in a cell with dimensions $a=13.519(3)$ Å, $b=22.400(5)$ Å, $c=27.374(6)$ Å and its volume is $7889(3)$ Å³. The crystal is a Wells-Dawson polyoxometalate and contains two polyoxotungstate clusters and free 4,4'-bipyridine groups between clusters.

In conclusion, many products were synthesized hydrothermally at the end of several experiments. The three novel compounds and their catalytic activities were discussed here. Also, the catalytic activities of the two known compounds were discussed. According to the results, it is possible to synthesize different organic-inorganic hybrid materials in glamorous crystalline form by changing the components and using the hydrothermal technique. For the catalytic study, it was observed that starch hydrolysis reactions by using hydrothermal synthesis and five different crystals were finished successfully at 150°C, 5h. from the results of Lugol's test and FT-IR ATR analysis. In order to obtain the optimum reaction conditions, optimization of temperature, time and catalyst amount reactions were also performed. Starch samples converted to D-glucose with glucose yields above 90 wt.% under optimum reaction conditions. Catalyst reusability was performed for each crystal. No appreciable loss was observed in activity after five reaction cycles for each crystal.

REFERENCES

1. West, A. R., *Solid State Chemistry and its Applications*. John Wiley and Sons: England, 1984.
2. Kickelbick, G., *Introduction to hybrid materials*. Wiley Online Library: 2007.
3. Hagrman, P. J.; Hagrman, D.; Zubieta, J., Organic-inorganic hybrid materials: From "simple" coordination polymers to organodiamine-templated molybdenum oxides *Angewandte Chemie-International Edition* **1999**, *38*, 2639-2684.
4. Rabenau, A., The Role of Hydrothermal Synthesis in Preparative Chemistry. *Angewandte Chemie-International Edition* **1985**, *24* (12), 1026-1040.
5. Laudise, R. A., Hydrothermal Synthesis of Crystals. *Chem. Eng. News* **1987**, *65* (39), 30-43.
6. Haman, S. D., Properties of electrolyte solutions at high pressures and temperatures. *Physics and Chemistry of the Earth* **1981**, *89* (13-14), 89-111.
7. Xu, R.; Pang, W.; Huo, Q., *Modern Inorganic Synthetic Chemistry*. Elsevier: 2010.
8. Byrappa, K.; Yoshimura, M., *Handbook of hydrothermal technology: a technology for crystal growth and materials processing*. William Andrew: New York, 2001.
9. Şahin, L. Hydrothermal Synthesis and Characterization of Transition Metal Oxides MSc thesis, İzmir Institute of Technology, İzmir, October 2004.
10. Smart, L.; Moore, E. A., *Solid state chemistry: An introduction*. Taylor & Francis: New York, 2005.
11. Seoane, J. R.; Llovet Ximenes, X., *Handbook of instrumental techniques for materials, chemical and biosciences research*. Centres Científics i Tecnològics: Universitat de Barcelona, 2012.
12. Goldstein, J., *Scanning electron microscopy and X-ray microanalysis*. Springer Us: 2003; Vol. 1.
13. Watt, I. M., *The Principles and Practice of Electron Microscopy*. Cambridge University Press: 1997.
14. Bartosova, A.; Soldan, M.; Sirotiak, M.; Blinova, L.; Michalikova, A., Application of FTIR-ATR Spectroscopy for Determination of Glucose in Hydrolysates of Selected Starches. *Research Papers Faculty of Materials Science and Technology in Trnava Slovak University of Technology in Bratislava*. **2013**, *21*, 116-121.

15. Steen Eric, V.; Callanan Linda, H., *Recent Advances in the Science and Technology of Zeolites and Related Materials*. Elsevier: 2004; Vol. 154C.
16. Feng, S. H.; Chen, J. S., *Frontiers of Solid State Chemistry: Proceedings of the International Symposium on Solid State Chemistry in China*. World Scientific Publishing Co. Pte. Ltd.: 2002.
17. Rao, C. N. R.; Natarajan, S.; Choudhury, A.; Neeraj, S.; Ayi, A. A., Aufbau Principle of Complex Open-Framework Structures of Metal Phosphates with Different Dimensionalities. *Accounts of Chemical Research* **2001**, 34 (1), 80-87.
18. Dey, K. C., Sharma V. , Study of the Heteropoly Metal Oxide Complexes: Principle of Their Synthesis, Structure and Applications. *International Journal of ChemTech Research* **2010**, 2 (1), 368-375.
19. Ammam, M., Polyoxometalates: formation, structures, principal properties, main deposition methods and application in sensing. *Journal of Materials Chemistry A*. **2013**, 1 (21), 6291-6312.
20. Casañ-Pastor, N.; Gómez-Romero, P., Polyoxometalates: from inorganic chemistry to materials science. *Frontiers in Bioscience* **2004**, 9, 1759-1770.
21. Gallegos, A. K. C. Organic/inorganic hibrid materials based on conducting organic polymers as electrodes for energy storage devices. PhD thesis, Materials Science Institute of Barcelona, 2003.
22. Sheshmani, S.; Fashapoyeh, M. A.; Mirzaei, M.; Rad, B. A.; Ghortolmesh, S. N.; Yousefi, M., Preparation, characterization and catalytic application of some polyoxometalates with Keggin, Wells-Dawson, and Preyssler structures. *Indian J. Chem.* **2011**, 50A, 1725-1729.
23. Xie, H. L.; Fan, Y. X.; Zhou, C. H.; Du, Z. X.; Min, E. Z.; Ge, Z. H.; Lia, X. N., A Review on Heterogeneous Solid Catalysts and Related Catalytic Mechanisms for Epoxidation of Olefins with H₂O₂. *Chem. Biochem. Eng.* **2008**, 22 (1), 25-39.
24. Mizuno, N., *Modern Heterogeneous Oxidation Catalysis: Design, Reactions and Characterization*. John Wiley & Sons: 2009.
25. Pulidindi, I. N.; Kimchi, B. B.; Gedanken, A., Can Cellulose be a Sustainable Feedstock for Bioethanol Production? *Renew Energy* **2014**, 71, 77-80.
26. Sanyang, M. L.; Ilyas, R. A.; Sapuan, S. M.; Jumaidin, R., Sugar Palm Starch-Based Composites for Packing Applications. In *Bionanocomposites for Packing Applications*, Springer: 2018; pp 125-147.
27. Tasic, M. B.; Konstantinovic, B. V.; Lazic, M. L.; Veljkovic, V. B., The Acid Hydrolysis of Potato Tuber Mash in Bioethanol Production. *Biochem Eng J.* **2009**, 43, 208-211.
28. Hermiati, E.; Azum, J.; Tsubaki, S.; Mangunwidjaj, D.; Sunarti, C. T.; Suparno,

- O.; Prasetya, B., Improvement of Microwave-assisted Hydrolysis of Cassava Pulp and Tapioca Flour by Addition of Activated Carbon. *Carbohydrate Polymers*. **2012**, *87*, 939-942.
29. Orozco, R. L.; Redwood, M. D.; Leeke, G. A.; Bahari, A.; Santos, R. C. D.; Macaskie, L. E., Hydrothermal Hydrolysis of Starch with CO₂ and Detoxification of the Hydrolysates with Activated Carbon for Bio-hydrogen Fermentation. *Int J Hydrogen Energy*. **2012**, *37*, 6545-6553.
30. Yamaguchi, D.; Hara, M., Starch Saccharification by Carbon-based Solid Acid Catalyst. . *Solid State Sciences*. **2010**, *12*, 1018-1023.
31. Emirdag-Eanes, M.; Önen, B.; McMillen, C. D., Hydrothermal synthesis and characterization of one dimensional chain structures of monolacunary Keggin polyoxoanions substituted with copper. *Inorg Chim Acta* **2015**, *427*, 219-225.
32. Wang, J.; Shen, Y.; Niu, J., Synthesis, characterization and crystal structure of a 1D heteropolytungstate [4,4'-bipyH₂]₂[4,4'-bipyH][PCoW₁₁O₃₉]•H₂O. *Journal of Coordination Chemistry* **2007**, *11*, 1183-1190.
33. Cheng, M.; Shi, T.; Wang, S.; Guan, H.; Fan, C.; Wang, X., Fabrication of Micellar Heteropolyacid Catalysts for Clean Production of Monosaccharides from Polysaccharides. . *Catalysis Communications*. **2011**, *12*, 1483-1487.
34. Kumar, V. B.; Pulidindi, I. N.; Gedanken, A., Selective Conversion of Starch to Glucose Using Carbon Based Solid Acid Catalyst. *Renewable Energy*. **2015**, *78*, 141-145.
35. Stax, O., Synthesis of Biological Micromolecules. In *Biology*, OpenStax, Cnx Biology: 2014.
36. Geddes, C. D.; Lakowicz, J. R., *Glucose Sensing*. Springer: New York, 2006.

APPENDIX A

BOND LENGTHS (Å) FOR (4,4'-bpyH₂)₃[PCuW₁₁O₃₉]

Table A.1. Bond lengths (Å) for (4,4'-bpyH₂)₃[PCuW₁₁O₃₉]

W(1) – O(34)	1.711(16)	W(10) – O(39)	2.458(14)
W(1) – O(1)	1.910(17)	W(11) – O(27)	1.881(19)
W(1) – O(29)	1.914(17)	W(11) – O(47)	1.920(16)
W(1) – O(2)	1.923(17)	W(11) – O(24)	1.942(17)
W(1) – O(6)	1.923(16)	W(11) – O(25)	1.953(16)
W(1) – O(15)	2.405(17)	W(11) – O(14)	1.962(16)
W(2) – O(32)	1.711(15)	W(11) – O(40)	2.446(15)
W(2) – O(4)	1.896(16)	W(12) – O(22)	1.883(17)
W(2) – O(42)	1.937(17)	W(12) – O(45)	1.893(16)
W(2) – O(13)	1.890(16)	W(12) – O(27)	1.932(18)
W(2) – O(5)	1.910(16)	W(12) – O(11)	1.946(16)
W(2) – O(28)	2.366(14)	W(12) – O(4)	1.976(16)
W(3) – O(7)	1.713(15)	W(12) – O(28)	2.433(15)
W(3) – O(8)	1.885(16)	P(1) – O(40)	1.539(15)
W(3) – O(6)	1.915(17)	P(1) – O(39)	1.563(13)
W(3) – O(44)	1.929(17)	P(1) – O(28)	1.583(15)
W(3) – O(42)	1.931(17)	P(1) – O(15)	1.608(16)
W(3) – O(15)	2.403(14)	Cu(12) – O(27)	1.932(18)
W(4) – O(31)	1.712(16)	N(3) – C(11)	1.31(3)
W(4) – O(11)	1.865(16)	N(3) – C(12)	1.32(3)
W(4) – O(12)	1.895(15)	N(1) – C(2)	1.27(3)
W(4) – O(2)	1.935(17)	N(1) – C(16)	1.36(3)
W(4) – O(13)	1.958(17)	N(2) – C(36)	1.37(3)
W(4) – O(28)	2.367(15)	N(2) – C(8)	1.39(3)
W(5) – O(19)	1.708(16)	N(5) – C(20)	1.31(3)
W(5) – O(14)	1.858(16)	N(5) – C(22)	1.39(4)
W(5) – O(16)	1.884(15)	N(6) – C(28)	1.37(4)
W(5) – O(29)	1.947(18)	N(6) – C(27)	1.40(4)
W(5) – O(44)	1.952(17)	N(4) – C(31)	1.24(4)
W(5) – O(15)	2.392(15)	N(4) – C(33)	1.34(5)
W(6) – O(33)	1.710(16)	C(7) – C(8)	1.29(4)
W(6) – O(47)	1.833(17)	C(7) – C(6)	1.36(3)
W(6) – O(43)	1.869(17)	C(4) – C(16)	1.35(4)
W(6) – O(16)	1.921(16)	C(4) – C(5)	1.36(3)
W(6) – O(21)	1.958(17)	C(5) – C(3)	1.38(3)

(cont. on the next page)

Table A.1. (cont.)

W(6) – O(39)	2.446(14)	C(5) – C(6)	1.50(3)
W(7) – O(35)	1.720(17)	C(2)- C(3)	1.36(4)
W(7) – O(24)	1.903(18)	C(13) – C(11)	1.32(4)
W(7) – O(23)	1.915(16)	C(13) – C(14)	1.42(4)
W(7) – O(46)	1.940(14)	C(12) – C(18)	1.36(4)
W(7) – O(22)	1.949(18)	C(14) – C(18)	1.37(3)
W(7) – O(40)	2.419(16)	C(14) – C(13)	1.42(4)
W(8) – O(36)	1.691(14)	C(14) – C(15)	1.51(4)
W(8) – O(45)	1.868(17)	C(15) – C(30)	1.34(4)
W(8) – O(23)	1.908(17)	C(15) – C(32)	1.40(4)
W(8) – O(26)	1.948(18)	C(6) – C(17)	1.43(3)
W(8) – O(43)	1.997(16)	C(20) – C(21)	1.26(4)
W(8) – O(39)	2.414(14)	C(24) – C(25)	1.40(4)
W(9) – O(37)	1.688(14)	C(24) – C(26)	1.42(4)
W(9) – O(46)	1.905(16)	C(24) – C(23)	1.47(4)
W(9) – O(5)	1.975(17)	C(26) – C(27)	1.37(4)
W(9) – O(37)	1.688(14)	C(25) – C(28)	1.27(4)
W(9) – O(46)	1.905(16)	C(21) – C(23)	1.45(4)
W(9) – O(5)	1.975(17)	C(17) – C(36)	1.33(4)
W(10) – O(30)	1.711(16)	C(23) – C(35)	1.29(4)
W(10) – O(21)	1.878(18)	C(22) – C(35)	1.30(5)
W(10) – O(1)	1.883(16)	C(30) – C(31)	1.42(5)
W(10) – O(26)	1.920(17)	C(32) – C(33)	1.36(5)
W(10) – O(12)	1.937(15)		

APPENDIX B

BOND ANGLES ($^{\circ}$) FOR $(4,4'$ -bpyH₂)₃[PCuW₁₁O₃₉]

Table B.1. Bond angles ($^{\circ}$) for $(4,4'$ -bpyH₂)₃[PCuW₁₁O₃₉]

O(34) – W(1) – O(1)	103.5(8)	O(21) – W(10) – O(39)	71.8(6)
O(34) – W(1) – O(29)	102.6(8)	O(1) – W(10) – O(39)	85.2(7)
O(1) – W(1) – O(29)	90.4(7)	O(26) – W(10) – O(39)	71.9(6)
O(34) – W(1) – O(6)	98.8(8)	O(12) – W(10) – O(39)	83.4(5)
O(1) – W(1) – O(6)	157.7(8)	O(27) – W(11) – O(47)	104.6(8)
O(29) – W(1) – O(6)	85.9(7)	O(27) – W(11) – O(24)	99.1(8)
O(34) – W(1) – O(2)	102.6(8)	O(47) – W(11) – O(24)	91.9(7)
O(1) – W(1) – O(2)	86.7(7)	O(27) – W(11) – O(25)	95.3(7)
O(29) – W(1) – O(2)	154.7(7)	O(47) – W(11) – O(25)	159.9(8)
O(6) – W(1) – O(2)	87.4(7)	O(24) – W(11) – O(25)	87.6(7)
O(34) – W(1) – O(15)	168.0(6)	O(27) – W(11) – O(14)	101.6(7)
O(1) – W(1) – O(15)	86.6(7)	O(47) – W(11) – O(14)	86.4(7)
O(29) – W(1) – O(15)	70.5(6)	O(24) – W(11) – O(14)	159.0(7)
O(6) – W(1) – O(15)	71.4(6)	O(25) – W(11) – O(14)	87.0(7)
O(2) – W(1) – O(15)	84.2(6)	O(27) – W(11) – O(40)	165.4(7)
O(32) – W(2) – O(13)	101.0(8)	O(47) – W(11) – O(40)	88.2(6)
O(32) – W(2) – O(4)	99.9(8)	O(24) – W(11) – O(40)	73.0(6)
O(13) – W(2) – O(4)	88.2(7)	O(25) – W(11) – O(40)	72.4(6)
O(32) – W(2) – O(5)	103.1(8)	O(14) – W(11) – O(40)	86.0(6)
O(13) – W(2) – O(5)	155.7(7)	O(22) – W(12) – O(45)	90.7(8)
O(4) – W(2) – O(5)	90.5(7)	O(22) – W(12) – O(27)	99.8(7)
O(32) – W(2) – O(42)	101.6(7)	O(45) – W(12) – O(27)	99.9(8)
O(13) – W(2) – O(42)	85.9(7)	O(22) – W(12) – O(11)	159.8(7)
O(32) – W(2) – O(28)	170.8(7)	O(22) – W(12) – O(4)	88.0(7)
O(13) – W(2) – O(28)	71.7(6)	O(45) – W(12) – O(4)	158.8(7)
O(5) – W(2) – O(28)	84.6(6)	O(11) – W(12) – O(4)	86.2(7)
O(42) – W(2) – O(28)	83.6(6)	O(22) – W(12) – O(28)	87.3(6)
O(7) – W(3) – O(8)	101.7(8)	O(45) – W(12) – O(28)	86.9(6)
O(7) – W(3) – O(6)	101.5(8)	O(27) – W(12) – O(28)	170.0(7)
O(8) – W(3) – O(6)	156.8(6)	O(40) – P(1) – O(39)	110.3(9)
O(7) – W(3) – O(44)	100.1(7)	O(40) – P(1) – O(28)	109.6(9)
O(8) – W(3) – O(44)	90.5(7)	O(39) – P(1) – O(28)	110.4(8)
O(6) – W(3) – O(44)	86.9(7)	O(40) – P(1) – O(15)	109.2(7)
O(7) – W(3) – O(42)	103.0(7)	O(39) – P(1) – O(15)	108.9(9)
O(8) – W(3) – O(42)	86.9(7)	O(28) – P(1) – O(15)	108.5(8)

(cont. on the next page)

Table B.1. (cont.)

O(6) – W(3) – O(42)	86.5(8)	O(40) – P(1) – O(39)	110.3(9)
O(44) – W(3) – O(42)	156.8(7)	O(40) – P(1) – O(28)	109.6(9)
O(7) – W(3) – O(15)	169.0(7)	O(39) – P(1) – O(28)	110.4(8)
O(8) – W(3) – O(15)	85.8(6)	O(40) – P(1) – O(15)	109.2(8)
O(6) – W(3) – O(15)	71.5(6)	O(39) – P(1) – O(15)	108.9(9)
O(44) – W(3) – O(15)	71.5(6)	O(28) – P(1) – O(15)	108.5(8)
O(42) – W(3) – O(15)	85.3(6)	W(10) – O(26) – W(8)	125.7(8)
O(31) – W(4) – O(11)	100.7(8)	W(4) – O(11) – W(12)	123.4(8)
O(31) – W(4) – O(12)	104.7(7)	W(2) – O(4) – W(12)	123.0(9)
O(11) – W(4) – O(12)	91.4(7)	P(1) – O(28) – W(2)	126.2(8)
O(31) – W(4) – O(2)	103.3(8)	P(1) – O(28) – W(4)	127.6(9)
O(11) – W(4) – O(2)	156.0(7)	W(2) – O(28) – W(4)	92.2(5)
O(12) – W(4) – O(2)	83.3(7)	P(1) – O(28) – W(12)	120.7(8)
O(31) – W(4) – O(13)	98.9(8)	W(2) – O(28) – W(12)	90.3(5)
O(11) – W(4) – O(13)	90.8(7)	W(4) – O(28) – W(12)	88.7(5)
O(12) – W(4) – O(13)	155.5(6)	W(3) – O(6) – W(1)	126.2(9)
O(2) – W(4) – O(13)	84.8(7)	W(12) – O(22) – W(7)	145.5(11)
O(31) – W(4) – O(28)	168.5(7)	W(5) – O(14) – W(11)	146.4(8)
O(11) – W(4) – O(28)	75.4(6)	P(1) – O(15) – W(5)	125.2(8)
O(12) – W(4) – O(28)	86.3(5)	P(1) – O(15) – W(3)	124.1(9)
O(2) – W(4) – O(28)	80.9(6)	W(5) – O(15) – W(3)	91.9(5)
O(13) – W(4) – O(28)	70.6(6)	P(1) – O(15) – W(1)	123.0(8)
O(19) – W(5) – O(14)	105.2(8)	W(5) – O(15) – W(1)	92.1(6)
O(19) – W(5) – O(16)	104.2(8)	W(3) – O(15) – W(1)	90.8(5)
O(14) – W(5) – O(16)	89.4(7)	W(11) – O(27) – Cu(12)	161.4(11)
O(19) – W(5) – O(29)	97.9(8)	W(11) – O(27) – W(12)	161.4(11)
O(14) – W(5) – O(29)	156.5(7)	Cu(12) – O(27) – W(12)	0.0(13)
O(16) – W(5) – O(29)	88.7(7)	W(4) – O(12) – W(10)	153.3(8)
O(19) – W(5) – O(44)	98.9(7)	W(10) – O(21) – W(6)	128.0(9)
O(14) – W(5) – O(44)	89.7(7)	W(8) – O(23) – W(7)	149.3(9)
O(16) – W(5) – O(44)	156.3(7)	W(9) – O(25) – W(11)	123.2(8)
O(14) – W(5) – O(15)	86.2(6)	W(3) – O(8) – W(9)	151.0(8)
O(16) – W(5) – O(15)	84.8(6)	W(7) – O(24) – W(11)	124.1(9)
O(29) – W(5) – O(15)	70.3(7)	W(2) – O(13) – W(4)	124.8(9)
O(44) – W(5) – O(15)	71.4(6)	W(1) – O(2) – W(4)	151.7(10)
O(33) – W(6) – O(47)	102.4(8)	W(1) – O(5) – W(9)	151.7(10)
O(33) – W(6) – O(43)	100.6(8)	P(1) – O(40) – W(9)	128.5(9)
O(47) – W(6) – O(43)	91.0(7)	P(1) – O(40) – W(7)	125.8(7)
O(33) – W(6) – O(16)	103.6(8)	W(9) – O(40) – W(7)	90.6(5)
O(47) – W(6) – O(16)	86.7(7)	P(1) – O(40) – W(11)	123.0(9)
O(43) – W(6) – O(16)	155.6(7)	W(9) – O(40) – W(11)	88.3(4)
O(33) – W(6) – O(21)	100.8(8)	W(7) – O(40) – W(11)	88.6(5)
O(47) – W(6) – O(21)	156.8(8)	P(1) – O(39) – W(8)	125.3(8)

(cont. on the next page)

Table B.1. (cont.)

O(43) – W(6) – O(21)	85.9(7)	P(1) – O(39) – W(6)	125.2(7)
O(16) – W(6) – O(21)	86.7(7)	W(8) – O(39) – W(6)	90.7(5)
O(33) – W(6) – O(39)	168.7(6)	P(1) – O(39) – W(10)	125.3(8)
O(47) – W(6) – O(39)	86.3(7)	W(8) – O(39) – W(10)	89.9(4)
O(43) – W(6) – O(39)	71.8(6)	W(6) – O(39) – W(10)	89.3(5)
O(16) – W(6) – O(39)	83.8(6)	W(1) – O(29) – W(5)	127.0(9)
O(21) – W(6) – O(39)	70.9(6)	W(8) – O(45) – W(12)	148.5(9)
O(35) – W(7) – O(24)	99.8(8)	W(3) – O(42) – W(2)	148.8(10)
O(35) – W(7) – O(23)	103.0(7)	W(6) – O(43) – W(8)	126.8(9)
O(24) – W(7) – O(23)	88.2(7)	W(3) – O(44) – W(5)	125.2(8)
O(35) – W(7) – O(46)	101.0(7)	W(9) – O(46) – W(7)	124.4(8)
O(24) – W(7) – O(46)	89.0(7)	W(6) – O(47) – W(11)	150.5(11)
O(23) – W(7) – O(46)	155.9(7)	C(11) – N(3) – C(12)	121(3)
O(35) – W(7) – O(22)	101.9(8)	C(2) – N(1) – C(16)	122(3)
O(24) – W(7) – O(22)	158.2(7)	C(8) – C(7) – C(6)	125(3)
O(23) – W(7) – O(22)	88.2(7)	C(36) – N(2) – C(8)	116(3)
O(46) – W(7) – O(22)	85.6(7)	C(7) – C(8) – N(2)	122(3)
O(35) – W(7) – O(40)	170.0(6)	C(16) – C(4) – C(5)	119(2)
O(24) – W(7) – O(40)	74.3(6)	C(4) – C(5) – C(3)	117(2)
O(23) – W(7) – O(40)	85.1(6)	C(4) – C(5) – C(6)	123(2)
O(46) – W(7) – O(40)	71.1(6)	C(3) – C(5) – C(6)	119(2)
O(22) – W(7) – O(40)	84.0(6)	N(1) – C(2) – C(3)	119(2)
O(36) – W(8) – O(45)	102.9(7)	C(11) – C(13) – C(14)	124(3)
O(36) – W(8) – O(23)	102.9(8)	N(3) – C(12) – C(18)	122(2)
O(45) – W(8) – O(23)	88.2(7)	C(18) – C(14) – C(13)	114(3)
O(36) – W(8) – O(26)	100.5(8)	C(18) – C(14) – C(15)	122(3)
O(45) – W(8) – O(26)	89.0(7)	C(13) – C(14) – C(15)	123(2)
O(23) – W(8) – O(26)	156.5(6)	N(3) – C(11) – C(13)	119(2)
O(36) – W(8) – O(43)	101.2(7)	C(2) – C(3) – C(5)	122(3)
O(45) – W(8) – O(43)	155.9(7)	C(30) – C(15) – C(32)	120(3)
O(23) – W(8) – O(43)	87.4(7)	C(30) – C(15) – C(14)	119(2)
O(26) – W(8) – O(43)	85.7(7)	C(32) – C(15) – C(14)	120(3)
O(36) – W(8) – O(39)	169.2(7)	C(7) – C(6) – C(17)	112(2)
O(45) – W(8) – O(39)	85.3(6)	C(7) – C(6) – C(5)	127(2)
O(23) – W(8) – O(39)	84.1(6)	C(7) – C(8) – N(2)	122(3)
O(26) – W(8) – O(39)	72.5(6)	C(17) – C(6) – C(5)	121(2)
O(43) – W(8) – O(39)	70.7(6)	C(20) – N(5) – C(22)	121(3)
O(37) – W(9) – O(25)	101.7(8)	C(28) – N(6) – C(27)	110(3)
O(37) – W(9) – O(46)	99.3(7)	C(21) – C(20) – N(5)	122(3)
O(25) – W(9) – O(46)	91.7(7)	C(25) – C(24) – C(26)	114(3)
O(37) – W(9) – O(8)	101.6(7)	C(25) – C(24) – C(23)	126(3)
O(25) – W(9) – O(8)	91.9(7)	C(26) – C(24) – C(23)	120(3)

(cont. on the next page)

Table B.1. (cont.)

O(46) – W(9) – O(8)	157.6(6)	C(27) – C(26) – C(24)	119(3)
O(37) – W(9) – O(5)	101.1(8)	C(28) – C(25) – C(24)	122(3)
O(25) – W(9) – O(5)	157.2(7)	C(20) – C(21) – C(23)	120(2)
O(46) – W(9) – O(5)	84.6(7)	C(36) – C(17) – C(6)	124(3)
O(37) – W(9) – O(40)	83.6(7)	C(2) – C(3) – C(5)	122(3)
O(25) – W(9) – O(40)	76.0(6)	C(4) – C(16) – N(1)	121(3)
O(46) – W(9) – O(40)	73.0(6)	C(12) – C(18) – C(14)	120(3)
O(8) – W(9) – O(40)	86.5(6)	C(25) – C(28) – N(6)	129(3)
O(5) – W(9) – O(40)	81.4(6)	C(35) – C(23) – C(21)	114(3)
O(30) – W(10) – O(21)	102.4(9)	C(35) – C(23) – C(24)	129(3)
O(30) – W(10) – O(1)	103.2(9)	C(21) – C(23) – C(24)	117(2)
O(21) – W(10) – O(1)	89.4(8)	C(35) – C(22) – N(5)	114(3)
O(30) – W(10) – O(26)	100.0(8)	C(26) – C(27) – N(6)	126(4)
O(21) – W(10) – O(26)	87.4(7)	C(31) – N(4) – C(33)	116(3)
O(1) – W(10) – O(26)	83.4(5)	C(15) – C(30) – C(31)	115(3)
O(27) – W(10) – O(47)	156.7(7)	N(4) – C(31) – C(30)	126(3)
O(30) – W(10) – O(12)	102.7(8)	C(33) – C(32) – C(15)	117(4)
O(21) – W(10) – O(12)	154.9(7)	N(4) – C(33) – C(32)	124(4)
O(1) – W(10) – O(12)	85.2(7)	C(17) – C(36) – N(2)	120(3)
O(26) – W(10) – O(12)	88.0(7)	C(23) – C(35) – C(22)	128(4)
O(30) – W(10) – O(39)	169.9(7)		

APPENDIX C

BOND LENGTHS (Å) FOR (4,4'-bpyH₂)[H₂PW₁₂O₄₀]₂.H₂O

Table C.1. Bond lengths (Å) for (4,4'-bpyH₂)[H₂PW₁₂O₄₀]₂.H₂O

W(1) – O(2)	1.647(13)	W(3) – O(13)	2.490(2)
W(1) – O(10)	1.844(18)	W(4) – O(8)	1.647(14)
W(1) – O(1)	1.853(18)	W(4) – O(9)	1.850(2)
W(1) – O(3)	1.924(18)	W(4) – O(11)	1.894(19)
W(1) – O(10)	1.940(2)	W(4) – O(9)	1.907(19)
W(1) – O(14)	2.420(2)	W(4) – O(5)	1.950(2)
W(2) – O(12)	1.669(18)	W(4) – O(16)	2.433(2)
W(2) – O(5)	1.836(17)	P(1) – O(13)	1.500(2)
W(2) – O(4)	1.869 (19)	P(1) – O(14)	1.620(4)
W(2) – O(4)	1.921(18)	P(2) – O(15)	1.490(2)
W(2) – O(11)	1.900(17)	P(2) – O(16)	1.590(3)
W(2) – O(15)	2.430(2)	N(1) – C(1)	1.350(3)
W(2) – O(15)	2.480(2)	C(1) – C(2)	1.370(3)
W(3) – O(6)	1.676(15)	C(2) – C(3)	1.430(3)
W(3) – O(3)	1.856(16)	C(3) – C(4)	1.460(4)
W(3) – O(7)	1.859(19)	C(4) – C(6)	1.380(3)
W(3) – O(1)	1.929(16)	N(2) – C(5)	1.340(3)
W(3) – O(7)	1.956(18)	C(5) – C(6)	1.400(3)
W(3) – O(13)	2.450(2)		

APPENDIX D

BOND ANGLES ($^{\circ}$) FOR (4,4'-bpyH₂)[H₂PW₁₂O₄₀]₂.H₂O

Table D.1. Bond angles ($^{\circ}$) for (4,4'-bpyH₂)[H₂PW₁₂O₄₀]₂.H₂O

O(2) – W(1) – O(10)	103.4(11)	O(11) – W(2) – O(15)	66.0(8)
O(2) – W(1) – O(1)	101.7(9)	O(4) – W(2) – O(15)	91.9(9)
O(10) – W(1) – O(1)	90.8(9)	O(12) – W(2) – O(15)	160.9(10)
O(2) – W(1) – O(3)	101.4(8)	O(5) – W(2) – O(15)	66.8(8)
O(10) – W(1) – O(3)	155.0(11)	O(4) – W(2) – O(15)	94.7(9)
O(1) – W(1) – O(3)	87.8(8)	O(11) – W(2) – O(15)	88.9(9)
O(2) – W(1) – O(10)	103.5(10)	O(4) – W(2) – O(15)	62.0(9)
O(10) – W(1) – O(10)	88.1(11)	O(15) – W(2) – O(15)	38.7(9)
O(1) – W(1) – O(10)	154.4(11)	O(6) – W(3) – O(3)	102.2(10)
O(3) – W(1) – O(10)	82.6(9)	O(6) – W(3) – O(7)	101.4(10)
O(2) – W(1) – O(14)	158.8(10)	O(3) – W(3) – O(7)	92.7(9)
O(10) – W(1) – O(14)	63.0(10)	O(6) – W(3) – O(1)	103.3(10)
O(1) – W(1) – O(14)	95.0(9)	O(3) – W(3) – O(1)	154.0(10)
O(3) – W(1) – O(14)	92.2(8)	O(7) – W(3) – O(1)	87.2(8)
O(1) – W(1) – O(14)	61.9(9)	O(6) – W(3) – O(7)	100.2(9)
O(12) – W(2) – O(5)	104.1(11)	O(3) – W(3) – O(7)	86.9(8)
O(12) – W(2) – O(4)	102.1(11)	O(7) – W(3) – O(7)	158.0(14)
O(5) – W(2) – O(4)	89.4(9)	O(1) – W(3) – O(7)	83.6(8)
O(12) – W(2) – O(11)	100.7(11)	O(6) – W(3) – O(13)	159.4(9)
O(5) – W(2) – O(11)	155.1(10)	O(3) – W(3) – O(13)	65.0(8)
O(4) – W(2) – O(11)	87.1(8)	O(7) – W(3) – O(13)	95.5(9)
O(12) – W(2) – O(4)	102.1(11)	O(1) – W(3) – O(13)	89.1(9)
O(5) – W(2) – O(4)	87.9(8)	O(7) – W(3) – O(13)	64.4(9)
O(4) – W(2) – O(4)	155.6(14)	O(6) – W(3) – O(13)	160.5(8)
O(11) – W(2) – O(4)	85.2(9)	O(3) – W(3) – O(13)	92.4(9)
O(12) – W(2) – O(15)	160.0(11)	O(7) – W(3) – O(13)	64.7(8)
O(5) – W(2) – O(15)	90.5(9)	O(1) – W(3) – O(13)	64.1(8)
O(4) – W(2) – O(15)	63.8(9)	O(7) – W(3) – O(13)	93.2(8)
O(12) – W(2) – O(11)	100.7(11)	O(6) – W(3) – O(13)	159.4(9)
O(5) – W(2) – O(11)	155.1(10)	O(3) – W(3) – O(13)	65.0(8)
O(4) – W(2) – O(11)	87.1(8)	O(7) – W(3) – O(13)	95.5(9)
O(12) – W(2) – O(4)	102.1(11)	O(1) – W(3) – O(13)	89.1(9)
O(5) – W(2) – O(4)	87.9(8)	O(7) – W(3) – O(13)	64.4(9)
O(4) – W(2) – O(4)	155.6(14)	O(6) – W(3) – O(13)	160.5(8)
O(11) – W(2) – O(4)	85.2(9)	O(3) – W(3) – O(13)	92.4(9)

(cont. on the next page)

Table D.1. (cont.)

O(12) – W(2) – O(15)	160.0(11)	O(7) – W(3) – O(13)	64.7(8)
O(5) – W(2) – O(15)	90.5(9)	O(1) – W(3) – O(13)	64.1(8)
O(4) – W(2) – O(15)	63.8(9)	O(7) – W(3) – O(13)	93.2(8)
O(13) – W(3) – O(13)	39.9(8)	O(13) – P(1) – O(14)	72.5(8)
O(8) – W(4) – O(9)	105.0(11)	O(13) – P(1) – O(14)	107.5(8)
O(8) – W(4) – O(11)	100.7(9)	O(14) – P(1) – O(14)	180.0(4)
O(9) – W(4) – O(11)	88.5(10)	O(15) – P(2) – O(15)	66.4(6)
O(8) – W(4) – O(9)	105.2(11)	O(15) – P(2) – O(15)	113.6(6)
O(9) – W(4) – O(9)	89.1(11)	O(15) – P(2) – O(15)	180.0(2)
O(11) – W(4) – O(9)	153.7(11)	O(15) – P(2) – O(16)	75.1(8)
O(8) – W(4) – O(5)	101.1(9)	O(15) – P(2) – O(16)	104.9(8)
O(9) – W(4) – O(5)	153.9(11)	O(16) – P(2) – O(16)	180.0(2)
O(11) – W(4) – O(5)	86.9(8)	P(1) – O(13) – W(3)	126.8(12)
O(9) – W(4) – O(9)	89.1(11)	O(15) – P(2) – O(15)	180.0(2)
O(11) – W(4) – O(9)	153.7(11)	O(15) – P(2) – O(16)	75.1(8)
O(8) – W(4) – O(5)	101.1(9)	O(15) – P(2) – O(16)	104.9(8)
O(9) – W(4) – O(5)	153.9(11)	O(16) – P(2) – O(16)	180.0(2)
O(11) – W(4) – O(5)	86.9(8)	P(1) – O(13) – W(3)	126.8(12)
O(9) – W(4) – O(5)	83.8(10)	P(1) – O(13) – W(3)	124.6(12)
W(2) – O(4) – W(2)	140.1(13)	W(4) – O(16) – W(4)	93.4(9)
W(3) – O(3) – W(1)	140.6(11)	C(1) – N(1) – C(1)	120.0(3)
W(3) – O(7) – W(3)	138.1(13)	N(1) – C(1) – C(2)	122.0(3)
W(4) – O(9) – W(4)	141.3(14)	C(1) – C(2) – C(3)	120.0(3)
W(2) – O(5) – W(4)	140.5(11)	C(2) – C(3) – C(2)	116.0(3)
W(4) – O(11) – W(2)	140.6(11)	C(2) – C(3) – C(4)	121.9(15)
W(1) – O(10) – W(1)	140.0(15)	C(6) – C(4) – C(6)	119.0(3)
O(13) – P(1) – O(13)	111.4(8)	C(6) – C(4) – C(3)	120.7(16)
O(13) – P(1) – O(13)	68.6(8)	C(5) – N(2) – C(5)	120.0(3)
O(13) – P(1) – O(13)	180.0(19)	N(2) – C(5) – C(6)	121.0(3)
O(13) – P(1) – O(13)	111.4(8)	C(4) – C(6) – C(5)	120.0(2)
O(13) – P(1) – O(14)	107.5(8)		

APPENDIX E

BOND LENGTHS (Å) FOR (4,4'-bpyH₂)₄[H₂P₂W₁₈O₆₂]₂

Table E.1. Bond lengths (Å) for (4,4'-bpyH₂)₄[H₂P₂W₁₈O₆₂]₂

W(1) – O(36)	1.67(3)	W(5) – O(19)	1.91(2)
W(1) – O(23)	1.89(2)	W(5) – O(50)	1.92(2)
W(1) – O(52)	1.89(2)	W(5) – O(38)	1.93(3)
W(1) – O(58)	1.92(2)	W(5) – O(75)	1.96(2)
W(1) – O(21)	1.93(2)	W(5) – O(65)	2.36(2)
W(1) – O(67)	2.37(2)	W(6) – O(49)	1.72(2)
W(2) – O(33)	1.73(2)	W(6) – O(22)	1.86(2)
W(2) – O(18)	1.84(2)	W(6) – O(26)	1.899(19)
W(2) – O(57)	1.85(2)	W(6) – O(59)	1.92(2)
W(2) – O(59)	1.89(2)	W(6) – O(93)	1.93(2)
W(2) – O(62)	1.95(2)	W(6) – O(69)	2.34(2)
W(2) – O(69)	2.41(2)	W(7) – O(7)	1.73(3)
W(3) – O(48)	1.72(3)	W(7) – O(21)	1.85(2)
W(3) – O(4)	1.93(2)	W(7) – O(39)	1.87(2)
W(3) – O(89)	1.93(2)	W(7) – O(28)	1.91(2)
W(3) – O(20)	1.959(18)	W(7) – O(26)	1.940(19)
W(3) – O(3)	1.966(18)	W(7) – O(72)	2.42(2)
W(3) – O(68)	2.34(2)	W(8) – O(106)	1.73(3)
W(4) – O(61)	1.71(2)	W(8) – O(14)	1.87(2)
W(4) – O(52)	1.89(2)	W(8) – O(89)	1.92(2)
W(4) – O(10)	1.91(2)	W(8) – O(97)	1.95(2)
W(4) – O(94)	1.93(2)	W(8) – O(34)	1.99(2)
W(4) – O(22)	1.93(2)	W(8) – O(74)	2.35(2)
W(4) – O(66)	2.33(2)	W(9) – O(54)	1.72(3)
W(5) – O(86)	1.75(3)	W(9) – O(94)	1.87(2)
W(9) – O(58)	1.95(2)	W(13) – O(71)	2.394(19)
W(9) – O(53)	1.96(2)	W(14) – O(41)	1.72(2)
W(9) – O(76)	2.38(2)	W(14) – O(15)	1.87(2)
W(10) – O(30)	1.70(3)	W(14) – O(8)	1.91(2)
W(10) – O(63)	1.89(3)	W(14) – O(23)	1.92(2)
W(10) – O(1)	1.92(2)	W(14) – O(9)	1.94(2)
W(10) – O(45)	1.92(2)	W(14) – O(67)	2.39(2)
W(10) – O(115)	1.94(2)	W(15) – O(60)	1.74(2)
W(10) – O(73)	2.34(2)	W(15) – O(42)	1.83(2)
W(11) – O(44)	1.65(3)	W(15) – O(15)	1.92(3)

(cont. on the next page)

Table E.1. (cont.)

W(11) – O(43)	1.88(2)	W(15) – O(11)	1.94(2)
W(11) – O(47)	1.90(2)	W(15) – O(39)	1.96(2)
W(11) – O(2)	1.93(2)	W(15) – O(72)	2.45(2)
W(11) – O(27)	1.95(2)	W(16) – O(25)	1.72(2)
W(11) – O(70)	2.31(2)	W(16) – O(20)	1.844(18)
W(12) – O(111)	1.72(3)	W(16) – O(1)	1.85(2)
W(12) – O(38)	1.87(3)	W(16) – O(43)	1.92(2)
W(12) – O(24)	1.88(2)	W(16) – O(14)	1.94(2)
W(12) – O(57)	1.94(2)	W(16) – O(70)	2.343(19)
W(12) – O(116)	1.97(3)	W(17) – O(80)	1.75(2)
W(12) – O(71)	2.38(2)	W(17) – O(53)	1.90(2)
W(13) – O(17)	1.72(3)	W(17) – O(50)	1.92(2)
W(13) – O(24)	1.91(2)	W(17) – O(95)	1.91(2)
W(13) – O(55)	1.93(2)	W(17) – O(84)	1.94(2)
W(13) – O(64)	1.93(2)	W(17) – O(76)	2.39(2)
W(13) – O(42)	1.94(2)	W(18) – O(51)	1.72(2)
W(18) – O(12)	1.87(2)	W(22) – O(79)	1.95(2)
W(18) – O(88)	1.89(2)	W(22) – O(16)	1.95(2)
W(18) – O(97)	1.89(2)	W(22) – O(98)	2.45(2)
W(18) – O(47)	1.90(2)	W(23) – O(32)	1.69(2)
W(18) – O(74)	2.34(2)	W(23) – O(10)	1.86(2)
W(19) – O(102)	1.69(3)	W(23) – O(84)	1.88(2)
W(19) – O(16)	1.86(2)	W(23) – O(19)	1.93(2)
W(19) – O(35)	1.89(2)	W(23) – O(18)	1.96(2)
W(19) – O(88)	1.89(2)	W(23) – O(66)	2.41(2)
W(19) – O(34)	1.94(2)	W(24) – O(31)	1.71(2)
W(19) – O(74)	2.34(2)	W(24) – O(11)	1.91(2)
W(20) – O(119)	1.73(3)	W(24) – O(64)	1.92(2)
W(20) – O(2)	1.86(2)	W(24) – O(113)	1.94(3)
W(20) – O(45)	1.87(2)	W(24) – O(6)	1.95(2)
W(20) – O(81)	1.90(3)	W(24) – O(77)	2.40(2)
W(20) – O(87)	1.92(3)	W(25) – O(108)	1.72(3)
W(20) – O(73)	2.34(2)	W(25) – O(9)	1.89(2)
W(21) – O(105)	1.74(3)	W(25) – O(95)	1.93(3)
W(21) – O(115)	1.85(2)	W(25) – O(13)	1.94(2)
W(21) – O(99)	1.85(3)	W(25) – O(46)	1.94(2)
W(21) – O(4)	1.86(2)	W(25) – O(76)	2.38(2)
W(21) – O(56)	1.96(2)	W(26) – O(103)	1.68(3)
W(21) – O(78)	2.38(2)	W(26) – O(109)	1.88(3)
W(22) – O(107)	1.78(2)	W(26) – O(5)	1.91(2)
W(22) – O(101)	1.85(3)	W(26) – O(40)	1.91(2)
W(22) – O(100)	1.91(2)	W(26) – O(99)	1.92(3)
W(26) – O(78)	2.38(2)	W(31) – O(116)	1.84(3)

(cont. on the next page)

Table E.1. (cont.)

W(27) – O(114)	1.75(3)	W(31) – O(62)	1.86(2)
W(27) – O(37)	1.87(2)	W(31) – O(6)	1.92(2)
W(27) – O(27)	1.87(2)	W(31) – O(90)	1.95(2)
W(27) – O(100)	1.88(2)	W(31) – O(77)	2.37(2)
W(27) – O(12)	1.96(2)	W(32) – O(121)	1.71(3)
W(27) – O(98)	2.33(3)	W(32) – O(109)	1.90(3)
W(28) – O(29)	1.72(2)	W(32) – O(110)	1.91(3)
W(28) – O(79)	1.86(2)	W(32) – O(117)	1.92(3)
W(28) – O(5)	1.89(2)	W(32) – O(101)	1.93(3)
W(28) – O(3)	1.893(19)	W(32) – O(85)	2.41(2)
W(28) – O(35)	1.95(2)	W(33) – O(122)	1.70(3)
W(28) – O(68)	2.41(2)	W(33) – O(82)	1.85(3)
W(29) – O(104)	1.63(2)	W(33) – O(56)	1.86(2)
W(29) – O(55)	1.87(2)	W(33) – O(118)	1.88(3)
W(29) – O(8)	1.89(2)	W(33) – O(63)	1.89(3)
W(29) – O(13)	1.90(2)	W(33) – O(91)	2.39(3)
W(29) – O(75)	1.92(2)	W(34) – O(124)	1.80(4)
W(29) – O(65)	2.38(2)	W(34) – O(81)	1.90(3)
W(30) – O(92)	1.74(2)	W(34) – O(110)	1.91(3)
W(30) – O(93)	1.90(2)	W(34) – O(37)	1.91(2)
W(30) – O(28)	1.91(2)	W(34) – O(83)	1.96(2)
W(30) – O(90)	1.92(2)	W(34) – O(85)	2.36(2)
W(30) – O(113)	1.93(3)	W(35) – O(120)	1.72(3)
W(30) – O(77)	2.39(2)	W(35) – O(117)	1.90(3)
W(31) – O(112)	1.73(3)	W(35) – O(123)	1.91(3)
W(35) – O(40)	1.92(2)	C(1) – C(3)	1.49(5)
W(35) – O(82)	1.95(3)	C(2) – C(3)	1.32(6)
W(35) – O(91)	2.34(3)	C(2) – C(13)	1.42(5)
W(36) – O(96)	1.76(3)	C(2) – C(24)	1.49(5)
W(36) – O(83)	1.87(2)	C(3) – C(16)	1.29(6)
W(36) – O(87)	1.91(2)	C(4) – C(5)	1.33(4)
W(36) – O(118)	1.94(3)	C(4) – C(27)	1.38(6)
W(36) – O(123)	1.96(3)	C(4) – C(6)	1.48(5)
W(36) – O(91)	2.32(3)	C(5) – C(10)	1.31(6)
P(1) – O(67)	1.51(2)	C(6) – C(22)	1.33(5)
P(1) – O(66)	1.53(2)	C(6) – C(29)	1.46(6)
P(1) – O(76)	1.58(3)	C(7) – C(15)	1.30(6)
P(2) – O(68)	1.52(2)	C(7) – C(17)	1.42(5)
P(2) – O(98)	1.52(3)	C(7) – C(8)	1.45(5)
P(2) – O(70)	1.59(2)	C(8) – C(25)	1.36(6)
P(2) – O(74)	1.65(2)	C(8) – C(18)	1.45(6)
P(3) – O(72)	1.46(2)	C(9) – N(1)	1.32(6)
P(3) – O(71)	1.48(2)	C(9) – C(15)	1.37(6)

(cont. on the next page)

Table E.1. (cont.)

P(3) – O(69)	1.53(2)	N(1) – C(11)	1.31(5)
P(3) – O(77)	1.57(2)	N(2) – C(40)	1.27(5)
P(4) – O(85)	1.51(2)	N(2) – C(42)	1.28(7)
P(4) – O(78)	1.52(3)	N(2) – Cu(1)	2.00(4)
P(4) – O(73)	1.56(2)	C(10) – N(5)	1.50(6)
P(4) – O(91)	1.63(3)	N(3) – C(14)	1.28(5)
Cu(1) – O(29)	4.00(4)	N(3) – C(12)	1.35(5)
C(1) – C(12)	1.34(5)	C(11) – C(17)	1.40(5)
C(13) – C(26)	1.34(5)	C(31) – C(41)	1.52(5)
C(14) – C(16)	1.45(6)	N(7) – C(45)	1.26(6)
C(18) – C(42)	1.21(7)	N(7) – C(36)	1.27(5)
C(19) – C(35)	1.36(5)	C(32) – C(33)	1.47(6)
C(19) – C(21)	1.46(6)	C(34) – C(44)	1.26(7)
C(19) – C(30)	1.48(5)	N(8) – C(38)	1.38(7)
N(4) – C(26)	1.27(5)	N(8) – C(37)	1.41(7)
N(4) – C(20)	1.32(5)	C(35) – C(36)	1.53(6)
C(20) – C(24)	1.26(6)	C(39) – C(50)	1.54(9)
N(5) – C(43)	1.26(7)	C(40) – C(25)	1.41(6)
C(21) – C(23)	1.32(6)	C(40) – Cu(1)	1.9(4)
C(21) – C(33)	1.38(6)	C(41) – C(46)	1.28(6)
C(22) – C(37)	1.52(6)	C(41) – C(48)	1.45(6)
C(23) – C(28)	1.31(7)	N(9) – C(50)	1.20(7)
C(25) – C(40)	1.41(6)	N(9) – C(44)	1.47(7)
C(27) – C(43)	1.60(7)	C(42) – C(18)	1.21(7)
C(28) – N(6)	1.41(6)	C(42) – Cu(1)	3.00(4)
C(29) – C(38)	1.27(6)	C(46) – C(49)	1.43(8)
C(30) – C(45)	1.38(7)	N(10) – C(47)	1.25(7)
N(6) – C(32)	1.30(5)	N(10) – C(49)	1.34(8)
C(31) – C(34)	1.29(6)	C(47) – C(48)	1.35(7)
C(31) – C(39)	1.34(7)		

APPENDIX F

BOND ANGLES ($^{\circ}$) FOR $(4,4'$ -bpyH₂)₄[H₂P₂W₁₈O₆₂]₂

Table F.1. Bond angles ($^{\circ}$) for $(4,4'$ -bpyH₂)₄[H₂P₂W₁₈O₆₂]₂

O(36) – W(1) – O(23)	100.1(11)	O(59) – W(2) – O(69)	72.7(8)
O(36) – W(1) – O(52)	104.3(11)	O(62) – W(2) – O(69)	81.0(9)
O(23) – W(1) – O(52)	155.4(9)	O(48) – W(3) – O(4)	98.6(11)
O(36) – W(1) – O(58)	93.4(11)	O(48) – W(3) – O(89)	96.4(11)
O(23) – W(1) – O(58)	89.8(9)	O(4) – W(3) – O(89)	164.7(10)
O(52) – W(1) – O(58)	85.8(9)	O(48) – W(3) – O(20)	101.7(10)
O(36) – W(1) – O(21)	99.3(11)	O(4) – W(3) – O(20)	89.0(9)
O(23) – W(1) – O(21)	92.1(9)	O(89) – W(3) – O(20)	85.3(9)
O(52) – W(1) – O(21)	86.9(9)	O(48) – W(3) – O(3)	99.8(10)
O(58) – W(1) – O(21)	166.6(9)	O(4) – W(3) – O(3)	92.9(9)
O(36) – W(1) – O(67)	173.4(10)	O(89) – W(3) – O(3)	87.2(9)
O(23) – W(1) – O(67)	74.2(8)	O(20) – W(3) – O(3)	157.9(8)
O(52) – W(1) – O(67)	81.3(8)	O(48) – W(3) – O(68)	173.7(9)
O(58) – W(1) – O(67)	83.3(9)	O(4) – W(3) – O(68)	82.7(9)
O(21) – W(1) – O(67)	84.5(8)	O(89) – W(3) – O(68)	82.6(9)
O(33) – W(2) – O(18)	98.5(10)	O(20) – W(3) – O(68)	84.5(7)
O(33) – W(2) – O(57)	100.7(10)	O(3) – W(3) – O(68)	73.9(7)
O(18) – W(2) – O(57)	91.9(10)	O(61) – W(4) – O(52)	103.4(10)
O(33) – W(2) – O(59)	100.7(10)	O(61) – W(4) – O(10)	101.8(10)
O(18) – W(2) – O(59)	89.0(10)	O(52) – W(4) – O(10)	154.6(10)
O(57) – W(2) – O(59)	158.2(10)	O(61) – W(4) – O(94)	95.2(10)
O(33) – W(2) – O(62)	97.7(10)	O(52) – W(4) – O(94)	85.9(10)
O(18) – W(2) – O(62)	163.8(10)	O(10) – W(4) – O(94)	89.8(10)
O(57) – W(2) – O(62)	83.4(10)	O(61) – W(4) – O(22)	100.6(10)
O(59) – W(2) – O(62)	89.7(10)	O(52) – W(4) – O(22)	87.8(9)
O(33) – W(2) – O(69)	173.3(9)	O(10) – W(4) – O(22)	89.6(10)
O(18) – W(2) – O(69)	83.1(9)	O(94) – W(4) – O(22)	163.9(9)
O(57) – W(2) – O(69)	85.8(9)	O(61) – W(4) – O(66)	173.9(9)
O(52) – W(4) – O(66)	82.0(9)	O(22) – W(6) – O(69)	83.1(8)
O(10) – W(4) – O(66)	72.7(9)	O(26) – W(6) – O(69)	83.4(8)
O(94) – W(4) – O(66)	82.2(9)	O(59) – W(6) – O(69)	73.9(8)
O(22) – W(4) – O(66)	82.3(8)	O(93) – W(6) – O(69)	82.2(9)
O(86) – W(5) – O(19)	100.7(10)	O(7) – W(7) – O(21)	99.3(11)
O(86) – W(5) – O(50)	97.4(11)	O(7) – W(7) – O(39)	102.0(11)
O(19) – W(5) – O(50)	88.8(10)	O(21) – W(7) – O(39)	93.1(10)

(cont. on the next page)

Table F.1. (cont.)

O(86) – W(5) – O(38)	97.9(11)	O(7) – W(7) – O(28)	93.8(11)
O(19) – W(5) – O(38)	88.2(10)	O(21) – W(7) – O(28)	165.8(9)
O(50) – W(5) – O(38)	164.7(10)	O(39) – W(7) – O(28)	89.5(9)
O(86) – W(5) – O(75)	97.3(10)	O(7) – W(7) – O(26)	100.0(10)
O(19) – W(5) – O(75)	162.0(10)	O(21) – W(7) – O(26)	87.2(9)
O(50) – W(5) – O(75)	89.4(10)	O(39) – W(7) – O(26)	157.6(9)
O(38) – W(5) – O(75)	88.8(10)	O(28) – W(7) – O(26)	85.0(8)
O(86) – W(5) – O(65)	171.5(9)	O(7) – W(7) – O(72)	176.2(10)
O(19) – W(5) – O(65)	87.8(8)	O(21) – W(7) – O(72)	84.2(9)
O(50) – W(5) – O(65)	83.5(9)	O(39) – W(7) – O(72)	76.1(9)
O(38) – W(5) – O(65)	81.4(9)	O(28) – W(7) – O(72)	83.0(8)
O(75) – W(5) – O(65)	74.3(8)	O(26) – W(7) – O(72)	81.7(8)
O(49) – W(6) – O(22)	97.0(11)	O(106) – W(8) – O(14)	104.2(13)
O(49) – W(6) – O(26)	99.4(10)	O(106) – W(8) – O(89)	102.7(14)
O(22) – W(6) – O(26)	87.0(9)	O(14) – W(8) – O(89)	86.5(10)
O(49) – W(6) – O(59)	103.3(10)	O(106) – W(8) – W(97)	100.4(14)
O(22) – W(6) – O(59)	90.6(10)	O(14) – W(8) – O(97)	91.1(10)
O(26) – W(6) – O(59)	157.3(9)	O(89) – W(8) – O(97)	156.7(10)
O(49) – W(6) – O(93)	97.8(11)	O(106) – W(8) – O(34)	96.6(13)
O(22) – W(6) – O(93)	164.8(9)	O(14) – W(8) – O(34)	159.1(9)
O(26) – W(6) – O(93)	87.1(9)	O(89) – W(8) – O(34)	87.6(9)
O(59) – W(6) – O(93)	89.5(10)	O(97) – W(8) – O(34)	86.4(9)
O(49) – W(6) – O(69)	177.2(10)	O(106) – W(8) – O(74)	165.8(13)
O(14) – W(8) – O(74)	87.9(9)	O(63) – W(10) – O(73)	80.2(10)
O(89) – W(8) – O(74)	85.2(9)	O(1) – W(10) – O(73)	83.3(9)
O(97) – W(8) – O(74)	71.5(9)	O(45) – W(10) – O(73)	71.1(8)
O(34) – W(8) – O(74)	71.6 (8)	O(115) – W(10) – O(73)	84.7(9)
O(54) – W(9) – O(94)	103.3(11)	O(44) – W(11) – O(43)	96.7(11)
O(54) – W(9) – O(46)	99.6(12)	O(44) – W(11) – O(47)	100.1(11)
O(94) – W(9) – O(46)	156.6(10)	O(43) – W(11) – O(47)	92.8(10)
O(54) – W(9) – O(58)	98.9(11)	O(44) – W(11) – O(2)	97.7(12)
O(94) – W(9) – O(58)	85.1(10)	O(43) – W(11) – O(2)	90.4(10)
O(46) – W(9) – O(58)	87.0(10)	O(47) – W(11) – O(2)	161.4(9)
O(54) – W(9) – O(53)	102.2(12)	O(44) – W(11) – O(27)	103.5(11)
O(94) – W(9) – O(53)	90.3(10)	O(43) – W(11) – O(27)	159.7(10)
O(46) – W(9) – O(53)	89.2(10)	O(47) – W(11) – O(27)	86.3 (9)
O(58) – W(9) – O(53)	158.9(10)	O(2) – W(11) – O(27)	84.5(10)
O(54) – W(9) – O(76)	172.1(11)	O(44) – W(11) – O(70)	169.2(10)
O(94) – W(9) – O(76)	83.7(9)	O(43) – W(11) – O(70)	72.6(8)
O(46) – W(9) – O(76)	73.8(9)	O(47) – W(11) – O(70)	82.0(8)
O(58) – W(9) – O(76)	85.3(9)	O(2) – W(11) – O(70)	81.5(9)
O(53) – W(9) – O(76)	73.7(9)	O(27) – W(11) – O(70)	87.2(8)
O(30) – W(10) – O(63)	101.7(12)	O(111) – W(12) – O(38)	99.7(12)

(cont. on the next page)

Table F.1. (cont.)

O(30) – W(10) – O(1)	95.9(12)	O(111) – W(12) – O(24)	99.4(11)
O(63) – W(10) – O(1)	161.8(10)	O(38) – W(12) – O(24)	91.4(11)
O(30) – W(10) – O(45)	99.1(11)	O(111) – W(12) – O(57)	102.1(11)
O(63) – W(10) – O(45)	92.2(11)	O(38) – W(12) – O(57)	89.9(10)
O(1) – W(10) – O(45)	89.7(10)	O(24) – W(12) – O(57)	157.9(10)
O(30) – W(10) – O(115)	105.1(12)	O(111) – W(12) – O(116)	97.3(12)
O(63) – W(10) – O(115)	84.4(11)	O(38) – W(12) – O(116)	162.5(11)
O(1) – W(10) – O(115)	86.5(10)	O(24) – W(12) – O(116)	89.9(11)
O(45) – W(10) – O(115)	155.8(9)	O(57) – W(12) – O(116)	82.5(10)
O(30) – W(10) – O(73)	170.1(11)	O(111) – W(12) – O(71)	172.5(10)
O(38) – W(12) – O(71)	81.8(9)	O(15) – W(14) – O(67)	82.2(8)
O(24) – W(12) – O(71)	73.1(9)	O(8) – W(14) – O(67)	84.8(8)
O(57) – W(12) – O(71)	85.3(9)	O(23) – W(14) – O(67)	73.3(8)
O(116) – W(12) – O(71)	81.9(9)	O(9) – W(14) – O(67)	80.9(8)
O(17) – W(13) – O(24)	98.7(12)	O(60) – W(15) – O(42)	102.7(11)
O(17) – W(13) – O(55)	100.1(12)	O(60) – W(15) – O(15)	99.6(10)
O(24) – W(13) – O(55)	91.8(10)	O(42) – W(15) – O(15)	88.7(10)
O(17) – W(13) – O(64)	95.8(12)	O(60) – W(15) – O(11)	98.2(11)
O(24) – W(13) – O(64)	85.3(10)	O(42) – W(15) – O(11)	87.1(10)
O(55) – W(13) – O(64)	164.1(10)	O(15) – W(15) – O(11)	162.1(8)
O(17) – W(13) – O(42)	106.1(12)	O(60) – W(15) – O(39)	101.5(11)
O(24) – W(13) – O(42)	154.3 (9)	O(42) – W(15) – O(39)	155.4(10)
O(55) – W(13) – O(42)	90.4(10)	O(15) – W(15) – O(39)	91.9(9)
O(64) – W(13) – O(42)	85.6(10)	O(11) – W(15) – O(39)	84.9(9)
O(17) – W(13) – O(71)	170.8(11)	O(60) – W(15) – O(72)	175.3(10)
O(24) – W(13) – O(71)	72.4(8)	O(42) – W(15) – O(72)	81.7(9)
O(55) – W(13) – O(71)	83.0(8)	O(15) – W(15) – O(72)	82.0(8)
O(64) – W(13) – O(71)	81.2(8)	O(11) – W(15) – O(72)	80.2(8)
O(42) – W(13) – O(71)	82.4(8)	O(39) – W(15) – O(72)	74.0(9)
O(41) – W(14) – O(15)	100.3(10)	O(25) – W(16) – O(20)	100.9(9)
O(41) – W(14) – O(8)	99.7(10)	O(25) – W(16) – O(1)	99.2(10)
O(15) – W(14) – O(8)	88.8(9)	O(20) – W(16) – O(1)	88.5(9)
O(41) – W(14) – O(23)	102.1(10)	O(25) – W(16) – O(43)	101.5(10)
O(15) – W(14) – O(23)	90.0(9)	O(20) – W(16) – O(43)	157.1(9)
O(8) – W(14) – O(23)	158.0(9)	O(1) – W(16) – O(43)	92.6(10)
O(41) – W(14) – O(9)	96.8(10)	O(25) – W(16) – O(14)	95.9(10)
O(15) – W(14) – O(9)	162.7(8)	O(20) – W(16) – O(14)	84.7(9)
O(8) – W(14) – O(9)	85.7(9)	O(1) – W(16) – O(14)	164.3(10)
O(23) – W(14) – O(9)	89.1(9)	O(43) – W(16) – O(14)	88.4(10)
O(41) – W(14) – O(67)	174.8(9)	O(25) – W(16) – O(70)	172.2(9)
O(20) – W(16) – O(70)	86.2(7)	O(12) – W(18) – O(74)	82.7(9)
O(1) – W(16) – O(70)	84.2(9)	O(88) – W(18) – O(74)	70.8(9)
O(43) – W(16) – O(70)	71.2(8)	O(97) – W(18) – O(74)	72.9(9)

(cont. on the next page)

Table F.1. (cont.)

O(14) – W(16) – O(70)	81.2(8)	O(47) – W(18) – O(74)	83.1(8)
O(80) – W(17) – O(53)	99.5(10)	O(102) – W(19) – O(16)	103.8(12)
O(80) – W(17) – O(50)	101.9(11)	O(102) – W(19) – O(35)	101.7(12)
O(53) – W(17) – O(50)	158.6(10)	O(16) – W(19) – O(35)	86.4(10)
O(80) – W(17) – O(95)	101.4(11)	O(102) – W(19) – O(88)	101.9(12)
O(53) – W(17) – O(95)	88.4(10)	O(16) – W(19) – O(88)	86.8(10)
O(50) – W(17) – O(95)	87.1(11)	O(35) – W(19) – O(88)	156.4(10)
O(80) – W(17) – O(84)	101.8(10)	O(102) – W(19) – O(34)	99.6(12)
O(53) – W(17) – O(84)	89.7(10)	O(16) – W(19) – O(34)	156.6(10)
O(50) – W(17) – O(84)	86.2(10)	O(35) – W(19) – O(34)	90.3(9)
O(95) – W(17) – O(84)	156.8(10)	O(88) – W(19) – O(34)	86.9(10)
O(80) – W(17) – O(76)	171.8(10)	O(102) – W(19) – O(74)	169.5(11)
O(53) – W(17) – O(76)	74.3(9)	O(16) – W(19) – O(74)	83.8(9)
O(50) – W(17) – O(76)	84.4(9)	O(35) – W(19) – O(74)	85.9(9)
O(95) – W(17) – O(76)	73.4(10)	O(88) – W(19) – O(74)	70.8(9)
O(84) – W(17) – O(76)	83.8(9)	O(34) – W(19) – O(74)	72.8(8)
O(51) – W(18) – O(12)	100.0(11)	O(119) – W(20) – O(2)	98.7(12)
O(51) – W(18) – O(88)	104.9(11)	O(119) – W(20) – O(45)	101.2(11)
O(12) – W(18) – O(88)	86.8(10)	O(2) – W(20) – O(45)	91.9(10)
O(51) – W(18) – O(97)	104.8(11)	O(119) – W(20) – O(81)	100.7(12)
O(12) – W(18) – O(97)	155.0(10)	O(2) – W(20) – O(81)	88.6(11)
O(88) – W(18) – O(97)	90.1(10)	O(45) – W(20) – O(81)	157.7(11)
O(51) – W(18) – O(47)	101.4(10)	O(119) – W(20) – O(87)	97.6(12)
O(12) – W(18) – O(47)	86.3(9)	O(2) – W(20) – O(87)	163.4(10)
O(88) – W(18) – O(47)	153.6(10)	O(45) – W(20) – O(87)	88.0(10)
O(97) – W(18) – O(47)	85.5(9)	O(81) – W(20) – O(87)	85.2(11)
O(51) – W(18) – O(74)	174.9(10)	O(119) – W(20) – O(73)	172.8(11)
O(2) – W(20) – O(73)	84.2(9)	O(101) – W(22) – O(98)	80.7(10)
O(45) – W(20) – O(73)	72.0(9)	O(100) – W(22) – O(98)	72.1(9)
O(81) – W(20) – O(73)	85.9(10)	O(79) – W(22) – O(98)	85.6(9)
O(87) – W(20) – O(73)	80.0(9)	O(16) – W(22) – O(98)	82.2(9)
O(105) – W(21) – O(115)	102.7(12)	O(32) – W(23) – O(10)	100.9(11)
O(105) – W(21) – O(99)	99.7(13)	O(32) – W(23) – O(84)	98.2(11)
O(115) – W(21) – O(99)	157.5(11)	O(10) – W(23) – O(84)	89.5(10)
O(105) – W(21) – O(4)	99.9(12)	O(32) – W(23) – O(19)	100.8(10)
O(115) – W(21) – O(4)	89.2(10)	O(10) – W(23) – O(19)	158.2(10)
O(99) – W(21) – O(4)	88.7(11)	O(84) – W(23) – O(19)	87.8(10)
O(105) – W(21) – O(56)	94.8(12)	O(32) – W(23) – O(18)	97.3(11)
O(115) – W(21) – O(56)	85.0(10)	O(10) – W(23) – O(18)	90.2(10)
O(99) – W(21) – O(56)	91.4(11)	O(84) – W(23) – O(18)	164.2(9)
O(4) – W(21) – O(56)	165.0(10)	O(19) – W(23) – O(18)	86.6(9)
O(105) – W(21) – O(78)	172.6(11)	O(32) – W(23) – O(66)	172.7(10)
O(115) – W(21) – O(78)	84.4(9)	O(10) – W(23) – O(66)	71.7(9)

(cont. on the next page)

Table F.1. (cont.)

O(99) – W(21) – O(78)	73.1(11)	O(84) – W(23) – O(66)	82.4(9)
O(4) – W(21) – O(78)	82.2(9)	O(19) – W(23) – O(66)	86.5(9)
O(56) – W(21) – O(78)	83.5(9)	O(18) – W(23) – O(66)	82.6(9)
O(107) – W(22) – O(101)	99.7(11)	O(31) – W(24) – O(11)	104.2(11)
O(107) – W(22) – O(100)	102.1(10)	O(31) – W(24) – O(64)	101.6(11)
O(101) – W(22) – O(100)	89.7(11)	O(11) – W(24) – O(64)	89.6(10)
O(107) – W(22) – O(79)	100.2(10)	O(31) – W(24) – O(113)	99.6(12)
O(101) – W(22) – O(79)	87.9(11)	O(11) – W(24) – O(113)	86.9(11)
O(100) – W(22) – O(79)	157.7(9)	O(64) – W(24) – O(113)	158.7(11)
O(107) – W(22) – O(16)	98.0(10)	O(31) – W(24) – O(6)	99.2(11)
O(101) – W(22) – O(16)	161.6(10)	O(11) – W(24) – O(6)	156.4(9)
O(100) – W(22) – O(16)	91.6(10)	O(64) – W(24) – O(6)	88.7(10)
O(79) – W(22) – O(16)	83.9(10)	O(113) – W(24) – O(6)	86.2(10)
O(107) – W(22) – O(98)	174.1(10)	O(31) – W(24) – O(77)	169.4(10)
O(11) – W(24) – O(77)	84.1(8)	O(5) – W(26) – O(78)	81.8(8)
O(64) – W(24) – O(77)	84.8(9)	O(40) – W(26) – O(78)	81.6(9)
O(113) – W(24) – O(77)	73.9(10)	O(99) – W(26) – O(78)	71.9(10)
O(6) – W(24) – O(77)	72.3(8)	O(114) – W(27) – O(37)	98.7(12)
O(108) – W(25) – O(9)	103.6(13)	O(114) – W(27) – O(27)	101.6(11)
O(108) – W(25) – O(95)	99.6(14)	O(37) – W(27) – O(27)	87.9(10)
O(9) – W(25) – O(95)	156.7(10)	O(114) – W(27) – O(100)	97.2(11)
O(108) – W(25) – O(13)	101.1(13)	O(37) – W(27) – O(100)	90.8 (10)
O(9) – W(25) – O(13)	86.7(9)	O(27) – W(27) – O(100)	161.2(10)
O(95) – W(25) – O(13)	86.7(10)	O(114) – W(27) – O(12)	97.8(11)
O(108) – W(25) – O(46)	101.1(13)	O(37) – W(27) – O(12)	163.4(10)
O(95) – W(25) – O(46)	91.1(11)	O(27) – W(27) – O(12)	88.7(10)
O(13) – W(25) – O(46)	157.5(10)	O(100) – W(27) – O(12)	87.3(10)
O(108) – W(25) – O(76)	171.1(13)	O(114) – W(27) – O(98)	172.5(10)
O(9) – W(25) – O(76)	83.6(9)	O(37) – W(27) – O(98)	82.5(10)
O(95) – W(25) – O(76)	73.5(10)	O(27) – W(27) – O(98)	85.9(9)
O(13) – W(25) – O(76)	84.4(9)	O(100) – W(27) – O(98)	75.3(10)
O(46) – W(25) – O(76)	73.5(9)	O(12) – W(27) – O(98)	81.1(10)
O(103) – W(26) – O(109)	103.9(12)	O(29) – W(28) – O(79)	100.8(10)
O(103) – W(26) – O(5)	100.3(11)	O(29) – W(28) – O(5)	99.4(10)
O(109) – W(26) – O(5)	87.4(10)	O(79) – W(28) – O(5)	91.7(9)
O(103) – W(26) – O(40)	96.7(11)	O(29) – W(28) – O(3)	98.5(10)
O(109) – W(26) – O(40)	85.4(11)	O(79) – W(28) – O(3)	159.7(9)
O(5) – W(26) – O(40)	162.7(9)	O(5) – W(28) – O(3)	91.4(8)
O(103) – W(26) – O(99)	101.6(12)	O(29) – W(28) – O(35)	96.5(10)
O(109) – W(26) – O(99)	154.5(11)	O(79) – W(28) – O(35)	85.1(9)
O(5) – W(26) – O(99)	89.8(10)	O(5) – W(28) – O(35)	164.1(8)
O(40) – W(26) – O(99)	89.9(11)	O(3) – W(28) – O(35)	86.5(9)
O(103) – W(26) – O(78)	173.2(11)	O(29) – W(28) – O(68)	172.1(10)

(cont. on the next page)

Table F.1. (cont.)

O(109) – W(26) – O(78)	82.6(10)	O(79) – W(28) – O(68)	87.0(8)
O(5) – W(28) – O(68)	81.6(8)	O(28) – W(30) – O(77)	85.8(8)
O(3) – W(28) – O(68)	73.6(7)	O(90) – W(30) – O(77)	73.9(9)
O(35) – W(28) – O(68)	82.7(8)	O(113) – W(30) – O(77)	74.1(10)
O(104) – W(29) – O(55)	97.6(11)	O(112) – W(31) – O(116)	103.1(12)
O(104) – W(29) – O(8)	100.0(11)	O(112) – W(31) – O(62)	103.7(11)
O(55) – W(29) – O(8)	89.0(10)	O(116) – W(31) – O(62)	84.2(11)
O(104) – W(29) – O(13)	98.4(11)	O(112) – W(31) – O(6)	99.7(11)
O(55) – W(29) – O(13)	164.1(9)	O(116) – W(31) – O(6)	89.1(10)
O(8) – W(29) – O(13)	87.7(10)	O(62) – W(31) – O(6)	156.6(10)
O(104) – W(29) – O(75)	100.6(11)	O(112) – W(31) – O(90)	99.6(11)
O(55) – W(29) – O(75)	88.7(10)	O(116) – W(31) – O(90)	157.3(11)
O(8) – W(29) – O(75)	159.4(9)	O(62) – W(31) – O(90)	90.2(10)
O(13) – W(29) – O(75)	89.0(10)	O(6) – W(31) – O(90)	87.4(9)
O(104) – W(29) – O(65)	175.1(10)	O(112) – W(31) – O(77)	170.4(10)
O(55) – W(29) – O(65)	81.6(9)	O(116) – W(31) – O(77)	83.6(10)
O(8) – W(29) – O(65)	84.8(8)	O(62) – W(31) – O(77)	83.6(9)
O(13) – W(29) – O(65)	82.6(8)	O(6) – W(31) – O(77)	73.3(8)
O(75) – W(29) – O(65)	74.6(8)	O(90) – W(31) – O(77)	73.9(9)
O(92) – W(30) – O(93)	101.5(11)	O(121) – W(32) – O(109)	103.5(12)
O(92) – W(30) – O(28)	100.5(10)	O(121) – W(32) – O(110)	100.8(13)
O(93) – W(30) – O(28)	85.9(10)	O(109) – W(32) – O(110)	155.3(11)
O(92) – W(30) – O(90)	100.2(11)	O(121) – W(32) – O(117)	95.8(13)
O(93) – W(30) – O(90)	87.4(10)	O(109) – W(32) – O(117)	83.8(12)
O(28) – W(30) – O(90)	159.2(9)	O(110) – W(32) – O(117)	89.1(12)
O(92) – W(30) – O(113)	101.1(11)	O(121) – W(32) – O(101)	100.8(13)
O(93) – W(30) – O(113)	157.3(11)	O(109) – W(32) – O(101)	90.3(11)
O(28) – W(30) – O(113)	90.7(10)	O(110) – W(32) – O(101)	89.8(12)
O(90) – W(30) – O(113)	88.0(11)	O(117) – W(32) – O(101)	163.3(11)
O(92) – W(30) – O(77)	172.3(10)	O(121) – W(32) – O(85)	172.5(12)
O(93) – W(30) – O(77)	83.3(9)	O(109) – W(32) – O(85)	83.1(9)
O(110) – W(32) – O(85)	72.4(10)	O(110) – W(34) – O(85)	73.7(10)
O(117) – W(32) – O(85)	81.3(10)	O(37) – W(34) – O(85)	83.4(9)
O(101) – W(32) – O(85)	82.5(10)	O(83) – W(34) – O(85)	83.4(9)
O(122) – W(33) – O(82)	103.5(14)	O(120) – W(35) – O(117)	103.4(13)
O(122) – W(33) – O(56)	101.8(13)	O(120) – W(35) – O(123)	100.3(14)
O(82) – W(33) – O(56)	90.4(11)	O(117) – W(35) – O(123)	93.0(13)
O(122) – W(33) – O(118)	99.9(14)	O(120) – W(35) – O(40)	102.2(13)
O(82) – W(33) – O(118)	87.8(12)	O(117) – W(35) – O(40)	85.3(11)
O(56) – W(33) – O(118)	158.1(11)	O(123) – W(35) – O(40)	157.3(12)
O(122) – W(33) – O(63)	103.0(13)	O(120) – W(35) – O(82)	100.9(13)
O(82) – W(33) – O(63)	153.5(12)	O(117) – W(35) – O(82)	155.6(12)
O(56) – W(33) – O(63)	83.1(11)	O(123) – W(35) – O(82)	85.1(13)

(cont. on the next page)

Table F.1. (cont.)

O(118) – W(33) – O(63)	88.8(12)	O(40) – W(35) – O(82)	87.2(11)
O(122) – W(33) – O(91)	169.6(13)	O(120) – W(35) – O(91)	168.8(12)
O(82) – W(33) – O(91)	71.7(11)	O(117) – W(35) – O(91)	85.0(11)
O(56) – W(33) – O(91)	87.6(10)	O(123) – W(35) – O(91)	71.6(12)
O(118) – W(33) – O(91)	71.2(11)	O(40) – W(35) – O(91)	85.7(10)
O(63) – W(33) – O(91)	82.4(10)	O(82) – W(35) – O(91)	71.2(11)
O(124) – W(34) – O(81)	99.4(14)	O(96) – W(36) – O(83)	102.3(11)
O(124) – W(34) – O(110)	102.4(14)	O(96) – W(36) – O(87)	101.8(12)
O(81) – W(34) – O(110)	158.2(12)	O(83) – W(36) – O(87)	86.2(10)
O(124) – W(34) – O(37)	97.5(13)	O(96) – W(36) – O(118)	100.8(12)
O(81) – W(34) – O(37)	85.7(11)	O(83) – W(36) – O(118)	156.9(11)
O(110) – W(34) – O(37)	91.8(11)	O(87) – W(36) – O(118)	90.4(11)
O(124) – W(34) – O(83)	96.3(13)	O(96) – W(36) – O(123)	102.2(13)
O(81) – W(34) – O(83)	85.6(10)	O(83) – W(36) – O(123)	89.3(11)
O(110) – W(34) – O(83)	91.6(11)	O(87) – W(36) – O(123)	156.0(12)
O(37) – W(34) – O(83)	164.7(9)	O(118) – W(36) – O(123)	84.6(12)
O(124) – W(34) – O(85)	176.1(12)	O(96) – W(36) – O(91)	170.5(12)
O(81) – W(34) – O(85)	84.5(10)	O(83) – W(36) – O(91)	84.8(10)
O(87) – W(36) – O(91)	84.8(10)	W(21) – O(4) – W(3)	162.2(13)
O(118) – W(36) – O(91)	72.1(11)	W(28) – O(5) – W(26)	162.4(12)
O(123) – W(36) – O(91)	71.3(12)	W(31) – O(6) – W(24)	123.2(12)
O(67) – P(1) – O(66)	110.8(12)	W(29) – O(8) – W(14)	150.7(13)
O(67) – P(1) – O(65)	111.2(12)	W(25) – O(9) – W(14)	151.6(12)
O(66) – P(1) – O(65)	113.0(12)	W(23) – O(10) – W(4)	125.3(13)
O(67) – P(1) – O(76)	106.8(13)	W(24) – O(11) – W(15)	147.9(13)
O(66) – P(1) – O(76)	107.4(13)	W(18) – O(12) – W(27)	150.2(13)
O(65) – P(1) – O(76)	107.3(13)	W(29) – O(13) – W(25)	148.9(13)
O(68) – P(2) – O(98)	113.4(13)	W(8) – O(14) – W(16)	151.5(13)
O(68) – P(2) – O(70)	110.7(11)	W(14) – O(15) – W(15)	163.0(12)
O(98) – P(2) – O(70)	109.1(12)	W(19) – O(16) – W(22)	152.7(14)
O(68) – P(2) – O(74)	108.9(12)	W(2) – O(18) – W(23)	161.5(13)
O(98) – P(2) – O(74)	108.3(13)	W(5) – O(19) – W(23)	146.0(13)
O(70) – P(2) – O(74)	106.1(11)	W(16) – O(20) – W(3)	152.0(11)
O(72) – P(3) – O(71)	111.8(12)	W(7) – O(21) – W(1)	163.7(13)
O(72) – P(3) – O(69)	109.6(13)	W(6) – O(22) – W(4)	162.9(13)
O(71) – P(3) – O(69)	112.8(12)	W(1) – O(23) – W(14)	123.2(11)
O(72) – P(3) – O(77)	109.6(13)	W(12) – O(24) – W(13)	124.6(13)
O(71) – P(3) – O(77)	107.1(12)	W(6) – O(26) – W(7)	150.7(11)
O(69) – P(3) – O(77)	105.6(12)	W(27) – O(27) – W(11)	146.9(13)
O(85) – P(4) – O(78)	111.9(14)	W(7) – O(28) – W(30)	151.7(11)
O(85) – P(4) – O(73)	111.5(13)	W(28) – O(29) – Cu(1)	106(5)
O(78) – P(4) – O(73)	112.0(13)	W(19) – O(34) – W(8)	121.6(11)
O(85) – P(4) – O(91)	106.9(14)	W(19) – O(35) – W(28)	150.3(13)

(cont. on the next page)

Table F.1. (cont.)

O(78) – P(4) – O(91)	108.9(14)	W(27) – O(37) – W(34)	165.6(13)
O(73) – P(4) – O(91)	105.3(13)	W(12) – O(38) – W(5)	162.1(14)
W(16) – O(1) – W(10)	165.2(14)	W(7) – O(39) – W(15)	122.3(12)
W(20) – O(2) – W(11)	166.4(14)	W(26) – O(40) – W(35)	150.5(14)
W(28) – O(3) – W(3)	121.6(10)	W(15) – O(42) – W(13)	155.4(14)
W(11) – O(43) – W(16)	124.0(12)	W(6) – O(69) – W(2)	89.9(7)
W(20) – O(45) – W(10)	124.8(11)	P(2) – O(70) – W(11)	127.5(11)
W(9) – O(46) – W(25)	122.1(13)	P(2) – O(70) – W(16)	128.3(11)
W(18) – O(47) – W(11)	153.7(12)	W(11) – O(70) – W(16)	92.0(7)
W(17) – O(50) – W(5)	148.9(13)	P(3) – O(71) – W(12)	128.8(11)
W(1) – O(52) – W(4)	153.0(13)	P(3) – O(71) – W(13)	129.0(12)
W(17) – O(53) – W(9)	121.9(12)	W(12) – O(71) – W(13)	89.2(7)
W(29) – O(55) – W(13)	161.6(14)	P(3) – O(72) – W(7)	129.6(13)
W(33) – O(56) – W(21)	151.1(14)	P(3) – O(72) – W(15)	127.9(13)
W(2) – O(57) – W(12)	152.3(14)	W(7) – O(72) – W(15)	87.1(8)
W(1) – O(58) – W(9)	149.2(13)	P(4) – O(73) – W(20)	128.9(13)
W(2) – O(59) – W(6)	123.3(11)	P(4) – O(73) – W(10)	128.1(13)
W(31) – O(62) – W(2)	153.4(14)	W(20) – O(73) – W(10)	91.9(8)
W(10) – O(63) – W(33)	155.8(15)	P(2) – O(74) – W(19)	123.8(12)
W(24) – O(64) – W(13)	148.2(14)	P(2) – O(74) – W(18)	124.8(12)
P(1) – O(65) – W(5)	126.8(12)	W(19) – O(74) – W(18)	92.2(8)
W(6) – O(22) – W(4)	162.9(13)	P(2) – O(74) – W(8)	121.2(12)
P(1) – O(65) – W(29)	128.1(12)	W(19) – O(74) – W(8)	94.0(8)
W(5) – O(65) – W(29)	90.7(7)	W(18) – O(74) – W(8)	92.3(8)
P(1) – O(66) – W(4)	128.8(13)	W(29) – O(75) – W(5)	120.4(11)
P(1) – O(66) – W(23)	126.5(13)	P(1) – O(76) – W(25)	125.4(13)
W(4) – O(66) – W(23)	90.2(7)	P(1) – O(76) – W(9)	125.1(13)
P(1) – O(67) – W(1)	129.0(12)	W(25) – O(76) – W(9)	90.2(9)
P(1) – O(67) – W(14)	128.5(12)	P(1) – O(76) – W(17)	124.9(14)
W(1) – O(67) – W(14)	89.1(7)	W(25) – O(76) – W(17)	90.1(8)
P(2) – O(68) – W(3)	129.0(12)	W(9) – O(76) – W(17)	90.1(8)
P(2) – O(68) – W(28)	125.4(12)	P(3) – O(77) – W(31)	126.6(12)
W(3) – O(68) – W(28)	90.3(7)	P(3) – O(77) – W(30)	125.1(11)
P(3) – O(69) – W(6)	129.6(12)	W(31) – O(77) – W(30)	90.5(7)
P(3) – O(69) – W(2)	127.0(12)	P(3) – O(77) – W(24)	123.0(11)
W(31) – O(77) – W(24)	91.1(7)	W(21) – O(99) – W(26)	125.3(15)
W(30) – O(77) – W(24)	89.9(7)	W(27) – O(100) – W(22)	123.7(13)
P(4) – O(78) – W(21)	128.0(14)	W(22) – O(101) – W(32)	163.8(16)
P(4) – O(78) – W(26)	128.2(14)	W(26) – O(109) – W(32)	154.5(15)
W(21) – O(78) – W(26)	89.6(9)	W(34) – O(110) – W(32)	124.0(15)
W(28) – O(79) – W(22)	151.1(13)	W(30) – O(113) – W(24)	122.1(15)
W(34) – O(81) – W(20)	151.2(16)	W(21) – O(115) – W(10)	151.3(14)
W(33) – O(82) – W(35)	125.8(15)	W(31) – O(116) – W(12)	152.8(16)

(cont. on the next page)

Table F.1. (cont.)

W(36) – O(83) – W(34)	149.8(13)	W(35) – O(117) – W(32)	152.6(17)
W(23) – O(84) – W(17)	151.5(12)	W(33) – O(118) – W(36)	124.9(15)
P(4) – O(85) – W(34)	128.6(13)	W(35) – O(123) – W(36)	123.2(17)
P(4) – O(85) – W(32)	127.0(14)	C(12) – C(1) – C(3)	123(3)
W(34) – O(85) – W(32)	89.8(8)	C(3) – C(2) – C(13)	130(4)
W(36) – O(87) – W(20)	151.7(14)	C(3) – C(2) – C(24)	124(4)
W(18) – O(88) – W(19)	126.2(13)	C(13) – C(2) – C(24)	106(3)
W(8) – O(89) – W(3)	149.1(14)	C(16) – C(3) – C(2)	132(4)
W(30) – O(90) – W(31)	121.8(12)	C(16) – C(3) – C(1)	110(4)
P(4) – O(91) – W(36)	125.4(15)	C(2) – C(3) – C(1)	116(4)
P(4) – O(91) – W(35)	122.9(14)	C(5) – C(4) – C(27)	119(3)
W(36) – O(91) – W(35)	93.8(10)	C(5) – C(4) – C(6)	125(3)
P(4) – O(91) – W(33)	122.4(14)	C(27) – C(4) – C(6)	117(3)
W(36) – O(91) – W(33)	91.9(9)	C(10) – C(5) – C(4)	127(3)
W(35) – O(91) – W(33)	91.3(10)	C(22) – C(6) – C(29)	121(4)
W(30) – O(93) – W(6)	149.9(14)	C(22) – C(6) – C(4)	122(3)
W(9) – O(94) – W(4)	152.5(13)	C(29) – C(6) – C(4)	117(3)
W(17) – O(95) – W(25)	122.7(14)	C(15) – C(7) – C(17)	118(4)
W(18) – O(97) – W(8)	123.3(12)	C(15) – C(7) – C(8)	127(4)
P(2) – O(98) – W(27)	129.4(14)	C(17) – C(7) – C(8)	114(3)
P(2) – O(98) – W(22)	124.1(14)	C(25) – C(8) – C(18)	117(4)
W(27) – O(98) – W(22)	88.9(8)	C(25) – C(8) – C(7)	123(3)
C(18) – C(8) – C(7)	119(3)	N(1) – C(9) – C(15)	115(4)
C(11) – N(1) – C(9)	128(4)	C(23) – C(28) – N(6)	116(4)
C(40) – N(2) – C(42)	118(4)	C(38) – C(29) – C(6)	118(4)
C(5) – C(10) – N(5)	113(4)	C(45) – C(30) – C(19)	115(4)
C(14) – N(3) – C(12)	126(4)	C(32) – N(6) – C(28)	119(4)
N(1) – C(11) – C(17)	114(3)	C(34) – C(31) – C(39)	122(4)
C(1) – C(12) – N(3)	116(3)	C(34) – C(31) – C(41)	125(3)
C(26) – C(13) – C(2)	127(3)	C(39) – C(31) – C(41)	113(4)
N(3) – C(14) – C(16)	115(4)	C(45) – N(7) – C(36)	128(5)
C(7) – C(15) – C(9)	124(4)	N(6) – C(32) – C(33)	124(3)
C(3) – C(16) – C(14)	126(4)	C(21) – C(33) – C(32)	113(4)
C(11) – C(17) – C(7)	119(4)	C(38) – N(8) – C(37)	120(5)
C(42) – C(18) – C(8)	118(5)	C(19) – C(35) – C(36)	121(4)
C(35) – C(19) – C(21)	122(3)	N(7) – C(36) – C(35)	114(4)
C(35) – C(19) – C(30)	117(4)	N(8) – C(37) – C(22)	115(4)
C(21) – C(19) – C(30)	121(3)	C(29) – C(38) – N(8)	125(5)
C(26) – N(4) – C(20)	123(4)	C(31) – C(39) – C(50)	114(5)
C(24) – C(20) – N(4)	121(4)	N(2) – C(40) – C(25)	123(4)
C(43) – N(5) – C(10)	131(4)	C(28) – C(23) – C(21)	128(5)
C(23) – C(21) – C(33)	120(4)	C(20) – C(24) – C(2)	125(4)
C(23) – C(21) – C(19)	122(4)	C(8) – C(25) – C(40)	115(4)
C(33) – C(21) – C(19)	118(4)	N(4) – C(26) – C(13)	118(4)
C(6) – C(22) – C(37)	119(4)		

APPENDIX G

BOND VALENCE SUMS OF (4,4'-bpyH₂)₃[PCuW₁₁O₃₉]

Table G.1. Bond valence sums of $(4,4'\text{-bpyH}_2)_3[\text{PCuW}_{11}\text{O}_{39}]$

	W(1)	W(2)	W(3)	W(4)	W(5)	W(6)	W(7)	W(8)	W(9)	W(10)	W(11)	W(12)	Cu(11)	Cu(12)	P(1)	Σ
O(1)	1.062												1.143			2.205
O(2)	1.025	0.987	1.004										0.889			2.018
O(3)		1.103											0.253			1.991
O(4)													0.891			2.245
O(5)																1.953
O(6)	1.025	1.062		1.048												2.073
O(7)					1.809											1.809
O(8)						1.136										2.087
O(9)						1.009										1.957
O(10)							0.948									2.637
O(11)								1.308								2.439
O(12)									0.987							2.093
O(13)										0.923						2.054
O(14)											0.964					2.408
O(15)	0.279		0.280													2.119
O(16)																2.170
O(17)																2.027
O(18)																2.056
O(19)																1.834
O(20)																2.430
O(21)																2.091
O(22)																2.425
O(23)																2.116
O(24)																2.334
O(25)																2.445
O(26)																1.992
O(27)																2.763
O(28)																2.310
	0.310		0.309													1.359

(cont. on the next page)

Table G.1. (cont.)

APPENDIX H

BOND VALENCE SUMS OF (4,4'-bpyH₂)[H₂PW₁₂O₄₀]₂.H₂O

Table H.1. Bond valence sums of (4,4'-bpyH₂)[H₂PW₁₂O₄₀]₂.H₂O

	W(1)	W(2)	W(3)	W(4)	W(5)	W(6)	W(7)	W(8)	W(9)	W(10)	W(11)	W(12)	W(13)	W(14)	W(15)	W(16)	W(17)	W(18)	P(1)	P(2)	Σ
O(1)	1.009																				2.235
O(2)	0.985																				2.134
O(3)	1.112																				2.183
O(4)	0.987	1.103																			2.090
O(5)																					2.172
O(6)	1.045																				2.178
O(7)																					2.149
O(8)																					2.273
O(9)																					2.035
O(10)																					2.220
O(11)																					2.107
O(12)																					2.217
O(13)																					2.137
O(14)																					2.102
O(15)																					2.201
O(16)																					2.062
O(17)																					2.125
O(18)																					2.198
O(19)																					2.097
O(20)																					1.352
O(21)																					2.249
O(22)																					2.069
O(23)																					1.737
O(24)	0.314	0.309																			1.853
O(25)		1.103																			2.162
O(26)		1.143																			2.258
O(27)		1.161																			2.168
O(28)			0.938																		2.133
				1.183																	2.121
					0.972																

(cont. on the next page)

Table H.1. (cont.)

(cont. on the next page)

APPENDIX I

BOND VALENCE SUMS OF (4,4'-bpyH₂)₄[H₂P₂W₁₈O₆₂]₂

Table I.1. Bond valence sums of (4,4'-bpyH₂)₄[H₂P₂W₁₈O₆₂]₂

	W(1)	W(2)	W(3)	W(4)	W(5)	W(6)	W(7)	W(8)	W(9)	W(10)	W(11)	W(12)	W(13)	W(14)	W(15)	W(16)	W(17)	W(18)	W(19)	W(20)
O(1)																				
O(2)																				
O(3)																				
O(4)																				
O(5)																				
O(6)																				
O(7)																				
O(8)																				
O(9)																				
O(10)																				
O(11)																				
O(12)																				
O(13)																				
O(14)																				
O(15)																				
O(16)																				
O(17)																				
O(18)																				
O(19)																				
O(20)																				
O(21)	1.006																			
O(22)																				
O(23)	1.121																			
O(24)																				
O(25)																				
O(26)																				
O(27)																				
O(28)																				

(cont. on the next page)

Table I.1. (cont.)

O(30)		1.874
O(31)		
O(32)		
O(33)	1.728	
O(34)		
O(35)		
O(36)	2.032	
O(37)		
O(38)		
O(39)		
O(40)		
O(41)		
O(42)		
O(43)		
O(44)		
O(45)		
O(46)		
O(47)		
O(48)		
O(49)		
O(50)		
O(51)		
O(52)	1.121	
O(53)		
O(54)		
O(55)		
O(56)		
O(57)		
O(58)	1.034	
O(59)	1.121	
O(60)		
O(61)		

(cont. on the next page)

Table I.1. (cont.)

O(62)	0.953
O(63)	
O(64)	
O(65)	
O(66)	0.341
O(67)	0.306
O(68)	0.275
O(69)	0.275
O(70)	0.332
O(71)	
O(72)	
O(73)	
O(74)	
O(75)	
O(76)	
O(77)	
O(78)	
O(79)	
O(80)	
O(81)	
O(82)	
O(83)	
O(84)	
O(85)	
O(86)	
O(87)	
O(88)	
O(89)	
O(90)	
O(91)	
O(92)	

(cont. on the next page)

Table I.1. (cont.)

	1.006	1.183	1.062	1.121	1.925	1.728	1.775	0.903	0.979	1.728										
O(93)																				
O(94)	1.006																			
O(95)																				
O(96)																				
O(97)																				
O(98)																				
O(99)																				
O(100)																				
O(101)																				
O(102)																				
O(103)																				
O(104)																				
O(105)																				
O(106)																				
O(107)																				
O(108)																				
O(109)																				
O(110)																				
O(111)																				
O(112)																				
O(113)																				
O(114)																				
O(115)																				
O(116)																				
O(117)																				
O(118)																				
O(119)																				
O(120)																				
Σ	6.62	6.609	5.962	6.36	5.982	6.457	6.469	6.077	6.199	6.374	6.707	6.29	6.115	6.323	6.189	6.637	6.093	6.623	6.694	6.584

(cont. on the next page)

Table I.1. (cont.)

	W(21)	W(22)	W(23)	W(24)	W(25)	W(26)	W(27)	W(28)	W(29)	W(30)	W(31)	W(32)	W(33)	W(34)	W(35)	W(36)	P(1)	P(2)	P(3)	P(4)	Σ
																	2.283				
																	2.222				
																	2.025				
																	2.222				
																	2.183				
																	1.987				
																	1.728				
																	2.183				
																	2.100				
																	2.278				
																	2.041				
																	2.111				
																	2.070				
																	2.162				
																	2.217				
																	2.169				
																	1.775				
																	2.211				
																	2.068				
																	2.200				
																	2.255				
																	2.222				
																	2.155				
																	2.214				
																	1.775				
																	2.073				
																	2.136				
																	2.124				
																	1.775				
1.216					0.953																
					1.062																
						1.216															
							1.062														
								0.979													
									0.928												
										1.121											
											1.121										
												1.034									
													1.112								
														1.112							
															1.062						
																1.062					
																	1.775				
																		1.775			
																			1.062		
																				1.062	
																					1.062

(cont. on the next page)

Table I.1. (cont.)

1.925	1.824										1.874
		0.953									1.824
			1.183								1.925
				1.062							1.728
					1.034						1.835
						2.074					2.074
							2.032				2.032
								2.245			2.245
									2.111		2.111
										2.189	2.189
											2.096
											1.775
											2.298
											2.186
											2.145
											2.217
											2.041
											2.182
											1.775
											1.775
											2.242
											2.019
											2.068
											1.775
											2.189
											2.144
											2.228
											1.987
											2.155
											1.682
											1.824

(cont. on the next page)

Table I.1. (cont.)

			1.216	1.121					2.169
					1.569				2.242
					1.569				2.040
					1.656				2.182
					1.612				2.185
					1.569				2.252
					1.334				2.219
					1.334				2.176
					1.796				2.024
					1.895				2.381
					1.895				2.410
					1.447				2.111
					1.134				2.121
					1.370				1.962
					1.370				2.256
					1.408				2.287
					1.612				2.169
					1.408				1.637
					1.612				2.182
					1.612				2.208
					1.612				2.202
					1.612				2.111
					1.612				2.131
					1.656				2.246
					1.656				1.637
					1.656				2.096
					1.656				2.242
					1.656				2.040
					1.656				1.987
					1.656				2.170
					1.656				1.682
					1.656				2.097
					1.656				2.097

(cont. on the next page)

Table I.1. (cont.)

		1.006														2.189
																2.068
																1.593
																2.074
	1.249	0.247														2.200
	1.062	1.034	0.341													2.283
	1.249		1.152													2.214
																2.255
																1.925
																1.978
																1.978
																2.264
																2.264
																1.682
																1.682
																1.728
																1.728
																1.509
																1.509
																1.775
																2.243
																2.243
																2.124
																2.124
																1.775
																1.728
																1.728
																1.985
																1.985
																1.637
																1.637
																2.228
																2.228
																2.186
																2.186
																2.125
																2.125
																2.131
																2.131
																1.728
																1.775
																1.824
																1.824
																1.990
																1.415
6.622	5.973	6.502	6.135	6.158	6.586	6.424	6.452	6.991	6.165	6.520	6.292	6.902	5.873	6.247	6.096	6.164
																5.692
																6.668
																5.912

VITA

PERSONAL INFORMATION

Surname, Name: ECE, Özlem
Nationality: Turkish (T.C.)
Date and Place of Birth: 02.12.1985, İzmir
Marital Status: Single
Phone: (+90) 555 200 4746
E-mail: eceozlem697@gmail.com

EDUCATION

Degree	Institution	Year
PhD	İzmir Institute of Technology	2019
MSc	İzmir Institute of Technology	2012
BSc	İzmir Institute of Technology	2008

WORK EXPERIENCE

Year	Place	Enrollment
2010-2018	İzmir Institute of Technology	Research Assistant
2007	İzmir Institute of Technology	Trainee

CONFERENCES

1. Advanced Materials World Congress, September 2013, İzmir, TURKEY. (Poster Presentation)
2. 8th of Aegean Analytical Chemistry Days, İzmir Institute of Technology, September 2012, İzmir, TURKEY.